A GATEKEEPER FUNCTION FOR P120 AND THE E-CADHERIN COMPLEX IN INTESTINAL TUMORIGENESIS

By

Sarah Palmer Short

Dissertation

Submitted to the Faculty of the

Graduate School of Vanderbilt University

In partial fulfillment of the requirements

for the degree of

DOCTOR OF PHILOSOPHY

in

Cancer Biology

May, 2015

Nashville, Tennessee

Approved:

Albert B. Reynolds, Ph.D.

Christopher S. Williams, M.D., Ph.D.

Jin Chen, M.D., Ph.D.

Robert J. Coffey, M.D.

William P. Tansey, Ph.D.

To my loving and patient husband, John

and

To the mice

ACKNOWLEDGEMENTS

I am endlessly grateful to the many amazing people that have contributed to my life and career. Thank you for helping me to achieve what I never thought possible and the opportunity to learn and grow into who I am today.

I would first like to thank my Ph.D. mentor, Dr. Al Reynolds. His imagination and excitement for science is contagious. While providing valuable suggestions and expertise, I appreciate the amount of freedom he allows students to follow their own intuitions and interest. While I am the first to admit my own intuitions are not always fruitful, this experience has given me the opportunity to grow confident in my own abilities. Al provided me with wonderful opportunities and I am truly grateful for my time spent in his lab.

I am also extremely grateful for my committee members: Dr. Chris Williams, Dr. Jin Chen, Dr. Bob Coffey, and Dr. Bill Tansey. Thank you for providing me with wonderful discussions that have helped shape the work presented here. It has truly been a pleasure discussing my research with you and the opportunity to hear everyone's unique perspective.

I would also like to thank the past and present members of the Reynolds lab. I could not ask for a more wonderful group of colleagues and friends. Dr. Rob Carnahan has been a wonderful teacher, whose insight, patience, and support has been invaluable. Drs. Dohn, Kurley, and Smalley-Freed, thank you for your patience and willingness to answer a young graduate student's many, many questions. Nichole Lobdell and Pam Martin, you have contributed more to my sanity than you will ever realize. Thank you for being a continuous source of love, laughter, and calm.

It is important to note that this dissertation would not be possible without Dr. Ann Richmond and the rest of the Richmond lab, particularly lab manager Linda Horton. Thank you Linda for taking a chance and hiring a girl who didn't know a 500ml bottle from a 50ml conical as a lab technician. It was in the Richmond lab that I learned how to do mouse work, western blots, and cell culture. I am immensely

grateful for the support and guidance from Ann and all the members of her lab, and it is not exaggeration to say that I would not be here today if it weren't for their support and guidance over the years.

They say it takes a village to raise a child, but it takes more than a village to grow a scientist! I would therefore like to thank all the wonderful people at Vanderbilt who have provided me opportunity to grow and learn throughout my graduate career. For valuable discussions, thoughtful feedback, and reasonable critiques, the Vanderbilt Cancer Biology Department is a wonderful group of scientists, researchers, and students who have made science a true pleasure.

I have a wonderful group of friends and family who have provided love and much needed distractions. My husband, John, has been by my side through my entire scientific career. I have a wonderful family, my Mom and Dad, and my sister Rebecca, and my in-laws, Rick and Paula. Thank you all for helping me celebrate the successes and move on from the failures.

The work in this dissertation was performed in the Department of Cancer Biology at Vanderbilt University from 2008-2014. This work was funded by the following grants: NIH RO1 CA111947 (to A.B.R.), NIH RO1 CA55724 (to A.B.R), Vanderbilt SPORE in GI Cancer project grant (to A.B.R), NRSA Predoctoral fellowship F31 CA165667-01 (to S.P.S), Vanderbilt Cancer Biology training grant (2T32CA009592-26).

TABLE OF CONTENTS

Page

LIST OF TABLES

LIST OF FIGURES

LIST OF ABBREVIATIONS

AIG	anchorage independent growth
AJ	adherens junction
APC	adenomatous polyposis coli
ARM	Armadillo repeat
BTB	bric-a-brac, tramtrack, broad-complex
BMP	bone morphogenic protein
BSA	bovine serum albumin
CBC	crypt based columnar cell
ChIP	chromatin immunoprecipitation
cKO	conditional knockout
CRC	colorectal cancer
DN	dominant negative
DNA	deoxyribonucleic acid
DSI	distal small intestine
E-cadherin	epithelial-cadherin
EGF	epidermal growth factor
eKBS	ENCODE Kaiso binding site
EMT	epithelial to mesenchymal transition

ENCODE	Encyclopedia of DNA Elements
FAP	Familial Adenomatous Polyposis
FBS	fetal bovine serum
GAP	GTPase associating/activating protein
GDP	guanosine diphosphate
GEF	guanine nucleotide exchange factor
GI	gastrointestinal
GTP	guanosine triphosphate
HGP	Human Genome Project
IF	immunofluorescence
IHC	immunohistochemistry
Ihh	Indian hedgehog
IP	intraperitineal
ISC	intestinal stem cell
JMD	juxtamembrane domain
KBS	Kaiso binding site
KD	knockdown
KO	knockout
LCM	laser capture microdissection
LOH	Loss of heterozygousity

MMP7	matrix metalloproteinase 7
mRNA	messenger RNA
MSI	middle small intestine
N-cadherin	neuronal-cadherin
NCID	Notch intra-cellular domain
NFkB	nuclear factor kappa B
OE	overexpressing
PBS	phospho-buffered saline
PCR	polymerase chain reaction
PEI	Polyethylenimine
POZ-ZF	poxvirus and zinc finger
PSI	proximal small intestine
qRT-PCR	quantitative reverse transcription PCR
RNA	ribonucleic acid
RTK	receptor tyrosine kinase
SB	Sleeping Beauty
shRNA	short hairpin RNA
TA	Transit amplifying
TAM	Tamoxifen
TCGA	The Cancer Genome Atlas

TGFβ	transforming growth factor beta
UTR	untranslated region
WT	wildtype
ZF	zinc finger

CHAPTER I

INTRODUCTION

Introduction to intestinal biology

By broadest definition, the gastrointestinal (GI) tract includes all structures between the mouth and anus, including the esophagus, stomach, and intestines (also commonly called bowel or gut). The intestine itself is divided in to two main components, the small intestine and the large intestine, which includes the colon, rectum, anus, and cecum, a pouch-like structure positioned at the junction of the large and small intestines. Together, these components form a hollow tube which carries digestive products from the stomach through the body before being expelled. Most proximal to the hollow space of the intestinal lumen is a single layer of columnar epithelial cells which serves as a barrier between the body and luminal contents, including digestive products, bile and other digestive enzymes, and the gut flora. In addition to serving as a physical barrier, this epithelial is also responsible for nutrient absorption, antigen processing, and immune regulation (reviewed in (Henderson et al, 2011)).

The small intestine is connected to the stomach by the pyloric sphincter, and is the primary site of absorption for fats, carbohydrates, and proteins. Structurally, the small intestine is divided into three segments, the duodenum, jejunum, and ileum which approximately correspond to proximal, middle, and distal segments (reviewed in (Schepers & Clevers, 2012)). While the primary function of the small intestine is to absorb nutrients, the large intestine absorbs water and salt from solid waste material before being expelled from the body. The colon makes up the bulk of the large intestine, which in humans is divided into ascending, transverse, descending, and sigmoid segments in reference to the position within the body cavity. However, the mouse does not share this complexity, and instead the mouse colon is divided only into proximal and distal segments.

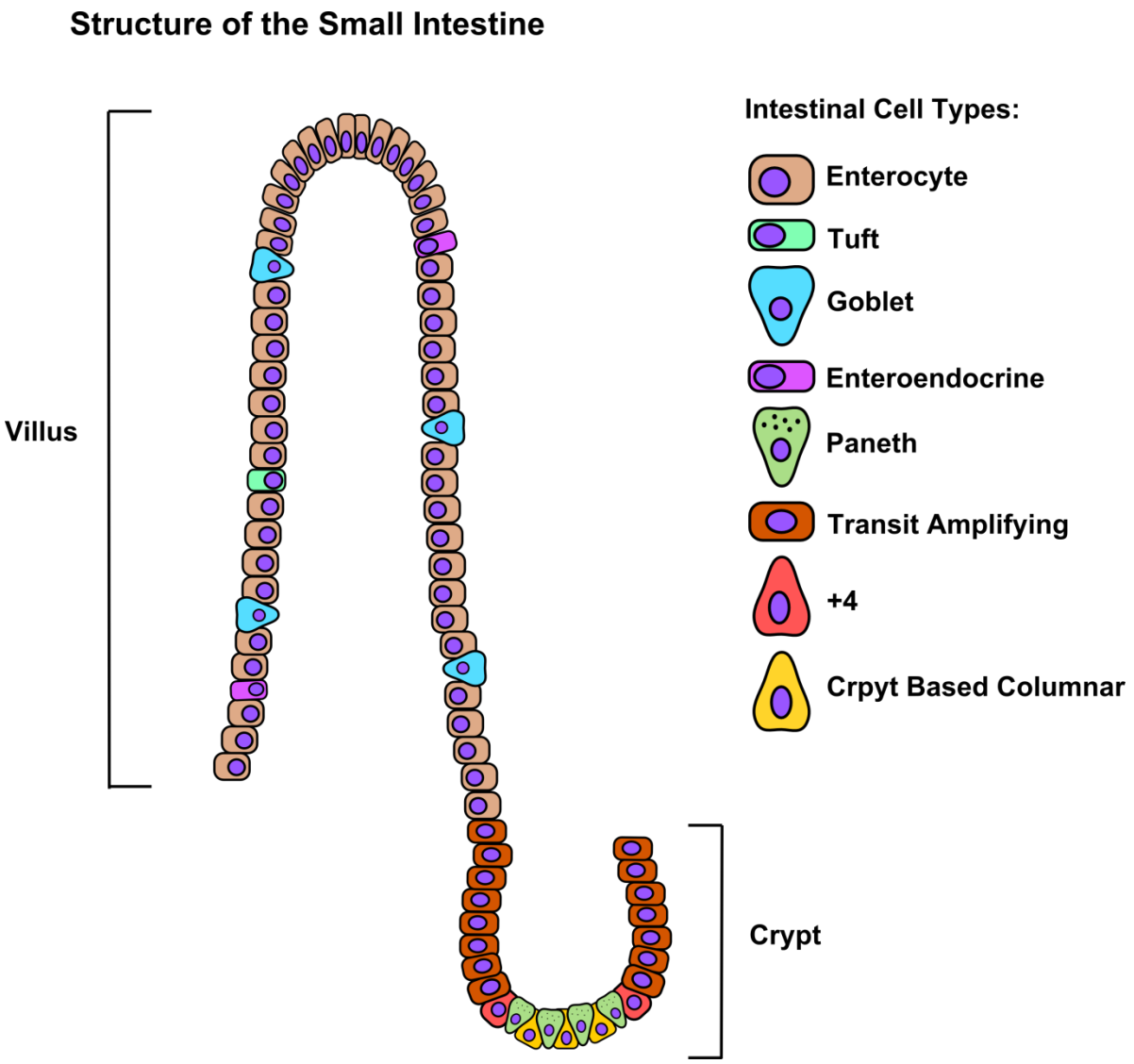

Figure 1. Schematic of the intestine and its cell types. The small intestine is divided into the villus (left) and crypt (right).The crypt houses the intestinal stem cells, including the proliferative crypt based columnar cells and the quiescent +4 population. These are directly adjacent to Paneth cells in the crypt base. Following stem cell division, daughter cells move into the region known as the transit-amplifying compartment, which is a rapidly dividing, undifferentiated population. After these rapid divisions, cells move upward onto the villus and differentiate, becoming one of two lineages: secretary or absorptive. Absorptive cells consist of enterocytes, while secretory cells include Paneth, enteroendocrine, tuft, and goblet cells.

Histologically, the intestinal epithelial layer contains two main structures, the villi and the crypts of Lieberkühn (reviewed in (Reya & Clevers, 2005; Schepers & Clevers, 2012)) (Figure 1). The crypts are glands extending down into the lamina propria, while villi are finger-like protrusions extending into the gut lumen to increase available surface area for nutrient absorption. Most villi cells also have subcellular structures called "microvilli," which are microscopic, actin-rich bundles protruding from the epithelial cells themselves. Collectively, the layer of microvilli is termed the "brush-border," and further aids absorption and mechanotransduction in the intestine (Mooseker, 1985).

The intestinal stem cell

The intestinal epithelium is a highly dynamic structure, characterized by rapid cell turnover such that the epithelium is almost entirely replaced every 3-5 days (Creamer et al, 1961; Hagemann et al, 1970). This massive amount of proliferation occurs in the intestinal crypt, and as cells age they are pushed from the crypt up the villus where they differentiate and are finally sloughed into the lumen at the villus tips (Creamer et al, 1961). Importantly, continuous proliferation is mostly maintained by a population known as "crypt-based columnar cells" (CBCs) (Barker et al, 2007; Cheng & Leblond, 1974). Originally described by Cheng and Leblond in 1974 , these slender cells were identified as the main intestinal stem cell population by the Clevers group in 2007 and designated by high expression of Lgr5, a transmembrane protein now known to be the receptor for the Wnt agonist, R-spondin (Barker et al, 2007; Cheng & Leblond, 1974; de Lau et al, 2011). Approximately 15 CBCs reside in the base of each crypt, dividing uniformly each day (Barker et al, 2007). The CBCs are intercalated between the Paneth cells, a fully differentiated cell type with major roles in host-microbe interactions due to their ability to synthesize and secrete antimicrobial peptides and proteins (reviewed in (Clevers & Bevins, 2013)). Interestingly, more recent studies have also shown Paneth cells are crucial in maintaining stem cell function through secretion of EGF, Wnt3a, and Notch ligands and even appear to determine stem cell fate (Sato et al, 2011b). As the Lgr5-expressing cells divide, the cell positioned next to the Paneth cell maintains stemness, while the daughter cells displaced away from the Paneth cell goes on to differentiate (Snippert et al, 2010). In addition to the CBC population, a second, quiescent stem cell population is postulated to reside at the "+4

position." Originally identified by label retention by Potten et al, this appears to be a somewhat heterogeneous cell population marked by expression of *Hopx*, *mTert*, *Bmi1*, and/or *Lrig1* (Montgomery et al, 2011; Potten, 1977; Powell et al, 2012; Sangiorgi & Capecchi, 2008; Takeda et al, 2011; Wong et al, 2012; Yan et al, 2012). Although generally quiescent, proliferation of +4 cells appears to be induced upon tissue injury or the loss of CBCs (reviewed in (Barker & Clevers, 2007)).

Following stem cell division, daughter cells moving away from the crypt are incorporated into a highly proliferative zone known as the transit-amplifying (TA) region. Cells in this region divide approximately every 16 hours, a rate even more frequently than the CBCs (reviewed in (Marshman et al, 2002; Schepers & Clevers, 2012)). As cells are finally forced out of the crypt and up the adjacent villi, proliferation halts and cells begin the complete the process to terminal differentiation into one of two main lineages: absorptive cells or secretory cells (reviewed in (Clevers & Batlle, 2013; Noah et al, 2011). The absorptive lineage primarily includes the enterocytes (or colonocytes in the colon), which are the most common intestinal cell type and function in nutrient absorption and transport. The secretory lineage includes the Paneth, goblet, tuft, and enteroendocrine cells (reviewed in (Clevers & Batlle, 2013; Noah et al, 2011)). Goblet cells are large, mucous-secreting cells which help protect the epithelial layer from the chemical and bacterial contents of the gut lumen. Enteroendocrine and tuft cells are much rarer, with roles in hormone secretion and chemical sensation, respectively. Importantly, the choice between the two lineages appears mostly determined by Notch signaling. Notch activation induces Hes1, which inhibits a major regulator of the secretory lineage, Atoh1 (Math1) (Shroyer et al, 2007). Thus, ectopic expression of the Notch Intracellular Domain (NCID) drastically decreases the number of secretory cells (Fre et al, 2005; Stanger et al, 2005; Zecchini et al, 2005), while Notch inhibition, such as overexpression of Atoh1, leads to a strong preference for a secretory phenotype (Shroyer et al, 2007; van Es et al, 2010; van Es et al, 2005).

The Wnt pathway in intestinal homeostasis and cancer

While Notch signaling plays a critical role in lineage specification, perhaps the signaling pathway with the most far reaching effects in the intestine is the Wnt pathway. The Wnt family of ligands is quite large, and most mammalian genomes contain 19 Wnt genes which function as close-range morphogens in a variety of tissues (reviewed in (Clevers & Nusse, 2012)). Interestingly, the Wnt1 gene was first discovered as a viral integration site for the mouse mammary tumor virus, leading to its classification as a proto-oncogene (Nusse & Varmus, 1992). Currently, Wnt receptor activation is thought to result in stimulation of one of three downstream pathways: the canonical Wnt/β-catenin cascade, the non-canonical planar cell polarity (PCP) pathway, or the Wnt/Ca2+ pathway (reviewed in (Clevers & Nusse, 2012)). The canonical Wnt pathway is the best understood, which commonly results in induction of pro-growth signaling mediated by downstream effectors such as c-Myc.

As mentioned previously, β-catenin plays a major role in AJ function, as it binds to E-cadherin and α-catenin to regulate the connection between the cadherin complex and the cytoskeleton (Rimm et al, 1995; Yamada et al, 2005) (Figure 2). Under homeostatic conditions, excess β-catenin not needed for AJ maintenance is degraded by a destruction complex consisting of the Adenomatous polyposis coli (APC) gene product, AXIN1, GSK3β, CK1α, and β-TrCP. β-catenin bound by this complex is sequentially phosphorylated, first by CK1α at Ser45, followed by GSK3β phosphorylation at Thr41, Ser37, and Ser33 (Liu et al, 2002). This final phosphorylated form is then ubiquitinated by the E3 ubiquitin ligase, β-TrCp, marking it for proteosomal degradation (Aberle et al, 1997; Kitagawa et al, 1999). However, in the presence of Wnt ligand, this destruction complex is inhibited by phosphorylation of the Wnt co-receptor LRP, which recruits the destruction complex to the membrane while simultaneously dissociating β-TrCP (Li et al, 2012b). Thus, free β-catenin is no longer degraded, which leads to its cytoplasmic accumulation and nuclear translocation. There is no clear consensus on the mechanism behind β-catenin's nuclear transport, and while it is thought to be independent of a nuclear localization sequence (NLS) and the importin machinery (Fagotto et al, 1998; Huber et al, 1996), much work remains in determining the exact mechanism governing β-catenin's translocation.

Once in the nucleus, β-catenin is able to bind transcriptional coactivators of the TCF/LEF family, specifically TCF4 (Behrens et al, 1996; Molenaar et al, 1996). Importantly, in the absence of active Wnt signaling, TCF family members act as transcriptional co-repressors though binding of Groucho/Grg/TLE proteins. Binding of β-catenin to TCF proteins relieves this repression by displacing Groucho and converting it into a transcriptional activator (Cavallo et al, 1998; Roose et al, 1998). While specific target genes vary depending on cell type and context, Wnt activation in the intestine results in transcription of numerous genes required for proliferation and stem cell function, such as *c-Myc*, CyclinD1, LGR*5*, *ASCL2*, *SOX9*, *EPHB2*, and *EPHB3* (Barker et al, 2007; Batlle et al, 2002; Blache et al, 2004; He et al, 1998; Shtutman et al, 1999; Tetsu & McCormick, 1999; van der Flier et al, 2009). Indeed, Wnt activation is believed to be the main driver of proliferation and stem cell maintenance in the crypt, in response to Wnt3a ligand secreted from either Paneth cells or nearby myofibroblasts (reviewed in (Clevers & Bevins, 2013; Medema & Vermeulen, 2011; Noah et al, 2011). Importantly, as cells move out of the crypt, increased distance from these secreted Wnt ligands halts proliferation and helps precipitate the differentiation process.

To maintain homeostasis, tight control over Wnt activation is required. Thus, other morphogens such as bone morphogenic proteins (BMPs) and Indian Hedgehog (Ihh) work to functionally oppose the Wnt pathway (reviewed in (Medema & Vermeulen, 2011)). In the intestine, BMP4 is expressed by cells of the inter-villus mesenchyme, which in turn acts on cells of the villus epithelium through paracrine signaling to augment differentiation. Ablation of BMP4 signaling in the intestine, either through ectopic overexpression of the BMP inhibitor Noggin or knockout of the BMP receptor, results in *de novo* crypt formation, increased proliferation, and higher expression of crypt-associated Wnt target genes such as *c-Myc* and *EphB3* (Haramis et al, 2004; He et al, 2004). Other studies have shown BMP activation is able to represses β-catenin/TCF4 driven transcription, and deletion of *Smad4* dramatically increases tumor formation in *Apc* mutant mice (Freeman et al, 2012). Ihh activation yields a similar effect as observed with BMP and Ihh deletion recapitulates many of the phenotypes seen upon BMP loss (Kosinski et al, 2010; van Dop et al, 2010). Interestingly, mechanistic studies have determined the effect of Ihh is likely due to aberrant BMP signaling, as Ihh stimulates expression of BMP4 in the mesenchymal cells (Kosinski et al, 2010). Thus, these pathways appear to cooperatively inhibit Wnt activation.

Because Wnt activation maintains the massive amount of proliferation needed to replenish the intestinal epithelium, it is perhaps not surprising that disruptions in Wnt activation can have drastic consequences on intestinal homeostasis. Loss of Wnt signaling, mediated by deletion of Wnt effectors (i.e. *Tcf4* or *c-Myc*) or ectopic overexpression of Wnt antagonists such as *Dkk1*, has been shown to result in complete loss of the crypt compartment and stem cell populations (Kuhnert et al, 2004; Muncan et al, 2006; Pinto et al, 2003; van de Wetering et al, 2002). Conversely, aberrant Wnt signaling through homozygous deletion of *Apc* immediately leads to increased cell proliferation and expansions of the undifferentiated cells (Sansom et al, 2004), resulting in a wide-spread "crypt-progenitor phenotype" which encompasses the entire intestinal epithelium and leads to morbidity within 5 days (Chapter 3).

Nowhere is the dramatic effect of aberrant Wnt activation as obvious as in the case of Familial Adenomatous Polyposis (FAP), a dominant hereditary polyposis resulting from the inheritance of a truncated *APC* allele (Kinzler et al, 1991; Nishisho et al, 1991). As APC serves as a scaffolding protein for the β-catenin destruction complex, its loss renders the complex non-functional and constitutively activates the Wnt signaling cascade. In the case of FAP, patients inherit one WT and one mutated *APC* allele, and tumor formation occurs when the wild type *APC* allele is lost through a process known as loss of heterozygousity (LOH) (Kinzler & Vogelstein, 1996; Oshima et al, 1995). In the case of FAP, the aberrant Wnt signaling which results from *APC* loss can lead to the formation of hundreds to thousands of adenomatous polyps, which often progress to invasive cancer. While FAP itself is quite rare, *APC* loss is widely applicable to the development of colorectal cancer (CRC). Importantly, *APC* mutations are found at the earliest stages of the adenoma-to-carcinoma progression prior to any other detectable mutations, and for many years has been thought to be the most common initiating event in human CRCs (Fearon & Vogelstein, 1990). Importantly, these early studies have been supported by recent, non-biased sequencing approaches, such as those utilized The Cancer Genome Atlas (TCGA). To-date, TCGA mutational analysis has reported *APC* mutations in an astounding 76% of patient CRC tumors, and when combined with other Wnt pathway mutations it appears that activation of the canonical Wnt cascade may be the initiating step in over 80% of human CRCs (2012).

Mouse models of CRC

Multiple mouse models have been developed to study intestinal tumorigenesis, with most mimicking the *APC* mutation found in FAP (Fodde et al, 1994; Moser et al, 1990; Oshima et al, 1995; Su et al, 1992). Thus, many of these models rely on inheritance of one truncated *Apc* allele, with tumor formation occurring when the remaining WT allele is lost. While similar in that each phenotype is mechanistically caused by *Apc* loss, differences between the models exist depending on the length of the inherited, truncated *Apc* allele. For example, mice with truncation at codon 716 display up to 300 tumors throughout the intestinal tract, while those mutated at codon 1638 only develop 3-5 tumors (Fodde et al, 1994; Oshima et al, 1995). The *ApcMin* model, whose inherited *Apc* allele is truncated at codon 850, lies in the middle, and develops approximately 100 polyps (Moser et al, 1990). Interestingly, different APC fragments vary in their ability to bind destruction complex members and inactivate β-catenin, which likely explains some variation observed in these tumor models. Indeed, β-catenin activation has been described by many as a threshold effect, and tumor formation only occurs only when critical signaling levels are reached (Albuquerque et al, 2002). As longer APC fragments still retain many of the domains necessary for β-catenin downregulation, the lower tumor number is likely due to mutant cells being less able to surpass the necessary threshold for transformation. However, it is interesting that ~200 tumors are found in mice lacking *Apc* completely, less that the number commonly found in the *ApcΔ716* model (Cheung et al, 2010). Thus, the ability of APC to degrade β-catenin may not be the only contributing factor to the differences observed in these model systems.

While mouse models of human CRC have proved invaluable in the experimental setting, it is also worth noting the major differences that exist between human CRC and the mouse tumor models. For one, the length of the truncations commonly used in mouse tumor models are much shorter that those observed in human tumors, although the *Apc1638* model is a notable exception that is relatively similar to human tumors in this respect (Rowan et al, 2000). Secondly, the tumors derived in mouse models are overwhelmingly adenomatous in nature, and while localized invasion can be seen in some models, metastasis is quite rare (Fodde et al, 1994; Moser et al, 1990; Oshima et al, 1995). Thus, while most human deaths are attributed to complications from distant metastases, mouse morbidity is generally due to GI

occlusion and/or chronic anemia due to high numbers of intestinal tumors. Finally, tumors in *Apc*-driven mouse models occur predominantly in the small intestine and not the colon, which is the primary site of involvement in human cancer. The mechanism behind this localization change is not yet known, and while mouse models have influenced much of what we know about intestinal biology, one must consider the possibility of unknown differences in the mouse and human intestine that may influence homeostasis and tumor development.

General Introduction to p120 and its cellular functions

p120-catenin (p120) was originally discovered as a substrate for tyrosine phosphorylation in Src-transformed fibroblasts (Reynolds et al, 1989). It was subsequently designated a catenin due to its interactions with cadherins (Daniel & Reynolds, 1995; Reynolds et al, 1994; Shibamoto et al, 1995), a large family of proteins that mediate cell-cell adhesion through homophilic interactions between adjacent cells. As cell-cell adhesion is perhaps a defining characteristic of multicellular organisms (Carnahan et al, 2010), cadherins are involved in a diverse range of basic cellular activities, including but not limited to tissue homeostasis, morphogenesis, and cancer (reviewed in (Gumbiner, 2005; Takeichi, 1995; Yap, 1998)).

p120 is the prototypical member of a family of armadillo-repeat proteins that includes δ-catenin (δ-catenin), ARVCF, p0071, and plakophilins (Anastasiadis & Reynolds, 2000). Importantly, p120 lacks enzymatic activity and instead functions primarily as a scaffolding protein (Figure 2). Perhaps its best known role in this regard is its role at the plasma membrane, where it binds to E-cadherin and stabilizes not only E-cadherin, but the entire cadherin complex. p120 is also known to modulate actin cytoskeleton dynamics by regulation of RhoGTPases, and may mediate transcriptional response through interactions with Kaiso (reviewed in (Anastasiadis, 2007; Daniel, 2007; van Roy & McCrea, 2005)).

p120 in cadherin stability

The classical cadherins (notably E-, N-, and VE-cadherin) are a large protein family of 20 known members, yet each is reliant on p120 for stabilization (Hulpiau & van Roy, 2009). p120 binds to the catenin juxtamembrane domain (JMD) through its first 5 armadillo repeats (Ireton et al, 2002; Thoreson et al, 2000), and lack of any one of p120's arm domains results in destabilized cadherins and reduced cell-cell adhesion. Re-expression of full-length p120 in these experiments doubles E-cadherin protein half-life with no concurrent change in mRNA levels, indicating p120 controls cadherin levels through protein stabilization (Ireton et al, 2002). Mechanistically, this is likely due to p120 masking a dileucine motif on E-cadherin necessary for clatherin-dependent endocytosis (Miyashita & Ozawa, 2007; Xiao et al, 2005).

The p120-bound cadherin normally exists in a complex at the plasma membrane along with α- and β-catenins (α-catenin, β-catenin) (Figure 2). Along with p120, these proteins bind the cadherin C-terminal tail where they physically and/or functionally link the cadherin to the actin cytoskeleton (Rimm et al, 1995; Yamada et al, 2005). Together, this structure is commonly referred to as the "cadherin complex," and is a crucial component of a cell-cell junction type known as the adherens junction (AJ). Importantly, in the event of p120 loss the entire complex is internalized and degraded, which culminates in decreased protein levels of E-cadherin, α-catenin, and β-catenin (Davis et al, 2003). This phenomenon is highly consistent across both *in vitro* and *in vivo* systems, as most tissues in which p120 is experimentally ablated demonstrate significant reductions in cadherin complex proteins (Bartlett et al, 2010; Davis et al, 2003; Davis & Reynolds, 2006; Elia et al, 2006; Marciano et al, 2011; Oas et al, 2010; Perez-Moreno et al, 2006; Smalley-Freed et al, 2010; Smalley-Freed et al, 2011; Stairs et al, 2011). Indeed, the majority of p120 ablation phenotypes appear due to disrupted cell-cell adhesion induced by loss of the adherens junction and cadherin complex proteins.

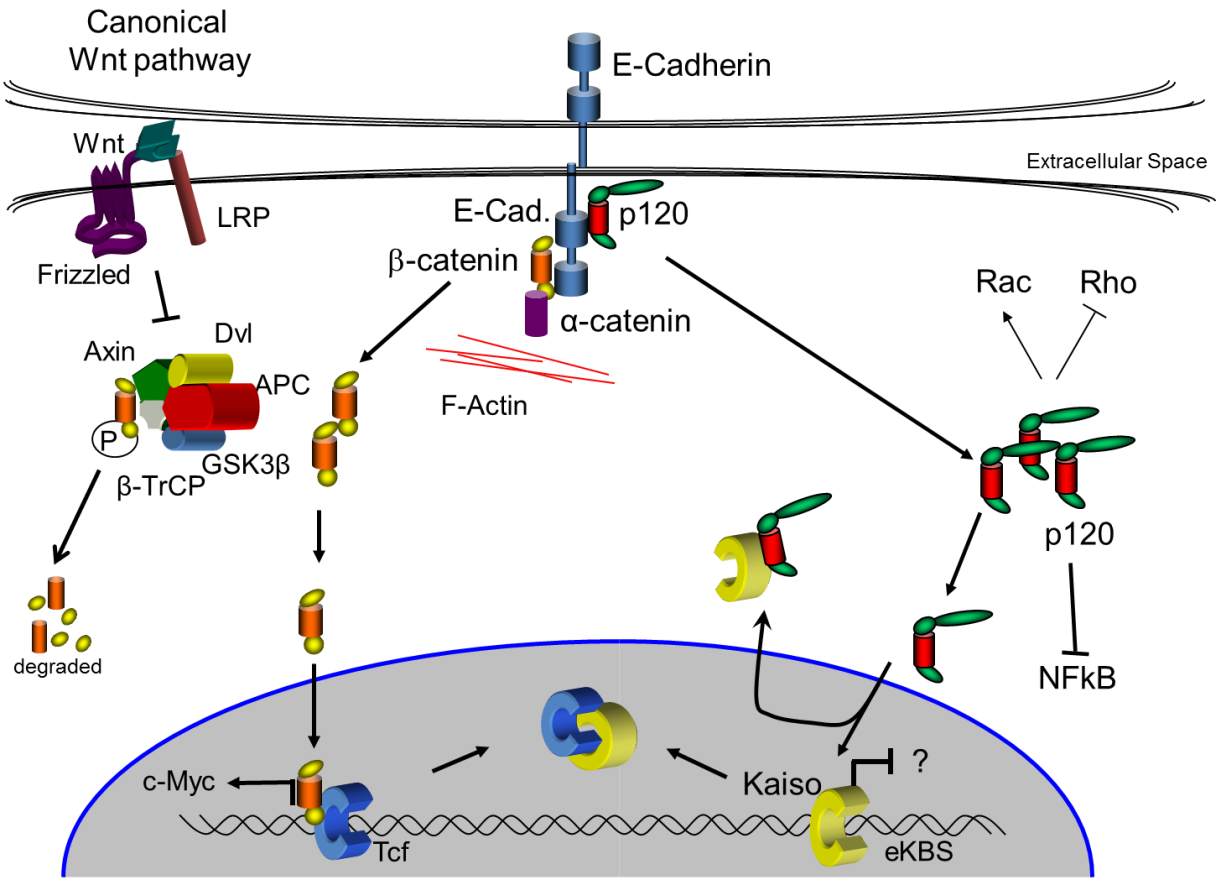

Figure 2. Roles for p120 and the canonical Wnt pathway. p120 binds classical cadherins and stabilizes the cadherin complex at the membrane. p120 also interacts with Rac and Rho GTPases, and is known to inhibit NFκB. p120 binds to a nuclear partner, Kaiso, and is thought to inhibit Kaiso-mediated repression by physical sequestration. Multiple components of p120 signaling interact with the canonical Wnt pathway (left), including β-catenin and Kaiso.

Activity modulation of Rho family GTPases by p120

In addition to roles in cadherin stability, p120 has also been implicated in control of Rho family small GTPases, such as RhoA and Rac (reviewed in (Anastasiadis, 2007)). GTPases function as binary switches, controlling important cellular processes such as adhesion and motility. Functionally, these proteins are controlled by binding to GTP or GDP, resulting in activation or inactivation, respectively (reviewed in (Jaffe & Hall, 2005)).

Over the years, p120 has been shown to modulate RhoA activity through a variety of non-mutually exclusive mechanisms. Phenotypically, RhoA activation often results in decreased migration and cell rounding due to increased cellular tension, while inhibition results in cell branching and increased formation of lamellapodia (reviewed in (Jaffe & Hall, 2005)). Interestingly, the opposite is seen with p120 overexpression in NIH-3T3 fibroblasts, which results in striking and widespread cell branching due to p120-mediated RhoA inhibition (Anastasiadis et al, 2000). Subsequent studies have shown p120 is able to bind directly to RhoA through the phosphorylated tyrosine 112 residue and/or amino acids 622-628 (Castano et al, 2007; Yanagisawa et al, 2008), and suggests a model in which p120 is responsible for maintaining RhoA in an inactive, GDP-bound state. Alternatively, p120 is modulate RhoA activity by binding p190 Rho GTPase activating protein (GAP), recruiting it to the cadherin complex to mediate local Rho inhibition (Wildenberg et al, 2006), or by binding to RhoA's downstream effector, ROCK1 (Smith et al, 2012; Smith et al, 2011). As p120 has been clearly shown to inhibit RhoA *in vivo*, together these studies suggest extensive crosstalk between RhoA and p120 in a variety of systems (Perez-Moreno et al, 2006).

On the other hand, p120 has been shown to activate another Rho family member, Rac1 (Goodwin et al, 2003; Johnson et al, 2010; Noren et al, 2000; Soto et al, 2008; Yanagisawa & Anastasiadis, 2006). In MBA-MD-231 and Neu-transformed MCF10A cells, p120 activates Rac1 to promote cell growth and invasion, although these results were not consistent in all cell lines tested (i.e. MCF7) (Johnson et al, 2010; Soto et al, 2008). Furthermore, p120 KD completely inhibits MDCK cell transformation by oncogenic Rac (Dohn et al, 2009). Interestingly, Rac and Rho signaling are often interdependent, thus p120 may not only be important the control of each individually, but likely plays a critical role in cross-talk between the two pathways. For example, Rac inhibits Rho through the well-characterized Bar-Sagi pathway (Nimnual et al,

2003), and this inhibition is dependent on both p120 and p190RhoGAP (Wildenberg et al, 2006). Thus, p120 may function as an important nexus which allows signal integration from both Rac1 and RhoA pathways.

p120 isoforms and EMT

p120 displays an amazing amount of complexity at the mRNA level. In mammals, this complexity stems in part from four alternative translational start sites and three alternatively spliced exons (i.e. A, B, and C), which yields a staggering 32 different isoforms (Keirsebilck et al, 1998; Mo & Reynolds, 1996). However, while multiple isoforms of p120 are expressed in cancer cell lines and tumor samples (Sarrio et al, 2004), a simplified approach focuses on just two main isoforms, termed 1A and 3A. Isoform 1A is the predominant p120 isoform in mesenchymal cells (e.g. fibroblasts), and includes the full length p120 protein with the N-terminal coiled-coiled domain. In epithelial cells, isoform 3A is primarily expressed (Mo & Reynolds, 1996), where the coiled-coiled domain and part of the N-terminal regulatory domain are removed by the use of a downstream translational start site (reviewed in (Reynolds & Roczniak-Ferguson, 2004)).

Evidence for distinct roles of the p120 isoforms is emerging. The difference in isoform expression patterns may be due in part to differences in cadherin expression, as isoform 1 shows a distinct preference for N-cadherin, the primary cadherin of mesenchymal cells, while isoform 3 more readily associates with the epithelial E-cadherin (Seidel et al, 2004). Importantly, differential expression of p120 isoforms appears to have major consequences on cell adhesion and migration (reviewed in (Pieters et al, 2012)), and is often associated with a phenomenon known as epithelial-to-mesenchymal transition (EMT) in which epithelial cells adopt a more migratory and invasive phenotype (reviewed in (Kalluri & Weinberg, 2009)). Cells undergoing EMT lose expression of E-cadherin, which helps maintain cell-cell contacts, cell polarity, and tissue integrity, and instead acquire expression of N-cadherin and other mesenchymal markers such as vimentin. These changes are often associated with increased migration and tumor cell invasion, thus EMT is thought to be a common phenomenon in tumor progression and metastasis. Interestingly, the E- to N-

cadherin switch induced by EMT is concurrent with a switch in p120 isoforms, going from predominant expression of 3A in epithelial cells to isoform 1A (Sarrio et al, 2004; Slorach et al, 2011). Indeed, p120 isoform 1 has been shown to increase cell migration and invasion in numerous cell culture systems (Slorach et al, 2011; Yanagisawa et al, 2008). Importantly, due to its role in EMT and E-cadherin regulation, p120 is often assumed to be an important player in late-stage tumor progression and the transition to metastasis.

An introduction to Kaiso

Kaiso (ZBTB33), a member of the BTB/POZ-ZF (broadcomplex, tramtrack, bric-a-brac/poxvirus and zinc finger) subfamily of transcription factors, was originally identified through a yeast two-hybrid screen as a p120 binding partner (Daniel & Reynolds, 1999). The interaction appears to involve the first 7 ARM repeats of p120 and all three ZF domains of Kaiso, although other binding elements are apparently required as Kaiso is unable to bind p120 isoform 1 (Daniel & Reynolds, 1999; Zhang et al, 2011). Because Kaiso requires all three zinc fingers for both high affinity DNA binding and interaction with p120, p120 has long been thought to inhibit Kaiso's transcriptional roles (Buck-Koehntop et al, 2012a; Buck-Koehntop et al, 2012b). Numerous studies have shown p120 does indeed mediate Kaiso-induced transcriptional changes, either by competitive binding or by inhibiting Kaiso through cytoplasmic sequestration (Kelly et al, 2004; Kim et al, 2004; Park et al, 2006; Spring et al, 2005). Interestingly, Kaiso has also been reported to bind the p120 family member, δ-catenin, and this interaction appears particularly important to neural development (Rodova et al, 2004).

Kaiso appears to have dual DNA specificity, and has been shown to bind DNA via a non-methylated consensus Kaiso binding site (KBS, TCCTGCNA), as well as methylated CpGs, possibly in a sequence-specific manner (Buck-Koehntop et al, 2012b; Daniel et al, 2002; Prokhortchouk et al, 2001; Ruzov et al, 2004; Sasai et al, 2010b). Interestingly, Kaiso's ability to bind methylated CGCGs is unique among its family members, as ZBTB4 and ZBTB38 are only able bind a single methylated CpG (Filion et al, 2006). In line with methyl binding, Kaiso is overwhelming thought to functional as a transcriptional repressor and has been shown to inhibit target genes such as *MMP7* (matrilysin), *CCND1* (CyclinD1),

WNT11, *CDKN2A* (p16), and *BCL6* though both KBS and CpG-mediated mechanisms (Daniel et al, 2002; Donaldson et al, 2012; Kim et al, 2004; Koh et al, 2013; Lopes et al, 2008). Kaiso is also known to form repressive protein complexes with N-CoR, HDAC1, and MTG16 (Barrett et al, 2012; Iioka et al, 2009; Yoon et al, 2003). Importantly, because only a limited number of methy-CpG-binding proteins exist, Kaiso has been suggested to be a major player in chromatin organization, genome stability, and epigenome maintenance (reviewed in (Defossez & Stancheva, 2011; Fournier et al, 2012)).

Interestingly, recent advances have called much of the above data into question. Kaiso was recently subject to a non-biased chromatin immunoprecipitation-sequencing (ChIP-seq) screen by an independent laboratory as part of the Human Genome Project (HGP), and subsequent analysis of Kaiso binding peaks in this study revealed surprising results. Strikingly, Kaiso was found at any of the previously reported target genes, and the full KBS sequence was only present in 5 of the 405 Kaiso-bound promoters analyzed (Chapter 4). Instead, these results identified a preference for a previously orphaned motif, the M8 motif, which is a common and well-conserved binding element in mammalian genomes (Raghav et al, 2012). This new binding site (eKBS) contains a central CGCG, and methylation at these sites appears to increase Kaiso's affinity in a manner consistent with earlier studies (Raghav et al, 2012). However, analysis of the Kaiso ChIP-seq data in conjunction with DNA methylation databases has found that Kaiso-bound promoters are largely unmethylated, suggesting Kaiso may instead contribute to promoter activation (Blattler et al, 2013). Indeed, eKBS genes are some of the most frequently transcribed, with roles in housekeeping, ribosomal assembly, and translation (Wyrwicz et al, 2007; Yamashita et al, 2007). Furthermore, mutation of the eKBS sequence has been shown to decreases transcription of promoters such as HNRNPK and FBN1 (Guo et al, 2008; Mikula et al, 2010). However, Kaiso-dependent changes in eKBS-driven transcripts have yet to be reported, nor have these results been recapitulated in *in vivo* systems.

p120 ablation in model organisms

p120 ablation studies *in vitro* invariably yield striking changes in cell-cell adhesion. Therefore, more recent studies have looked to characterize the effects of p120 ablation *in vivo* across a variety of tissue and organ systems. Interestingly, attempts at global p120 KO in mice, zebrafish, and *Xenopus* have shown p120 expression to be an absolute requirement for vertebrate development (Carnahan et al, 2010). To sidestep issues with early lethality, later studies have relied on use of inducible mouse models to control tissue and temporal specificity of p120 KO. Two models of p120 floxed alleles were concurrently developed, the first of which introduced loxP sites flanking all four transcriptional start sites (Davis & Reynolds, 2006). The second model floxes exon 7, corresponding to parts of ARM repeats 1, 2, and 3, which results in a frameshift mutation and mRNA degradation (Elia et al, 2006). Importantly, both models are able to generate complete p120 loss and have been extensively characterized in a variety of tissues.

Although effects vary widely depending on the organ system and context, phenotypes associated with tissue-specific p120 ablation are often severe (Table 1). Phenotypes are mostly attributed to p120-dependent changes in cadherin levels, resulting in defects in adhesion, migration, and cell polarity. For example, p120 KO targeted to the salivary gland results in perinatal death, due to complete failure to form acinar structures. This model also demonstrated deformed ducts and an epithelial phenotype which resembled intraepithelial neoplasia (Davis & Reynolds, 2006). Likewise, the developing mammary gland doesn't form at all in the absence of p120, and while limited ablation allows formation of a mammary ductal tree, p120 null cells are lost due to inability to participate in collective cell migration (Kurley et al, 2012). p120-ablated kidneys are unable to develop tubules and over time develop hyperplastic kidney cysts (Marciano et al, 2011). Importantly, the requirement for p120 is not just limited to ductal epithelial cells. Targeting p120 ablation to the vasculature results in embryonic lethality and hemorrhaging, and mice with p120 loss in the enamel-producing ameloblasts exhibit considerable wasting and tooth erosion (Bartlett et al, 2010; Oas et al, 2010). Thus, the absence of p120 leads to cell-cell adhesion defects and disruption of tissue homeostasis across almost all tissues reported to-date. A notable exception to the severity of p120 ablation is in the adult prostate gland, which has no discernable phenotype despite extensive p120 ablation.

Tissue	Phenotype	Citation
Global null	Embryonic lethal	Unpublished
Salivary gland	Blocked acinar development, malformed ducts, intraepithelial neoplasia	Davis et al., 2006
Skin	Chronic inflammation, hyperplasia, no barrier defect	Perez-Moreno et al., 2006, 2008
Dorsal Forebrain	Reduced spine density and synapse formation	Elia et al., 2006
Schwann cells	Reduced myelination, lack of Schmidt-Lanterman incisures	Perrin-Tricaud et al., 2007
GI tract	Terminal bleeding, inflammation, neutrophil recruitment, adenoma formation	Smalley-Freed et al., 2010, 2011
Teeth	Ameloblast detachment, reduced enamel, sinusoid formation	Bartlett et al., 2010
Vasculature	Lethal e11.5, angiogenic remodeling defects, hemorrhaging	Oas et al., 2010
Esophagus	Inflammation, invasive squamous cell carcinoma	Stairs et al., 2011
Kidney	Hypoplastic cystic kidney, disrupted glomerulogenesis	Marciano et al., 2011
Cochlea	Convergent extension defects, defects in planar cell polarity	Chacon-Heszele et al., 2012
Mammary gland	Delayed pubertal development, disrupted terminal end buds, decreased collective migration	Kurley et al., 2012
Prostate	No phenotype in aged animal	ABR unpublished

Table 1. The effect of p120 ablation in mouse models

In addition to cadherin- and Rho-mediated phenotypes, p120 loss also induces striking inflammatory responses in some systems. p120 KO in the skin, a stratified epithelium, results in little change to cell-cell adhesion and barrier function is still maintained (Perez-Moreno et al, 2006). However, aged mice show epidermal hyperplasia and chronic inflammation, a phenotype attributed to cell-autonomous inactivation of NFκB and pro-inflammatory signaling. Inflammation also drives a striking phenotype in the oral cavity and esophagus, where p120 null cells secrete a host of inflammatory factors and chemoattactants (e.g. TNFα and M-CSF), which leads to extensive immune cell infiltration and activation (Stairs et al, 2011). Long term, this highly reactive microenvironment induces severe dysplasia and invasive squamous cancer, and was one of the first studies to show a tumor suppressor role for p120 *in vivo*. However, it is currently unclear in these instances whether p120-mediated cell-cell adhesion contributed materially to tumor development.

The effect of p120 ablation in the intestine

Previous work in our lab has focused on detailing the effects of p120 loss in the intestinal epithelium. Using a constitutively active *Villin-Cre* driver, we induced widespread p120 ablation in the intestine beginning at embryonic day 9.5 (Smalley-Freed et al, 2010). These mice were born; however, p120 ablation in 50% or more of the intestinal epithelium led to adhesive defects, massive inflammation, and intestinal bleeding that was lethal in all mice by 21 days of age. We then constructed a second-generation model using a tamoxifen-inducible *Villin-CreER* to enable limited p120 KO and long-term experiments (Smalley-Freed et al, 2011). A tamoxifen regime inducing p120 KO in ~10% of the intestinal epithelium turned out to be well tolerated, and resulting colonies of p120 null cells were at little or no disadvantage and persisted for the life of the animal. Surprisingly, this limited p120 ablation resulted in tumor formation in 45% of the animals, albeit at relatively long latencies of 12 – 18 months. Interestingly, the p120-null cells themselves were not found in the tumors, and tumor formation was attributed to long-term chronic inflammation due to defects in intestinal barrier function and recruitment of Cox2 (+) neutrophils by adjacent p120-null cells. Importantly, inflammatory diseases such as Crohn's colitis and ulcerative colitis are a well-known risk factor for development of human CRC (reviewed in (Peterson &

Artis, 2014)), thus these studies suggest a widely-applicable tumor suppressive role for p120 in the development of intestinal cancers.

p120's *in vitro* effect on cadherin levels have been recapitulated in all tissues examined to date. Classical cadherin levels (namely E-cadherin) drop by approximately 50% following p120 ablation in the GI tract, epidermis, and salivary gland, while ablation in the mammary gland and prostate reduces cadherins to almost undetectable levels (Davis & Reynolds, 2006; Kurley et al, 2012; Perez-Moreno et al, 2006; Smalley-Freed et al, 2010; Smalley-Freed et al, 2011). Importantly, this consequence is strictly limited to cadherins and the AJ. While many model systems have reported changes in barrier function, a role primarily associated with tight junctions, p120 ablation has to-date shown no effect on the formation of tight junctions or expression of their primary proteins (Dohn et al, 2009; Smalley-Freed et al, 2010). Likewise unaffected are desmosomes and desmosomal proteins, suggesting that consequences of p120 ablation are solely due to changes in cadherin and AJ function (Dohn et al, 2009).

Cadherin and catenin function in the intestine

As suggested by the above studies analyzing the effects of p120 KO in the intestine, proper cadherin function plays an important role in intestinal homeostasis. Early studies in which a dominant-negative (DN) cadherin was expressed in the intestinal epithelium resulted in widespread, Crohn's disease-like inflammation and adenoma development, pointing to the necessity of functional cadherins in maintaining barrier function and homeostasis in the intestinal epithelium (Hermiston & Gordon, 1995). Interestingly, the mechanism behind the DN-cadherin appears to be through p120 itself, as p120 is able to bind the cytoplasmic domain of the truncated cadherin, which sequesters and prevents p120 from binding and stabilizing endogenous cadherins (Xiao et al, 2003). Thus, it was perhaps not surprising that p120 KO in the intestine also induced a barrier defect and inflammatory consequences much as those seen with the DN-cadherin model (Smalley-Freed et al, 2010).

E-cadherin is the predominant cadherin in the intestinal epithelium and is highly expressed in both crypt and villus units (Dogan et al, 1995). However, studies have reported a slight decrease in E-cadherin expression in the crypt, particularly in the lower 1/3 which houses the intestinal stem cells (Escaffit et al, 2005; Tan et al, 2013). Interestingly, while subtle, this expression change may have important biological consequences for crypt homeostasis. Cells in the crypt are quite mobile, and E-cadherin may be decreased to support the cell rearrangements necessary with intestinal stem cell (ISC) and TA cell proliferation and/or crypt budding (Tan et al, 2013). Crypt cells, particularly the ISCs and Paneth cells, are also excluded from the collective migration responsible for moving differentiated cells up to the villus (as are the TA cells until they finish their proliferative programs). Importantly, cadherin expression has been shown to be required for collective migration in a variety of scenarios (reviewed in (Friedl, 2004; Friedl et al, 2004; Theveneau & Mayor, 2012)). Therefore, lower expression of E-cadherin may help maintain compartmentalization of the intestinal crypt, and higher E-cadherin expression acquired upon differentiation helps join cells to the intestinal "conveyor belt" to move up the villus.

Like p120, proper E-cadherin function is vital for intestinal homeostasis. Widespread E-cadherin KO induces striking defects in cell-cell adhesion, culminating in increased cell shedding, apoptosis, and bloody diarrhea which leads to death of the animal within 6 days (Schneider et al, 2010). Cell positioning and cell differentiation were also severely impaired, particularly in cells of the secretory lineages. Furthermore, loss of E-cadherin increases cell proliferation and expands the proliferative zone, thus taken together E-cadherin loss appears to affect migration, differentiation, and proliferation. Conversely, studies which overexpress E-cadherin report decreased proliferation and migration along the crypt villus axis (Hermiston et al, 1996). While decreased proliferation itself can impair migration, both phenotypes were separately caused by the ectopic E-cadherin. Indeed, restricting overexpression only to the villus recapitulated the defect in migration, while alleviating the proliferation phenotype observed in the crypt. Collectively, these data point to a major regulatory role for E-cadherin in various aspects of intestinal epithelial cell function and homeostasis.

Interestingly, the presence of a classical cadherin alone is insufficient to rescue many defects observed with E-cadherin alteration. Studies which express N-cadherin through the E-cadherin promoter report that, while these mice are born normally (suggesting that N-cadherin can structurally substitute for E-cadherin in development and morphogenesis), there were dramatic changes in the intestinal epithelium which grew more pronounced as the mice aged (Libusova et al, 2010). N-cadherin expressing mice show increased cell proliferation, expansion of the proliferative zone, morphological defects, and polyp formation, and together these alterations result in death of the mutant mice within ~2-3 weeks. However, while both are members of the classical cadherin family, the differences between N-cadherin and E-cadherin are quite extensive. Thus, the differences in biological function (e.g. EMT) may account for some of the dramatic results these authors report, and this study has not yet been duplicated with a member of the cadherin family more similar to E-cadherin, such as P-cadherin. However, taken together, these studies illustrate that proper E-cadherin expression and function are both required to maintain intestinal homeostasis, and cadherin alteration may affect the intestinal epithelium in a manner more complex than solely regulating cell-cell adhesion.

The role of α-catenin *in vivo* is not as well characterized as many of its AJ binding members, particularly in the intestine. However, in line with *in vitro* studies, the effects of α-catenin knockout appear to be both cadherin- and non-cadherin-specific. Loss of α-catenin function blocks mouse embryonic development at the blastocyst stage, much like targeted loss of E-cadherin (Torres et al, 1997). Furthermore, α-catenin knockout in neural precursors or skin reduces adhesion and results in cell polarity defects, as would be expected with AJ and cadherin complex loss (Lien et al, 2006; Vasioukhin et al, 2001). However, the adhesive defect observed with skin-specific α-catenin knockout is actually more severe than that seen with loss of E-cadherin, as is the hyperproliferation phenotype (Vasioukhin et al, 2001). While this discrepancy could be due to family member compensation for E-cadherin (i.e. P-cadherin), α-catenin appears to more directly mediate other cellular roles, such as contact inhibition. Indeed, α-catenin-dependent control of YAP1 is thought to be a major contributor to its phenotype in the skin (Schlegelmilch et al, 2011; Silvis et al, 2011). However, much work still remains to be done in determining the exact role of α-catenin *in vivo*, especially in other organ and tissue systems.

Cadherin and catenins in CRC

Due to their well-described roles in EMT and cell migration, cadherin complex proteins have been a frequent subject of IHC-based pathology studies in an attempt to define them as prognostic markers. While the prognostic value of these proteins is still a topic of debate, various studies report decreased immunoreactivity and/or mislocalization of p120 in CRC samples (Bellovin et al, 2005; Bondi et al, 2006; Gold et al, 1998; Karatzas et al, 1999; Skoudy et al, 1996). Indeed, altered p120 status was reported in some studies in as many as 86% of samples, and was often found to correlate with increased tumor progression, decreased 5- and 10-year survivals, and/or increased lymph node metastasis (Bellovin et al, 2005; Gold et al, 1998). However, complete loss of p120 protein was fairly rare, and tumors with regional loss were often much more advanced than those showing only downregulation or mislocalization (Gold et al, 1998). Consistent with p120-dependent regulation, changes in E-cadherin levels were often seen in tumors with altered p120 (Bellovin et al, 2005; Bondi et al, 2006; Skoudy et al, 1996). Interestingly, alterations in E-cadherin and p120 have also been reported in non-cancerous intestinal polyps, including one study which found decreased p120 staining in 20/20 hyperplastic polyps (Valizadeh et al, 1997). Thus, while commonly associated with events late in tumor progression, these studies raise the possibility that p120 and cadherin complex proteins may contribute to tumorigenesis much earlier than previously thought.

In line with a role in early tumorigenesis, both E-cadherin and α-catenin have been shown to mediate formation of intestinal adenomas in *Apc*-dependent mouse models. A study by Smits et al. demonstrated that loss of one E-cadherin allele increased tumor formation 10-fold in the *Apc1638* model, with no change in tumor progression or invasion (Smits et al, 2000). While striking, the mechanism of this increase is unknown and appears to be independent of E-cadherin's conventional roles in invasion and EMT. Interestingly, this study only included analysis of heterozygous animals and included no homozygous cohort. This may be because long-term E-cadherin loss is poorly tolerated and therefore not conducive to tumor studies (Schneider et al, 2010). Another possibility, however, is that complete loss of E-cadherin is specifically not tolerated within the intestinal adenomas, as we see with p120 (Chapter 3). Indeed, a tumor suppressive mutation identified by the Noda group was determined to be a loss of function in α-catenin (Shibata et al, 2007). As α-catenin loss in the skin leads to hyperproliferation and tumor

formation, it was surprising to find that in the intestine, α-catenin actually appears to be necessary for tumor development. Collectively, these studies point to a role for cadherins and catenins in early intestinal tumorigenesis and suggest a more complex function not restricted to late stage progression and metastasis.

Opportunities for cadherin involvement in early tumorigenesis

β-catenin is an essential molecule for both cell-cell adhesion and induction of the canonical Wnt cascade, thus it is perhaps not surprising that the cadherin complex itself is thought to have roles in Wnt activation and CRC. Because both cadherins and Wnt signaling appear to rely on the same pool of β-catenin, it has long been thought that disruption of the E-cadherin complex releases β-catenin from its role at the plasma membrane and increases the cytoplasmic pool available for Wnt signal transduction. This is supported by cadherin overexpression studies in *Xenopus* and drosophila, which recapitulate phenotypes observed with Wnt inhibition (Fagotto et al, 1996; Heasman et al, 1994). Likewise, cadherin overexpression in CRC cell lines triggers membrane recruitment of β-catenin and decreased expression of Wnt/TCF target genes (Gottardi et al, 2001; Sadot et al, 1998; Shtutman et al, 1999), while E-cadherin KD is able to augment Wnt activation (Kuphal & Behrens, 2006). Indeed, increases in Wnt activation are consist even across multiple mechanisms of cadherin removal and/or inhibition, including cadherin cleavage (Maretzky et al, 2005; Reiss et al, 2005) and GFR-induced cadherin internalization (Morali et al, 2001). However, it is also important to note that cadherin loss alone is not sufficient to activate the Wnt cascade, particularly in cells with a functional β-catenin destruction complex (Herzig et al, 2007; Kuphal & Behrens, 2006). Taken together, these studies reveal an important functional contribution for the cadherin complex in Wnt regulation. Furthermore p120, as a major regulator of cadherin function and stability, may be an important mediator of Wnt and early CRC development.

p120 may also influence Wnt signaling through its interaction with its nuclear binding partner, Kaiso. Kaiso has been shown to influence Wnt activation in a variety of model systems by interfering with TCF binding (to either β-catenin or DNA) and by direct repression of canonical Wnt targets such as *c-Myc* and *CyclinD1* (Donaldson et al, 2012; Kim et al, 2004; Park et al, 2005; Ruzov et al, 2009; Spring et al, 2005). Importantly, cytoplasmic p120 is known to alleviate Kaiso-mediated Wnt repression by sequestering Kaiso from the nucleus, which may be necessary for Wnt signal transduction (Kelly et al, 2004; Spring et al, 2005). Thus, disruption of the cadherin complex may augment Wnt signaling in a two-pronged approach, simultaneously releasing both β-catenin and p120 from the membrane to potentiate Wnt activation. However, while reported in cell culture and *Xenopus* systems, Kaiso-mediated changes in Wnt signaling have yet to be recapitulated in live mammalian systems. Instead, studies of Kaiso null mice report delayed tumor formation and increased survival in the *ApcMin* model. Conversely, Kaiso overexpression in the intestine leads to an increased progenitor zone, although the effects on proliferation in this model are not well understood (Chaudhary et al, 2013; Prokhortchouk et al, 2006). Furthermore, increased Kaiso expression (both cytoplasmic and nuclear) has been reported in infiltrating ductal carcinomas and triple negative carcinomas of the breast, as well as non-small cell lung cancer and prostate cancer, and this increase often correlated with increased aggressiveness and/or worse prognosis. (Dai et al, 2009; Jones et al, 2014; Jones et al, 2012; Vermeulen et al, 2012). Thus overall, Kaiso appears to have a positive role in multiple tumor types, contributing to growth and aggressiveness though yet unknown mechanisms.

While roles in Wnt activation are perhaps the best studied possibility, the cadherin complex is extensively coupled to other signaling pathways which may influence intestinal tumorigenesis, such as receptor tyrosine kinase (RTK) signaling. Colocalization of cadherin and RTKs has been frequently reported, although the functional consequences are not always the same (Crepaldi et al, 1994; Hoschuetzky et al, 1994; Pece & Gutkind, 2000). While in some cases cadherin involvement can result in RTK activation and protumorigenic signaling (Cheung et al, 2011; Pece & Gutkind, 2000), more frequently cadherins appear to shut down ligand-dependent RTK activation (Laprise et al, 2004; Qian et al, 2004; Takahashi & Suzuki, 1996). Thus, cadherin/RTK crosstalk may constitute a major tumor suppressive role *in vivo*, and activation of RTKs, such as the epidermal growth factor receptor (EGFR) or its family member ERBB3, has been shown necessary for tumor establishment in the *ApcMin* model (Lee et al, 2009; Roberts

et al, 2002). Taken together RTK activation may provide another mechanistic outlet for cadherin involvement in intestinal tumorigenesis.

Interestingly, cadherin-mediated changes in RTK activation were often density dependent, and over the years adhesion proteins have been identified as effectors of a phenomenon known as contact inhibition of cell growth. Extensively studied *in vitro*, contact inhibition induces a change from proliferation to quiescence upon monolayer formation, a change mediated in part by cadherin-based inhibition of growth factor dependent signaling (Kim et al, 2011; Takahashi & Suzuki, 1996). However, in addition to RTKs, contact-dependent growth control is also heavily mediated by the HIPPO pathway and its downstream effector, YAP1. Originally discovered in Drosophila, signaling from Hippo (or its mammalian homologs MST1 and MST2) initiates a kinase cascade which ends with the oncoprotein Yorkie (YKI, YAP1 and TAZ in mammals) (reviewed in (Pan, 2010)). This phosphorylation event sequesters YAP1 in the cytoplasm, thus inhibiting its nuclear translocation (Lei et al, 2008; Zhao et al, 2007). However, in the absence of phosphorylation, YAP1 acts as a co-activator with transcription factors such as p73, RUNX2, and members of the TEAD/TEF family, the latter of which has lately emerged as the most likely candidate for mediating YAP1's growth-inducing signals (Ota & Sasaki, 2008; Strano et al, 2001; Vassilev et al, 2001; Yagi et al, 1999; Zhao et al, 2008). However, as transcriptional outputs have varied between organ and tissue systems, these studies suggest YAP1 may function in a highly context-specific manner.

While multiple upstream inputs exist to ensure dynamic regulation of tissue homeostasis, the cadherin complex appears to be one of the most potent regulators of HIPPO activation. Both depend on each other for proper function; YAP1 is inhibited in a density-dependent manner that is directly dependent on E-cadherin (Varelas et al, 2010; Zhao et al, 2007), while intact HIPPO signaling is required for E-cadherin mediated growth suppression (Kim et al, 2011). Interestingly, another upstream HIPPO mediator is the "4.1, Ezrin, Radixin, Moesin" (FERM) domain-containing protein, Merlin, which has been widely characterized as a tumor suppressor in a variety of tissue systems (Giovannini et al, 1999; Hamaratoglu et al, 2006; McClatchey et al, 1998). Merlin is able to regulate many of the protumorigenic signaling components listed above, such as EGFR, Rac1, and YAP1, and directly interacts with cadherin components

to regulate junction stability (reviewed in (Curto & McClatchey, 2008)). Thus, the regulation of contact inhibition and HIPPO pathway activation sits squarely at the membrane, revolving around the cadherin complex and its associated proteins.

Recently, the study of contact inhibition has moved out of the cell culture dish into animal models, and the HIPPO pathway is now known to have major roles in regulating organ size, tissue differentiation, and tumorigenesis (reviewed in (Pan, 2010)). In the intestine, YAP1 activity is highest in the undifferentiated progenitor zone of the intestinal crypt, and increased YAP1 signaling leads to alterations in tissue structure, hyperplasia, and tumor formation (Barry et al, 2013; Cai et al, 2010; Camargo et al, 2007; Zhou et al, 2011). Interestingly, we observe decreased p120 staining in the same cell population with active YAP1, and p120 staining increases after differentiation and the transition to quiescence. Thus, it is tempting to speculate that the cadherin complex may regulate a form of "contact inhibition" *in vivo*, with reduced functionality of the cadherin complex allowing for active YAP1 and RTK signaling in the crypt and/or tumor. Indeed, E-cadherin modulation in the intestine influences proliferation and cell differentiation in a manner consistent with this hypothesis (Hermiston et al, 1996), and α-catenin KO phenotypes appear to be YAP1-dependent in many organ systems (Schlegelmilch et al, 2011; Silvis et al, 2011). Thus, p120 and the cadherin complex likely contribute to adhesion-based regulation of proliferation and cell-growth both *in vivo* and *in vitro*.

Finally, p120 may modulate early tumor formation through regulation of RhoA and its ability to modulate anoikis, a type of programed cell death induced by cell detachment. Importantly, anoikis is associated with anchorage-independent cell growth (AIG), which is imperative for tumor progression as it allows cancer cells to survive detachment, invasion, circulation, and colonization (reviewed in (Taddei et al, 2012)). Interestingly, p120 has been previously shown to mediate AIG through its ability to inhibit RhoA activation (Dohn et al, 2009). Experiments in which AIG was used as a readout for MDCK cell transformation have illustrated that p120 is required for both Src- and Rac-induced transformation and AIG, which was rescued by inhibiting of any component of the RhoA signaling cascade (i.e. RhoA, ROCK, or LIMK). Taken together, these data suggest p120 may function to mediate survival of early transformed cells, and can contribute to tumor formation by overcoming RhoA-induced cell death.

Hypothesis

For my thesis work, it is my hypothesis that p120-catenin directly contributes to early tumorigenesis in the intestine. This seems likely, as p120 ablation in a variety of organ systems has led to tumor formation, and the pathology literature describes multiple changes to p120 and cadherin complex proteins in both early and late tumorigenesis. Furthermore, it is likely that an involvement for p120 in CRC will center around the cadherin complex, although there are many ways in which this could occur. On the other hand, it is also possible that p120 does not actively contribute to tumor formation, as our previous studies with p120 KO in the intestine speculate that tumor formation is due to indirect inflammatory mechanisms. However, chronic inflammation is a well-known risk factor for CRC, thus even an indirect effect on tumor formation may contribute to CRC development. Thus, the primary objective of my work will not only contribute to our understanding of p120 biology, but also to the functional relevance of p120 to CRC.

CHAPTER II

MATERIALS AND METHODS

Animals

Mice containing the floxed p120 allele (f) were generated as described previously by our lab (Davis & Reynolds, 2006) and backcrossed onto a C57bl/6 background. *p120f/f* mice were crossed with *Vil-CreERT2* mice (el Marjou et al, 2004) to target tamoxifen-inducible p120 ablation to the small intestine and colon. *p120f/f; Vil-CreERT2* mice were then crossed with *Apc1638* or *ApcMin* tumor models to generate experimental populations for tumor studies. After genotyping, p120 KO was induced by IP injection of 1 mg/20g mouse weight of tamoxifen (TAM) dissolved in corn oil for 3 consecutive days. Mice were sac'd when moribund and tumors counted macroscopically on a Zeiss Stemi 2000-C dissecting microscope. For p120 KO in established tumors, *ApcMin; p120 f/f; Vil-CreERT2* mice were aged at least 3 months prior to TAM treatment.

To generate p120 heterozygous mice, *p120f/f* mice were crossed with transgenic mice expressing Cre-recombinase gene under the control of the adenovirus *EIIA* promoter. Resulting *p120f/ΔCre* pups were verified to express only one p120 allele and then crossed into C57bl/6 strain to yield the *p120+/-* line. These mice were crossed with *ApcMin* to yield *ApcMin; p120+/+* and *ApcMin; p120+/-* littermate sets. Matched mice were sac'd when one reached tumor burden endpoint, or sac'd at 4 weeks for microadenoma analysis.

For conditional *Apc* ablation, Apc cKO mice were obtained from Jackson labs and crossed with *Lrig1-CreERT2/+* mice. Homozygous *Apc* flox mice expressing *Lrig1-CreERT2* were injected with 1mg TAM dissolved in corn oil by IP to induce complete *Apc* loss. Littermate control mice were treated with corn oil alone.

Kaiso global null mice have been reported previously. To investigate the consequences of Kaiso loss in the context of *Apc* ablation, Kaiso null mice were crossed with the Apc cKO model to yield *KaisoΔ/y; Apcf/f; Lrig1-CreER* and *Kaiso+/y; Apcf/f; Lrig1-CreER* cohorts. As Kaiso is X-linked, experiments were limited to male littermate mice with and without Kaiso. Mice were treated by IP with 1mg TAM to induce *Apc* loss and sacrificed 5 days post TAM for immunohistochemical analysis.

All experiments involving animals were approved by the Vanderbilt University Institutional Animal Care and Use Committee. Mice were maintained under a strict 12-hour light/dark cycle and with free access to chow and water. Genotyping was done as described previously (Davis & Reynolds, 2006; el Marjou et al, 2004; Kuraguchi et al, 2006; Powell et al, 2012; Prokhortchouk et al, 2006).

Immunohistochemistry

Swiss-rolled intestinal tissue was fixed in 10% neutral buffered formalin overnight at 4°C and then embedded in paraffin. Tissue processing and H&E staining were performed by the Vanderbilt Translational Pathology Shared Resource using standard technique. For fluorescent IHC, sodium citrate antigen retrieval was used for the majority of antibodies. After blocking, samples were incubated with primary and secondary antibodies overnight at 4°C and for 2 hr at room temperature, respectively. See Table 2 for a list of primary antibodies. Secondary antibodies were conjugated to either 488 or 594 Alexa-fluor dyes (Invitrogen). Nuclei were visualized by brief incubation in 1μg/ml Hoechst dye. Fluorescence images were taken on an Axioplan 2 microscope (Carl Zeiss, Inc.) with a Hamamatsu Orca-ER digital camera. Images were analyzed and processed with MetaMorph (MDS Analytical Technologies) software. To quantify proliferative and apoptotic cells and total nuclei, the MetaMorph count nuclei application was used. For microadenoma analysis, sections from 4-week *ApcMin; p120+/+* and *ApcMin; p120+/-* mice were serial sectioned every 50μm for 1mm. Slides were stained with β-catenin to visualize microadenomas.

Human small adenoma and FAP samples were compiled by Vanderbilt pathologist, Dr. Kay Washington, and IHC for Kaiso and β-catenin was done by Frank Revetta in the Vanderbilt Pathology Department. For IHC, each sample was scored on a 0-4 intensity scale, where 0 = negative, 1 = faint expression, 2 = low expression, 3 = moderate expression, and 4 = high expression. Scores were recorded for total protein and for nuclear and cytoplasmic cell fractions. Statistical analysis and agreement report was done by Greg Ayers of the Vanderbilt Biostatistics Department.

Cell culture

HEK293, HCT116, SW480, LS174T, and CaCo2 cell lines were obtained from ATCC and cultured in DMEM supplemented with antibiotics and 10% heat-inactivated fetal bovine serum (FBS). IEC6 cells were further supplemented with 10μg/ml insulin (Invitrogen). To stimulate various signaling pathways, cells were treated with 50mM LiCl, 100ng/ml BMP4 (R&D), and 5μM DAPT for 24 hours, 5μM etoposide (Sigma) for 48 hours, or Wnt3a conditioned media as needed. To generate conditioned media, Wnt3a expressing and non-expressing L-cells were ordered from ATCC and grown in DMEM with antibiotics and 10% fetal bovine serum. Confluent 10-cm plates were split 1:10 and seeded into a 15-cm plate with 20ml media and grown for 5 days. After 5 days, conditioned media was harvested and filtered through a 0.45μm filter. Media was mixed 1:1 with fresh media for Wnt3a stimulation experiments.

Lentiviral and Retroviral manipulation

For generation of lentivirus, 2μg vector DNA and 1μg each pCMV-PAX2 and pMD2.G (Addgene) was transfected into HEK293T cells via Polyethylenimine (PEI). For retroviral constructs, 4μg target vector was transfected into Phoenix (ϕ) packaging cells. Virus was harvested 48 hours post-transfection. CRC cells were infected with lentivirus or retrovirus containing media supplemented with 4μg/ml polybrene for 6 hours, followed by drug selection by puromycin or neomycin 48 hours post-infection.

Antibody	Company/Catalog #	Species/Isotype	Concentration (in µg/ml)
pp120(p120)	BD 610134	Mouse IgG1	0.6
F1αSH (p120)	Reynolds Lab	Rabbit	1:500
8D11 (p120)	Reynolds Lab	Mouse IgG2a	1
E-cadherin	BD 610181	Mouse IgG2a	0.5
β-catenin	Sigma C2206	Rabbit	1:800*
β-catenin	BD 610154	Mouse IgG1	2.5
α-catenin	Sigma C2081	Rabbit	1:800*
Kaiso	Reynolds Lab	Rabbit	1:3000
Cleaved Caspase-3 (Asp 175)	Cell Signaling 9661	Rabbit	1:400
Phosphorylated Histone H3	EMD Millipore 06-570	Rabbit	2
Ki67	Abcam ab15580	Rabbit	1:2000*
Hnrnpk	Abcam ab24170	Rabbit	1:400*
Banp	Abcam ab84376	Rabbit	1:400*

Table 2. Antibodies used for immunohistochemistry.

*antibodies were diluted 1:1 in glycerol if necessary before determining working concentration.

For Kaiso KD, 5 Sigma MISSION shRNA constructs were used (#358, #751, #1539, #1799, and #2600) along with a scrambled, nontarget control sequence. Construct #1539 consistently yielded the best knockdown in almost all cells tested, followed by #2600 and #358, thus were designated shRNA #1, shRNA #2, and shRNA #3, respectively. For Kaiso overexpression, pDONR Kaiso cDNA was obtained from the Harvard PlasmID resource and shuttled into an LZRS-neo-flag vector using the Gateway cloning system (Invitrogen) to generate the LZRS-neo Kaiso-Flag construct. The puromycin selectable DN-TCF4 plasmid (EdTP) is previously described (Fuerer & Nusse, 2010) (Addgene). To generate the control EP plasmid, the EdTP was cut with BamHI and self-ligated.

Cell Immunofluorescence

Cells were plated on glass coverslips and fixed in 3% paraformaldehyde for 30 minutes. After PBS washes, cells were permeabilized in PBS with 0.2% TritonX-100 for 5 minutes. After more PBS washes, non-specific binding was blocked using 3% nonfat milk. Cells were incubated in primary antibody, anti-Flag (1:1000, Sigma) and anti-Kaiso (1:1000, Reynolds lab), for 30 minutes. Coverslips were then washed and incubated in secondary antibody for 30 minutes (Alexa-Fluor, 1:800, Invitrogen). After final washes, nuclei were stained using 0.5μg/ml Hoechst dye. Coverslips were coated in ProLong gold (Invitrogen) and mounted on glass slides.

Western Blot Analysis

Protein was isolated as previously described (Mariner et al, 2004). Briefly, cells were washed with PBS, lysed in RIPA buffer [50 mM Tris (pH 7.4), 150 mM NaCl, 1% Nonidet P-40, 0.5% Deoxycholic Acid, 0.1% sodium dodecyl sulfate] containing inhibitors (1mM henylmethylsulfonyl fluoride, 5 μg/mL leupeptin, 2 μg/mL aprotinin, 1mM sodium orthovanadate, 1mM EDTA, 50mM NaF,) and spun at 14,000rpm at 4°C for 10 minutes. For whole intestinal lysates, intestines were harvested and flushed with ice-cold PBS. 2cm sections of mouse ileum were splayed and lysed on ice in RIPA buffer containing 20μl/mL protease (Sigma P8340) and phosphatase inhibitor cocktails (Sigma P004 and P5726).

Samples were homogenized with a motor fitted with a Kontes Microtube Pellet Pestle Rod and cleared by spinning at 14,000rpm at 4^{o}C for 10 minutes. Cleared total protein from all sources was quantified using a bicinchoninic acid assay (Pierce). 10-40 μg of protein per sample was boiled in 2X Laemmli sample buffer and separated by SDS-polyacrylamide gel electrophoresis. Proteins were transferred to nitrocellulose (PerkinElmer), and non-specific binding was blocked by incubating membranes in Odyssey blocking buffer (LI-COR) prior to addition of primary and secondary antibodies. Anti-p120/pp120 (0.1μg/mL, BD Biosciences), anti-p120/F1αSH (0.25μg/ml, Reynolds lab), anti-E-cadherin (0.1μg/mL, BD Biosciences), anti-tubulin/DM1α (1:1000, VAPR), anti-β-catenin (1:5000, Sigma), anti-α-catenin (1:1000, Sigma), anti-Kaiso (1:1000, Reynolds lab), anti-cleaved caspase 3 (1:1000, Cell Signaling Technology), anti-p53 (1:1000, Cell Signaling Technology), anti-phospho-p53 (1:1000, Cell Signaling Technology), anti-Flag (1:500, Sigma) and anti-TCF4 (4μg/mL, Sigma Aldrich) antibodies were used. The Odyssey system was used for detection of secondary goat anti-mouse IgG IRDye 800 and goat anti-rabbit IgG IRDye 700 antibodies (1:10,000 LI-COR).

CTNND1 mRNA expression

CTNND1 mRNA expression was queried from Illumina HiSeq RNASeqV2 data available through the TGCA colon adenocarcinoma (COAD) dataset. Samples include normal adjacent tissue (n=39) and colon adenocarcinoma (n=264). Normalized RSEM expression data was Log2 transformed and median-centered at 1 for visualization.

Real-time qPCR

Cell pellets or 2cm of whole mouse ileum were homogenized in Trizol. Total RNA was purified with RNeasy Mini kit with on-column DNaseI treatment (Qiagen) according to manufacturer's instructions. cDNA synthesis performed using the SuperScript VILO cDNA synthesis kit (Life Technologies). Real-time PCR was performed on a BioRad CFX96 real-time cycler using LuminoCT SYBR green master mix (Sigma). After pre-incubation at 95^{o}C, two-step cycling was performed from 95^{o}C (10s) to 60^{o}C (30s) for 40 cycles. *GAPDH* was used to calculate normalized fold change. Melting curves of the resulting PCR products were analyzed using CFX Manager software (BioRad) to exclude amplification of nonspecific products. Primers not previously cited were designed using NCBI-GENE-'Pick Primers' function with PCR product limited to 120 bp. See Tables 3-5 for complete primer lists.

Laser capture microdissection

Tissue was collected into adhesive caps using the Veritas Laser Capture Microdissection System and processed for DNA using the Pico Pure DNA extraction kit (Arcturus cat# KIT0103). 10-30 μL of proteinase K solution was used per sample. Extracted DNA was PCR amplified for the p120 null or floxed alleles and run on 2% agarose gels for viewing.

ENCODE ChIP-seq analysis

Results from Kaiso ChIP-seq screens were queried from HCT116, HEPG2, GM12878, and K56 cell lines. Peaks were called and assigned to target promoters manually. Analysis yielded 405 genes with Kaiso binding peaks in multiple cell lines. Pathway analysis and promoter analysis were done with the help of Steven Chen in the Vanderbilt Department of Biostatistics.

Gene Symbol	Forward Sequence	Reverse Sequence	Citation/PrimerBank ID
Axin2	TGACTCTCCTTCCAGATCCCA	TGCCCACACTAGGCTGACA	31982733a1
cMyc	ATGCCCCTCAACGTGAACTTC	GTCGCAGATGAAATAGGGCTG	293629266c1
Lgr5	CCAATGGAATAAAGACGACGGCAACA	GGGCCTTCAGGTCTTCCTCAAAGTCA	Jaks et al. Nature genetics. 2008
Cdh1	CCAACAGGGACAAAGAAACAAAGG	GATGACACGGCATGAGAATAGAGG	Slorach et al.
Ctnna1	GCCAAGCAGATGTGCATGATC	CAGAGGTGTTTTTGAGTGGACCTT	Slorach et al.
Ctnnb1	GGGTGGCATAGAGGCTCTTGT	GCTCAGTGATGTCTTCCCTGTCA	Slorach et al.
Ctnnd1	AGCTTGTGGAGAATTGTGTTTGC	TGCCTGTGGGATTTCACGAT	Slorach et al.
Zbtb33	GAACTCCTTGAATGAACAGCGT	CCCAGCAACTGAGAAGAGC	9937986a1
Gapdh	TGACCTCAACTACATGGTCTACA	CCGTGAGTGGAGTCATACTGG	n/a
Id1	CCTAGCTGTTCGCTGAAGGC	CTCCGACAGACCAAGTACCAC	31077096a1
Smad6	GCAACCCCTACCACTTCAGC	GTGGCTTGTACTGGTCAGGAG	12836011a1
Smad7	GGCCGGATCTCAGGCATTC	TTGGGTATCTGGAGTAAGGAGG	6678778a1
Lyz2	ATGGAATGGCTGGCTACTATGG	ACCAGTATCGGCTATTGATCTGA	8393739a1
Muc2	ATGCCCACCTCCTCAAAGAC	GTAGTTTCCGTTGGAACAGTGAA	23956200a1
Serpine1	TTCAGCCCTTGCTTGCCTC	ACACTTTTACTCCGAAGTCGGT	6679373a1
Cdkn1a	CCTGGTGATGTCCGACCTG	CCATGAGCGCATCGCAATC	6671726a1
Cdkn1b	TCAAACGTGAGAGTGTCTAACG	CCGGGCCGAAGAGATTTCTG	31542372a1
Cdkn1c	CGAGGAGCAGGACGAGAATC	GAAGAAGTCGTTCGCATTGGC	31981849a1
Cdkn2a	CGCAGGTTCTTGGTCACTGT	TGTTCACGAAAGCCAGAGCG	6753390a1
EphB2	GCGGCTACGACGAGAACAT	GGCTAAGTCAAAATCAGCCTCA	414594a1
Tcf7	AGCTTTCTCCACTCTACGAACA	AATCCAGAGAGATCGGGGGTC	6678245a1
mTert	AGCGGGATGGGTTGCTTTTAC	CACCCATACTCAGGAACGCC	Munoz et al., 2012
Olfm4	TGGCCCTTGGAAGCTGTAGT	ACCTCCTTGGCCATAGCGAA	Munoz et al., 2012
Lrig1	AAGGGAACTCAACTTGGCGAG	ACGTGAGGCCTTCAATCAGC	Munoz et al., 2012
Hopx	CATCCTTAGTCAGACGCGCA	AGGCAAGCCTTCTGACCGC	Munoz et al., 2012
Bmi1	GGAGAAGAAATGGCCCACTACC	TTGGCCTTGTCACTCCCAGA	Munoz et al., 2012
Snai1	CACACGCTGCCTTGTGTCT	GGTCAGCAAAAGCACGGTT	6755586a1
Atoh1	GAGTGGGCTGAGGTAAAAGAGT	GGTCGGTGCTATCCAGGAG	Kazanjian et al., 2010
Hes1	CCAGCCAGTGTCAACACGA	AATGCCGGGAGCTATCTTTCT	Kazanjian et al., 2010
Dll1	AACCATGAACAACCTAGCCAATT	CATGGTCCCCGTGAAAGTC	Kazanjian et al., 2010
Spdef	AAGGCAGCATCAGGAGCAATG	CTGTCAATGACGGGACACTG	Kazanjian et al., 2010
Hey1	CCGACGAGACCGAATCAATAAC	TCAGGTGATCCACAGTCATCTG	117606331c1

Table 3. List of mouse qRT-PCR primers.

Gene Symbol	Forward Sequence	Reverse Sequence	Citation/PrimerBank ID
Gapdh	GGTGTGAACCACGAGAAATA	TGAAGTCACAGGAGACAACC	n/a
Siah2	TGCCTTGTTTTTGACACAGC	AGTTGTGGGTCCTGACTTGG	n/a
Alpl	CAGCCACCGCCTATCTCTGT	TGCTGTTGCACTGGTTGAATC	n/a
Vil1	GCAGCTGCCATCTACACAACA	CGCTCTCATGGCCTTGGA	n/a
Axin2	ACATGAGCAATGGGGGACTG	AACCACGGTGGGTGAAAGTT	n/a
Id1	GCTCTACGACATGAACGGCT	TGCTCACTTTGCGGTTCTGA	n/a
Lgr5	TCCAACCTCAGCGTCTTCAC	GCATTTCCAGCAAGACGCAA	n/a
Smad7	TGCGAGAAGGTGGTGTGTTT	TCGTGAGATGTCTGGAGGGT	n/a
Smad6	AGCATGTCTCCAGATGCCAC	GCCTGGTCATACACCGCATA	n/a
Pai1	AGGGGCAGCAGATAGACAGA	ATAACACAAGGCGGCTGTCA	n/a
P21	TTGTCGCTGTCTTGCACTCT	TTTTCGGCCCTGAGATGTCC	n/a
Kaiso 1	GACACAGGTCCAGCCTAACC	CACAGGAGTGGGAAGCTGAG	n/a
Kaiso 2	AAGCCAAGTGCTATGCCTGT	CTGGAGGCTCTTTTCCAGCA	n/a

Table 4. List of rat qRT-PCR primers.

Gene Symbol	Forward Sequence	Reverse Sequence	Citation/ PrimerBank ID
ATF4	CCCTTCACCTTCTTACAACCTC	TGCCCAGCTCTAAACTAAAGGA	33469973c3
BANP	GGAAGAGGACTACCCCAATGG	TGACACCGGATGCCGTAGA	109698607c3
BUB1B	GCACCGACAATTCCAAGCTC	TGTGCTTCGTTGTGGTACAGA	168229167c3
CCNC	CCTTGCATGGAGGATAGTGAATG	AAGGAGGATACAGTAGGCAAAGA	61676092c1
CDC20	GCTTTGAACCTGAACGGTTTTG	TCTGGCGCATTTTGTGGTTTT	118402581c3
CUL3	GATGCACTGCCTTGACAAATCA	CCTTGCTCCCTCAAATAGGAACT	380714661c3
DDX20	TGGCTCCTACAAGAGAAATTGC	ACATGACACTCTAAGCCTTCCA	256223452c2
DENR	AAGACCGTACCACAAAAGGTTAC	CCTCCCCTGTTACTGAGGCA	55749880c2
DIDO1	GAGCCCGAGAACGATCAGG	TGGGGTCGTAACCCTCACATT	301129169c3
MAD1L1	GGGGAGGATCTCGGAACTG	CTGCTCGTGGTCTGCTCTT	62243373c2
MKL2	TTATAGGCGTTGGGAAGGAGG	CCGGAGACAAAGCGTCACT	38569479c3
PDRG1	AGGAATCAGAATCGAGAGGGC	CATGTTCCCGAAGCAAACCAT	40807483c1
PHB	GACCACGTAATGTGCCAGTCA	CATCATAGTCCTCTCCGATGCT	6031190c2
PRDX1	CCACGGAGATCATTGCTTTCA	AGGTGTATTGACCCATGCTAGAT	320461710c1
RPL26	GACTTCCGACCGAAGCAAGAA	TGCACCCGTTCAATGTAGATAAC	78190467c1
RPS19	AAGCTGAAAGTCCCCGAATGG	AGTTCTCATCGTAGGGAGCAAG	48255921c1
SIRT4	GCTTTGCGTTGACTTTCAGGT	CCAATGGAGGCTTTCGAGCA	300795832c1
UHRF2	GCCTTGGTGCTTGGTTTGAAG	AGACGTAGAGGGTACACTGTC	324120894c3
WDR77	GGTAGCAAAGACATCTGCATCA	TTGTCCTCGCTGCATGAAAGA	20127622c3
XPC	CATCGTGGGAGCCATCGTAAG	CTCACCATCGCTGCACATTTT	224809301c3
ZBTB2	ATCAGACCAGTGAGTGTGTCC	ACTTGATGCCCTGTTCTAATCG	24308240c2
UBE2D3	CAGGTCCAGTTGGGGATGATA	CCGCCTTGATATGGGCTGTC	259155308c1
ATF2	AATTGAGGAGCCTTCTGTTGTAG	CATCACTGGTAGTAGACTCTGGG	368711268c1
ATF7	GAGACGACAGACCGTTTGTGT	AGGCGTTTGATCTGCAATGAT	331999949c1
MAP3K7	ATTGTAGAGCTTCGGCAGTTATC	CTGTAAACACCAACTCATTGCG	21735563c2
MAPK14	TCAGTCCATCATTCATGCGAAA	AACGTCCAACAGACCAATCAC	194578904c2
RPS11	TTCAGACTGAGCGTGCCTAC	GCCCTCAATAGCCTCCTTGG	34335149c1
RPS15	CCCGAGATGATCGGCCACTA	CCATGCTTTACGGGCTTGTAG	71284430c1
RPS15A	GTGCAACTCAAAGACCTGGAA	TCCCTCCTGTGTGTTTTCGTC	71772358c2
RPS2	GGCCTCTCTCAAGGATGAGGT	GTCCCCGATAGCAACAAATGC	70609878c1
RPS28	GACACGAGCCGATCCATCATC	TGACTCCAAAAGGGTGAGCAC	71565158c1
RPS3A	TGGATCTTACCCGTGACAAAATG	TGACATCAACGTGAGCTTCAATC	70609888c3
RPS6	AGGGTTATGTGGTCCGAATCA	TTGGTCTGTAACAGGAATGCC	17158043c2
RPS7	CCAAGTCCGGCTAGTACGC	TCGAGTTGGCTTAGGCAGAAT	71164880c3
RPS9	GAAATCTCGTCTCGACCAAGAG	GGTCCTTCTCATCAAGCGTCA	71164881c1
ZBTB33	TGGAAGACCGAAAATTCCGGG	CAACTTGCCCAGCAACAGAG	296179375c2
TCF4	AGAAACGAATCAAAACAGCTCCT	CGGGATTTGTCTCGGAAACTT	226371626c1
ATOH1	GCAGGAGGAAAACAGCAAAA	ACTTGCCTCATCCGAGTCAC	Kazanjian et al., 2010
HES1	AGCACACTTGGGTCTGTGC	TGAAGAAAGATAGCTCGCGG	Kazanjian et al., 2010
SPDEF	GCACTGCAGCAGACAGCTC	GGGGATACGCTGCTCAGAC	Kazanjian et al., 2010
CCND1	TGGAGCCCGTGAAAAAGAGC	TCTCCTTCATCTTAGAGGCCAC	77628152c2
AXIN2	CAACACCAGGCGGAACGAA	GCCCAATAAGGAGTGTAAGGACT	195927058c1

Table 5. List of human qRT-PCR primers.

Statistics

Statistical analyses were performed using GraphPad Prism software (GraphPad La Jolla, California, USA). For assays with or without normal distribution, two-tailed Student's t-tests or Mann-Whitney tests were performed, respectively. A p-value of <0.05 was considered statistically significant.

Intestinal enteroid and tumoroid culture

Cultures from the small intestine and *ApcMin* tumoroids were established based on published protocols (Mahe et al, 2013; Sato et al, 2011a). Detailed protocols for establishment of small intestinal enteroids and tumoroids as well as organoid passaging, freezing, paraffin embedding, and lentiviral infection are described in Appendix B.

CHAPTER III

A GATEKEEPER FUNCTION FOR THE E-CADHERIN COMPLEX IN INTESTINAL TUMORIGENESIS

Introduction

The vast majority of human colorectal cancer (CRC) is triggered by inactivation of the tumor suppressor, Adenomatous Polyposis Coli (APC), a key negative regulator of canonical Wnt signaling (2012; Fearon & Vogelstein, 1990). Progression to malignancy occurs over many years and is typically driven by frequently encountered alterations in a handful of "major" drivers (e.g., *APC*, *K-Ras*, *SMAD4*, *p53*), and evidently, a substantially larger number of so called "minor" drivers, genes mutated infrequently but too often to be accounted for by chance. Mortality is generally caused by complications arising from metastasis, a phenomenon often linked to downregulation or loss of the epithelial cell-cell adhesion molecule E-cadherin. Indeed, E-cadherin-loss is typically observed in advanced tumors (Berx et al, 1998; Moll et al, 1993; Palacios et al, 2003; Vos et al, 1997) and thought to be causally associated with the transition to metastasis(Birchmeier & Behrens, 1994; Perl et al, 1998; Vleminckx et al, 1991; Yap, 1998).

E-cadherin is responsible for the major cell-cell adhesion system in epithelial cells and widely viewed as a master organizer of the epithelial phenotype (Takeichi, 1995). Its cell-cell adhesion activity is mediated by a tetrameric protein complex comprised of transmembrane E-cadherin and cytoplasmic binding partners p120-, α-, and β-catenins (Yamada et al, 2005). Assembled in stages, E-cadherin translocates with β-catenin to the cell surface and is then retained by p120, which blocks endocytic reuptake via physical interaction with the cadherin juxtamembrane domain (Davis et al, 2003; Ireton et al, 2002; Xiao et al, 2003). α-catenin bridges the complex to the actin cytoskeleton through interaction with β-catenin. Loss of any one of these core activities eliminates an essential function and abrogates adhesion.

Although E-cadherin well established as a tumor and metastasis suppressor, the mechanisms underlying this activity are not fully understood. Maintenance of cell-cell adhesion is clearly critical, but the E-cadherin complex also suppresses Wnt signaling through sequestration of β-catenin (Fagotto et al, 1996; Gottardi et al, 2001) and regulates density-dependent growth inhibition (aka contact inhibition) through modulation of several effectors including EGFR, the tumor suppressor Merlin, and components of the HIPPO pathway (e.g. YAP/TAZ) (Azzolin et al, 2014; Curto et al, 2007; Kim et al, 2011; Takahashi & Suzuki, 1996). E-cadherin is a *bona fide* classical tumor suppressor in lobular carcinoma of the breast and familial gastric cancer, where mutations are relatively common and loss of expression for both alleles contributes causally to tumorigenesis (Berx et al, 1995; Machado et al, 1999). In the vast majority of carcinoma types, however, E-cadherin downregulation occurs epigenetically (e.g., promoter methylation) or by various mediators of the epithelial-to-mesenchymal-transition (EMT) (Berx et al, 1998; Bolos et al, 2003; Cano et al, 2000; Graff et al, 1995; Ma et al, 2010). Downregulation or loss by these mechanisms typically occur in late stage cancer and are believed to play a major role in the transition to malignancy. Curiously, in CRC (and many other carcinoma types), E-cadherin is rarely mutated, as is also the case for p120 and α-catenin.

In cultured epithelial cells and in mice, p120 ablation is followed rapidly by E-cadherin endocytosis and degradation, resulting usually in morphological alterations and impaired cell-cell adhesion (Bartlett et al, 2010; Davis et al, 2003; Davis & Reynolds, 2006; Ireton et al, 2002; Kurley et al, 2012; Perez-Moreno et al, 2006; Smalley-Freed et al, 2010; Stairs et al, 2011). Thus, it is widely suspected that p120 itself may behave as a tumor and/or metastasis suppressor. Indeed, the frequent occurrence of p120 downregulation in most epithelial cancers, including CRC, is extensively documented, but not well understood (Bellovin et al, 2005; Bondi et al, 2006; Gold et al, 1998; Karatzas et al, 1999; Skoudy et al, 1996). In cKO mouse models, the extent of E-cadherin loss upon p120 KO varies widely from 50- to near 100%, depending on the tissue. Phenotypes are often severe, but vary widely depending on tissue, timing and context. In the skin and esophagus, both squamous epithelia, retain barrier function but nonetheless develop significant cell autonomous inflammatory phenotype and eventually cancer. While development of cancer is quite rare, most other epithelia exhibit some degree of adhesion phenotypes and altered morphology. At one extreme, the nascent mammary gland doesn't form at all because the cells lose

adhesiveness altogether and dissociate into the lumen. Conversely, p120 KO in the prostate has no obvious phenotype although it persists through the life of the animal (ABR unpublished data).

p120 knockout in more than 50% of the intestinal epithelium is ultimately lethal. Barrier defects, inflammation and mucosal damage accumulate leading to intestinal bleeding and death by 21 days of age (Smalley-Freed et al, 2010). To study long-term effects of p120 KO, a tamoxifen regime was developed to limit the extent of p120 KO (Smalley-Freed et al, 2011). Reducing p120 KO to ~10% of the intestinal epithelium (hereafter "limited" p120 KO) produced long-lived animals, outwardly indistinguishable from controls. Stochastic p120 ablation was clearly compatible with stem and progenitor cell function as immunostaining revealed clonal microdomains of p120 null cells interspersed with normal epithelium that persisted for life. Unexpectedly, over 45% of the animals developed tumors, none of which exhibited outright loss of p120. The majority, however, showed evidence of Wnt pathway activation, including sharply elevated levels of β-catenin, suggesting a molecular explanation for the tumors but few clues as to the role of p120.

Here we identify p120 as an obligatory haploinsufficient tumor suppressor in *Apc*-sensitized mice. Although early experiments targeted both p120 alleles, biallelic ablation was restricted to wild type tissue and never observed in the context of a tumor. Similarly, the mutant *Apc* allele was initially expected to be synergistic. Instead, biallelic p120 ablation and *Apc*-LOH are mutually exclusive. Nonetheless, "limited" p120 KO induced a 10-fold increase in tumor multiplicity, apparently driven by the by loss of one p120 allele. Given that p120 is rarely mutated in CRC, a relevant question is whether the outcome of halving p120 levels by any means is in fact meaningful in the larger scheme of tumor progression. Interestingly, the Sleeping Beauty transposon introduces mutations randomly throughout the genome in a fashion that approximates the forces at work in human tumors (reviewed in (Mann et al, 2014)). The method strongly selects for tumor drivers and does it in a way that puts a legitimate number on the relative tumor promoting potency of a hundreds of candidate drivers. Remarkably, α-catenin and p120 ranked 2nd and 3rd, respectively, among the 919 candidates identified in an *Apc*-sensitized background. At number 37, E-cadherin is nonetheless among the top 4%. Notably, although obligatory haploinsufficiency is relatively rare, our findings and evidence from the literature indicate that α-catenin and E-cadherin behave like p120.

Results

Characterization of p120 expression in the small intestine before and after *APC* LOH.

To characterize p120 in the intestine, we first colocalized p120 and β-catenin in the normal small intestine and in intestinal adenomas induced by APC loss (Figure 3). As expected, p120 and β-catenin colocalized at basolateral membranes, but in both cases staining in the crypt was reduced relative to that along the villus (Figure 3A, white brackets). Interestingly, p120 staining was also reduced in adenomas derived from *ApcMin* and *Apc1638* mouse models of intestinal cancer (Figures 3B and 3C, respectively, white arrowheads). *ApcMin* mice typically develop 30-100 tumors per animal, whereas mice carrying the substantially weaker *Apc1638* allele present with 2-7 tumors (Fodde et al, 1994; Moser et al, 1990). The strength of the *Min* allele is often reflected by high levels of cytoplasmic/nuclear β-catenin (Figure 3B, arrowheads). Note that p120 and β-catenin staining vary together, as before, in untransformed parts of the tumor, but diverge sharply in adenomatous areas where β-catenin accumulates in the cytoplasm and nucleus. Curiously, as illustrated at lower magnification in a typical *Apc1638* adenoma (Figure 3C), reduced p120 staining was a consistent feature of adenomatous transformation.

Importantly, p120 staining was also reduced in early adenomas obtained from Familial Adenomatous Polyposis (FAP) patients (Figure 3D). As with *Apc* mutant mice, FAP patients inherit a mutant *APC* allele and are thus predisposed to CRC (Nakamura et al, 1992; Nishisho et al, 1991). Although small human adenomas are generally quite advanced relative to the adenomas from mice, we were able to histologically identify seven very small human adenomas (i.e., well under the 0.5 cm extraction benchmark used for colonoscopy) that were in the same general size range as their mouse counterparts. Notably, 100 percent (7/7) of these "micro" FAP adenomas displayed regions of markedly reduced p120 staining (Figure 3D, arrowheads) relative to adjacent normal tissue. The effect was clearly evident in the smallest sample, a single crypt microadenoma (first panel), and in each of the six small adenomas (represented by second panel).

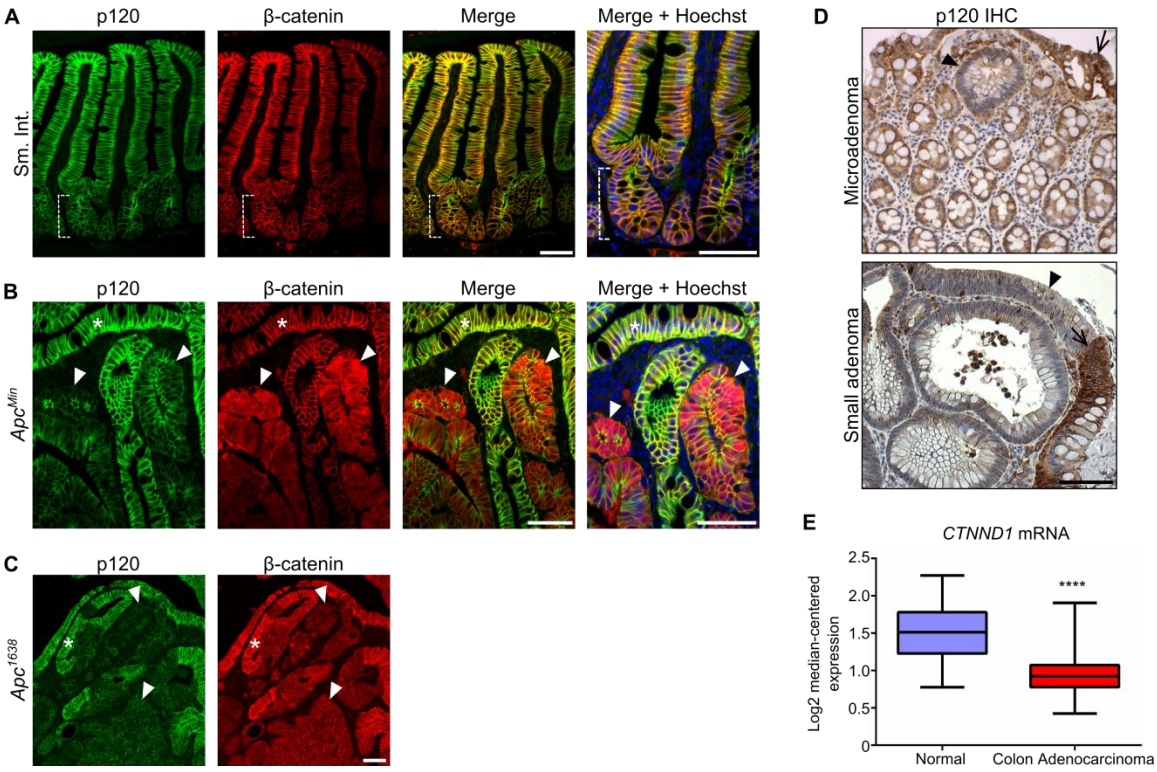

Figure 3. p120-catenin (p120) staining is decreased following *APC* loss. (A) Mouse small intestine (B) *ApcMin* tumor and (C) *Apc1638* tumor were stained for p120 (green), β-catenin (red), and Hoechst (blue). Tumor tissue shows decreased p120 staining concurrent with altered β-catenin (arrowhead) as compared to adjacent WT tissue (asterisk). Decreased p120 staining is also seen in the crypt (brackets). Scale bar 50μm. (D) IHC analysis shows decreased p120 staining in small adenomas (arrowhead) from human FAP patients compared to adjacent WT tissue (arrow). Scale bar 100μm. (E) p120 mRNA (*CTNND1*) is decreased in TGCA adenocarcinomas samples as compared to normal tissue controls. Data was Log2 transformed and median centered (****P < 0.0001, Students t-test).

We searched the publically available databases for evidence of molecular alterations in human CRC that could be consistent with the observed reduction in p120 staining. Notably, analysis of CRC genomes from The Cancer Genome Atlas (TCGA) project indicated that the gene encoding p120 (aka *CTNND1*) is not frequently mutated (2012). Other TCGA data, however, reveal compelling evidence for partial *CTNND1* loss at the mRNA level (TCGA research network) (Figure 3E).While the mechanism has not been identified, the evidence is consistent with partial loss of p120 as a factor contributing to tumor progression.

Next we asked whether reduced p120 staining in the crypt is indeed a function of reduced p120 levels (Figure 4). Driven by canonical Wnt signaling, most of the crypt is dedicated to the rapid mitotic expansion of progenitor cells (Barker et al, 2012; Schepers & Clevers, 2012). Stem cells at the base give rise to progenitors, which undergo 4 – 5 rapid rounds of mitosis as they rise through the transit-amplifying region. Under normal circumstances, this so called "crypt-progenitor" phenotype then gives way to terminal differentiation and growth arrest as the cells transition over to the villus. The mature cells then migrate to the villus tip over 3 – 5 days, at which point they are lost to the lumen. In contrast, early stage adenomas induced by *Apc*-LOH are maintained in a crypt-progenitor–like state by autonomous Wnt signaling and continue to proliferate (Sansom et al, 2004; van de Wetering et al, 2002).

To better resolve this region for qualitative and quantitative biochemical comparisons, we used an *Lrig1-CreER* driver and tamoxifen (TAM) in a homozygous *Apc* floxed background (Apc cKO) to induce synchronous *Apc* KO in the progenitor compartment across the entire intestine (Figure 4A) (Kuraguchi et al, 2006; Powell et al, 2012). Following induction, the intestinal epithelium was harvested daily and processed for immunochemical and/or biochemical analyses. Under the constitutive influence of cell autonomous Wnt signaling (i.e. *Apc* ablation), the progenitor population failed to differentiate as the cells moved up onto the villus and continue in their undifferentiated state to the villus top. As illustrated in figure 4A, the upward progress of the crypt-progenitor phenotype over time (white dotted lines) is marked by reduced p120 staining. Likewise, these cells show high levels of expression for p120's nuclear binding partner Kaiso, which is normally confined to the crypt. Figure 4B shows the p120 low/Kaiso high population also displayed altered β-catenin localization, as expected with homozygous *Apc* loss.

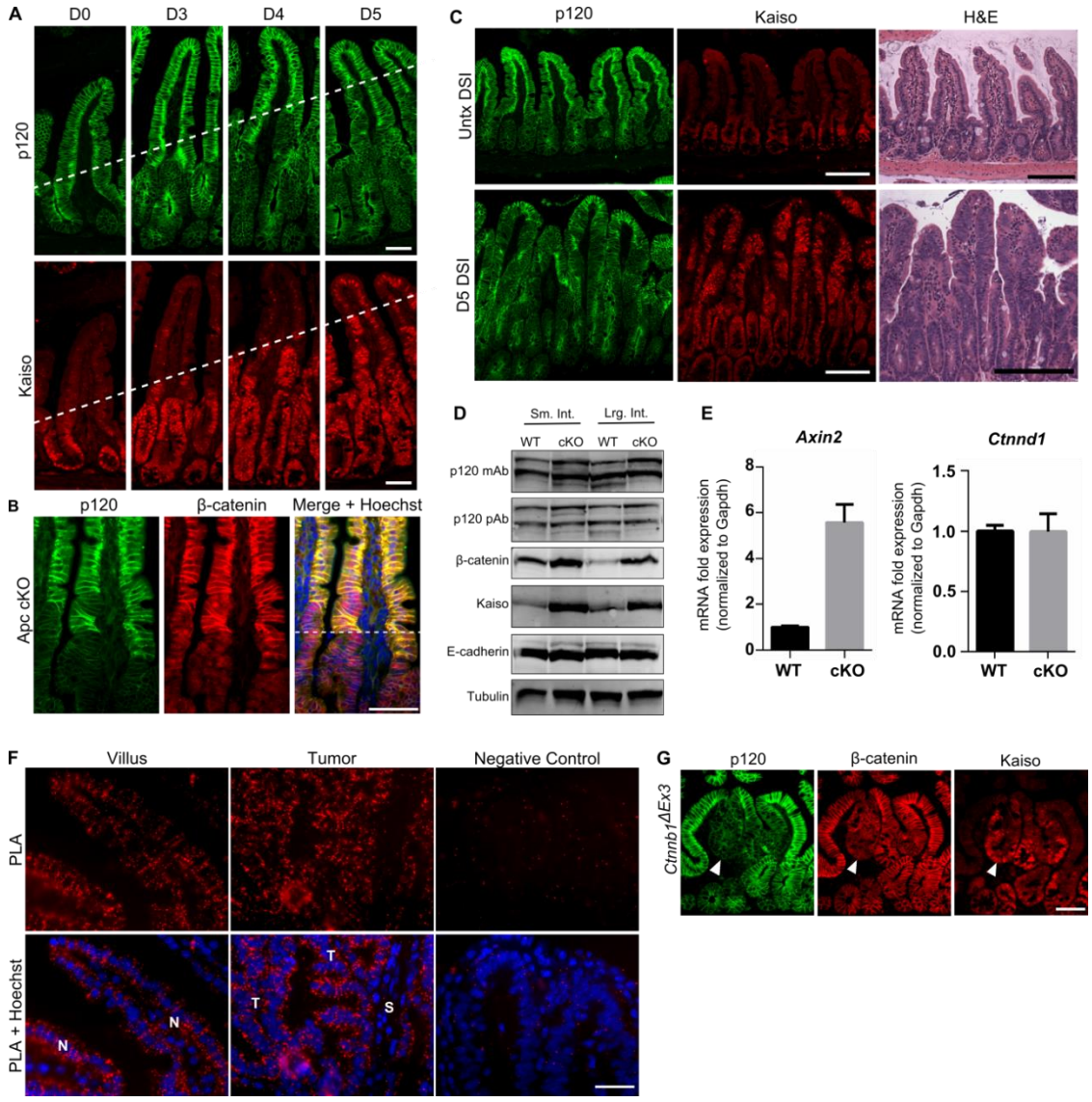

Figure 4. Decreased p120 staining does not reflect altered levels of cadherin complex components. Homozygous *Apc* floxed mice were crossed with the *Lrig1-CreER* line to drive TAM-inducible *Apc* KO in the intestinal epithelium (Apc cKO). (A) Time-course analysis of p120 (green) and Kaiso (red) staining in the ileum at day 0 and days 3, 4, and 5 post TAM. Kaiso staining marks upward progress of *Apc* null/p120-low cells over time (dotted line). (B) p120 (green), β-catenin (red) and Hoechst (blue) staining in *Apc* WT (above line) and KO (below line) tissue shows mislocalized β-catenin concurrent with p120 decrease. (C) WT (top) and cKO (bottom) ileum stained with p120 (green), Kaiso (red), and H&E shows transformed *Apc* null cells comprise the majority of the intestinal epithelium by 5 days post TAM. Scale bars 100μm. (D) No change in p120 protein was detected with p120 monoclonal (mAb) or polyclonal (pAb) antibodies in protein lysates from day 5 corn oil (WT) or TAM (cKO) treated mice. Tubulin = loading control. (E) No change in p120 mRNA from day 5 WT and cKO samples by qRT-PCR. (n=5 mice per group). *Axin2* used for positive control. (F) Proximal ligation assay (PLA) detects p120/E-cadherin protein complexes. No decrease in binding was seen in tumor tissue as compared to normal villus, despite overall reduced p120 staining. Scale bars 50μm. (G) Representative *Lrig1-Cre; Ctnnb1ΔEx3* adenoma shows similar expression for p120.Increased Kaiso marks adenoma (arrowhead). Scale bars 50μm.

Because immunofluorescence is notoriously unreliable for protein quantification, epithelial tissue from the distal ileum was isolated at day 5 post-TAM and proteins were quantified directly by SDS PAGE and Western blotting (Figures 4C and 4D). Figure 4C illustrates the WT control (top) and TAM-induced *Apc* KO tissue at this time point immunolabeled for p120, Kaiso or by H&E stain. Kaiso robustly marks every cell in the WT crypt and is then extinguished at the crypt/villus boundary. In contrast, the crypt-progenitor-like phenotype extends to the top of the villi in tissue from the TAM-treated animal. Yet despite the large discrepancy in immunofluorescence staining intensity, biochemical quantification reveals no difference in protein levels for p120 or E-cadherin (Figure 4D) following *Apc* deletion. β-catenin and Kaiso levels, on the other hand, show the expected increase. Similarly, mRNA levels for *Ctnnd1* do not change, but an increase in excess of five-fold is observed for established Wnt target *Axin2* (Figure 4E). Consistent with the Western result, we found no evidence of punctate staining due to E-cadherin internalization (and subsequent degradation) in our immunofluorescent studies. Together with the unchanged protein levels detect via Western blot, these data suggest that individual E-cadherin complexes are likely retained intact at the plasma membrane, but perhaps redistributed in a fashion that affects detection.

To directly visualize intact cadherin complexes, as opposed to conventional immunofluorescence localization of individual proteins, WT (villus) and tumor tissue were labeled by Proximity Ligation Assay (PLA) with E-cadherin and p120 antibodies (Figure 4F). PLA differs from conventional double-immunofluorescence in that the secondary antibodies are coupled to oligonucleotides. To generate a signal, the two secondary antibodies must be close enough to one another for the oligonucleotides to anneal. Thus, staining puncta reflect highly amplified signals based on a single protein-protein interaction and predicated generated by the original binary annealing. Interestingly, similar staining amounts were seen in both WT and tumor tissue. Interestingly, these PLA experiments suggest that that the aforementioned staining discrepancy is unlikely to reflect dissolution of the cadherin core complex (CCC) and that it remains intact at the cell membrane.

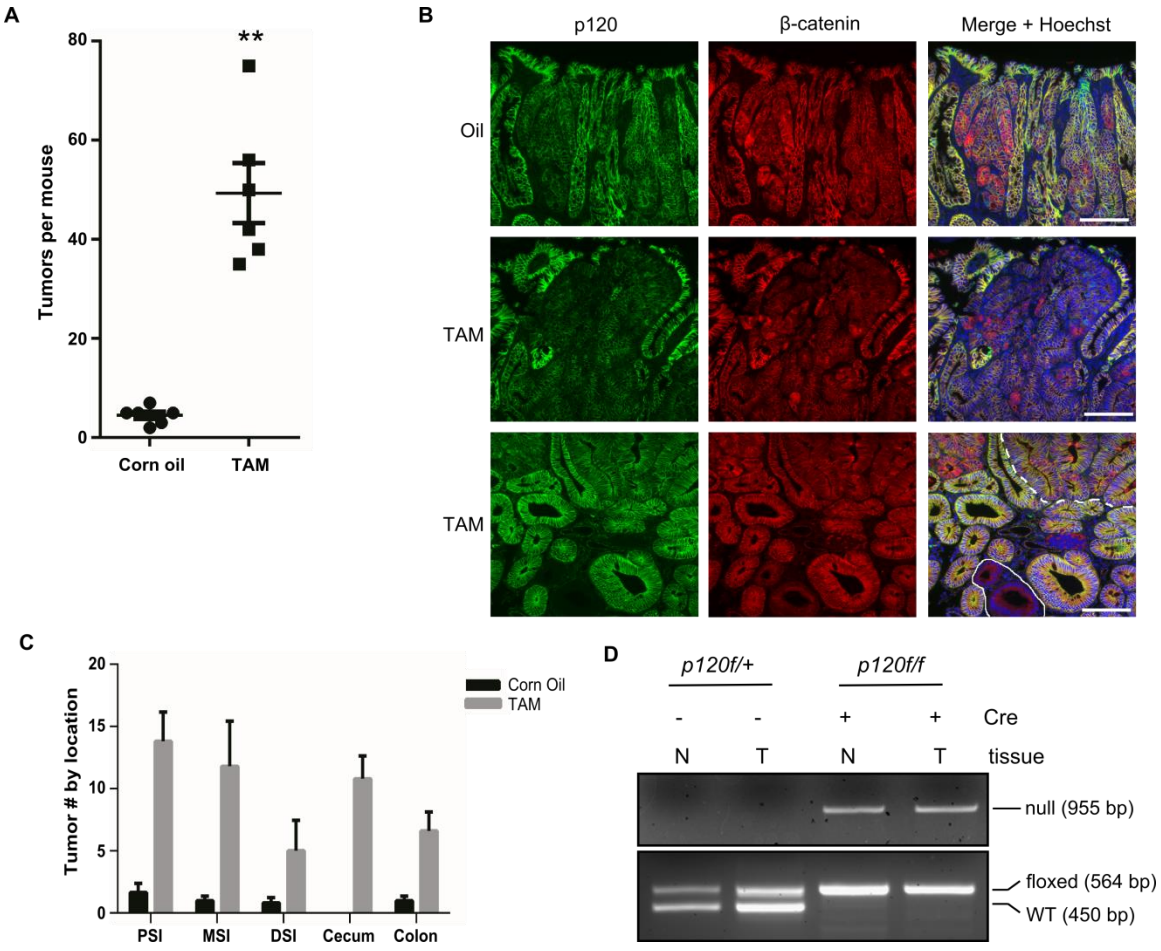

Figure 5. Limited p120 loss increases tumor number following *Apc* mutation. *Apc1638; Vil-CreER; p120f/f* mice were treated with corn oil alone or with TAM (n=6 per group) to induce p120 loss. (A) Tumor multiplicity increased 10-fold in p120 KO mice (49±6 vs 4.5±1, **P < 0.01, Mann-Whitney test). Error bars represent SEM. (B) Representative images from *Apc1638* tumors show that complete p120 KO was never seen in the tumor tissue (bottom panel, dotted line), but is readily observed in adjacent tissue (solid line). Tumors from p120 KO mice (middle, bottom) have a similar staining decrease as control tumors (top). Scale bars 100μm. (C) Intestines were divided into the proximal (PSI), middle (MSI), and distal (DSI) small intestine, cecum, and colon. Limited p120 KO increased tumor number in in all areas of the intestine. (D) DNA extracted from tumor (T) and adjacent normal (N) tissue from *Apc1638; Vil-CreER; p120f/f* mice simultaneously detects both floxed and recombined p120 alleles, indicating loss of only one floxed allele.

Also notable is that adenomas generated by activated β-catenin transgenes (e.g. *Ctnnb1ΔEx3/+*) (Figure 4G) were essentially indistinguishable from *Apc*-generated adenomas, and recapitulated the crypt-progenitor phenotype shown in other parts of Figure 4. Indeed, p120 staining is decreased and Kaiso is highly expressed in the nucleus, similar to their appearance in the WT crypt. In all cases, it appears that the alterations to both p120 and Kaiso are ultimately Wnt-driven and comprise elements of the larger molecular program behind the crypt-progenitor phenotype (van de Wetering et al, 2002). Furthermore, *Apc* loss constitutively activates this progenitor program, as evidenced in part by the extension of crypt-like p120 and Kaiso staining patterns to virtually all APC and/or β-catenin-initiated adenomas (Sansom et al, 2004).

p120 functions as an obligatory haploinsufficient tumor suppressor following loss of *Apc*

To clarify the long term effects of p120 loss in the intestine, we crossed the "limited" p120 ablation model onto an *Apc1638* background (*Apc1638; p120f/f; Vil-CreER*) and TAM-induced to determine how p120 loss might impact tumorigenesis or tumor progression in an *Apc* mutant background (Figure 5). Experimental (+TAM) and control (corn oil alone) mice were treated and sacrificed after 9 months for analysis of tumor burden. Surprisingly, the TAM-treated p120 KO cohort showed a 10-fold increase in tumor number relative to controls (Figure 5A), but none of the tumors were in fact null for p120. Instead, Figure 5B shows a further decrease in p120 staining in a typical adenoma from the TAM treated cohort (middle panel) relative to the reduction associated above with the crypt progenitor phenotype (top panels, oil only) (Table 6). Of the 52 total tumors analyzed by IHC from the TAM-treated cohort, none exhibited complete loss of p120, despite the presence of p120 negative pockets distributed throughout the surrounding WT epithelium (Figure 5B, bottom panels). Gross tumor distribution was largely unaffected by p120 ablation except for the selective appearance of significant numbers of cecal tumors (average = 11 per mouse vs none in *Apc1638* control) (Figure 3C). Further analysis by Laser Capture Microdissection (LCM) and PCR (Figure 5D) revealed loss of a single p120 allele, not both, suggesting not just haploinsufficiency, but also obligatory retention of at least one p120 allele within the tumor tissue. This condition is apparently restricted to the tumor as pockets of biallelic p120 ablation in normal epithelium exhibited no evidence of negative selection over the 9 month time-span.

Genotype	# of Tumors	Score (Mean ± SD)
Apc1638	8	2.38 ± 0.52
Apc1638/ p120 KO	35	1.09 ± 0.28

Table 6. p120 staining in *Apc1638* and *Apc1638/p120 KO* tumors. Tumors from *Apc1638* and *Apc1638/ p120 KO* mice were stained for p120 and then scored according to level of staining. Scoring Scale: 0= complete p120 KO; 1+= staining similar to that seen in tumors confirmed to only have 1 allele of p120; 4+=wild type levels of p120; 2+ and 3+ are respectively higher than the levels seen with loss of 1 p120 allele, but less than wild type levels.
n=3 mice per genotype. *P=.043

To examine this phenomenon further, we repeated the above experiments in an *ApcMin* background (Figure 6). Notably, when *p120f/+* and *p120f/f* mice were compared in this background (with *ApcMin; p120+/+* mice as controls), the results were essentially identical, with a similar increase in tumor number (Figure 6A) and decreased survival (Figure 6C). Tumors from all groups displayed similar upregulation of β-catenin (Figure 6B), and despite the association of cell-cell adhesion loss with tumor progression and metastasis, p120 loss did not increase invasion in either the *ApcMin* or *Apc1638* mouse models. Furthermore, while no difference in proliferation was observed (Figure 6D), both *p120f/+* and *p120f/f* tumors showed a minor increase in apoptotic index (Figure 6E). Although the tumor fold increase in this model (just under 2-fold) was small compared to the 10-fold increase in the *Apc1638* background, the absolute increase in tumor number was similar. Differences in performance between the models are likely a function of inherent differences in potency and timeframe (9 months vs. 5 months) of the *Apc* alleles, whereas the effects of p120 reduction reflect a similar, if not identical phenomenon.

While clearly suggestive of a haploinsufficient tumor suppressor function, we wanted to rule out possible field effects due to relatively ubiquitous p120 null "microenvironments," (e.g., inflammation, ROS) which were associated with the limited p120 ablation model. Indeed, in that context, "limited" p120 ablation by itself induced intestinal tumors in mice, albeit at substantially reduced levels, likely due to chronic inflammation. To address this issue we generated a heterozygous (*p120+/-*) mouse by germline inactivation of one p120 floxed allele. These heterozygous mice show clear reduction in p120 staining across the entire intestinal epithelium (Figure 6F), and western blot analysis revealed obvious quantitative reduction of p120 levels to about half that of WT epithelium (Figure 7A). As expected, decreased p120 levels were accompanied by loss of E-cadherin, α-, and β-catenin protein, but not mRNA (Figure 7B). Despite global reduction of p120 and cadherin complex proteins, these mice appeared relatively normal, with no change in basal rates of proliferation and apoptosis, and no overt differences in intestinal linage or stem cell markers. A slight increase in cellular migration rate, however, was consistently observed (Figure 7C).

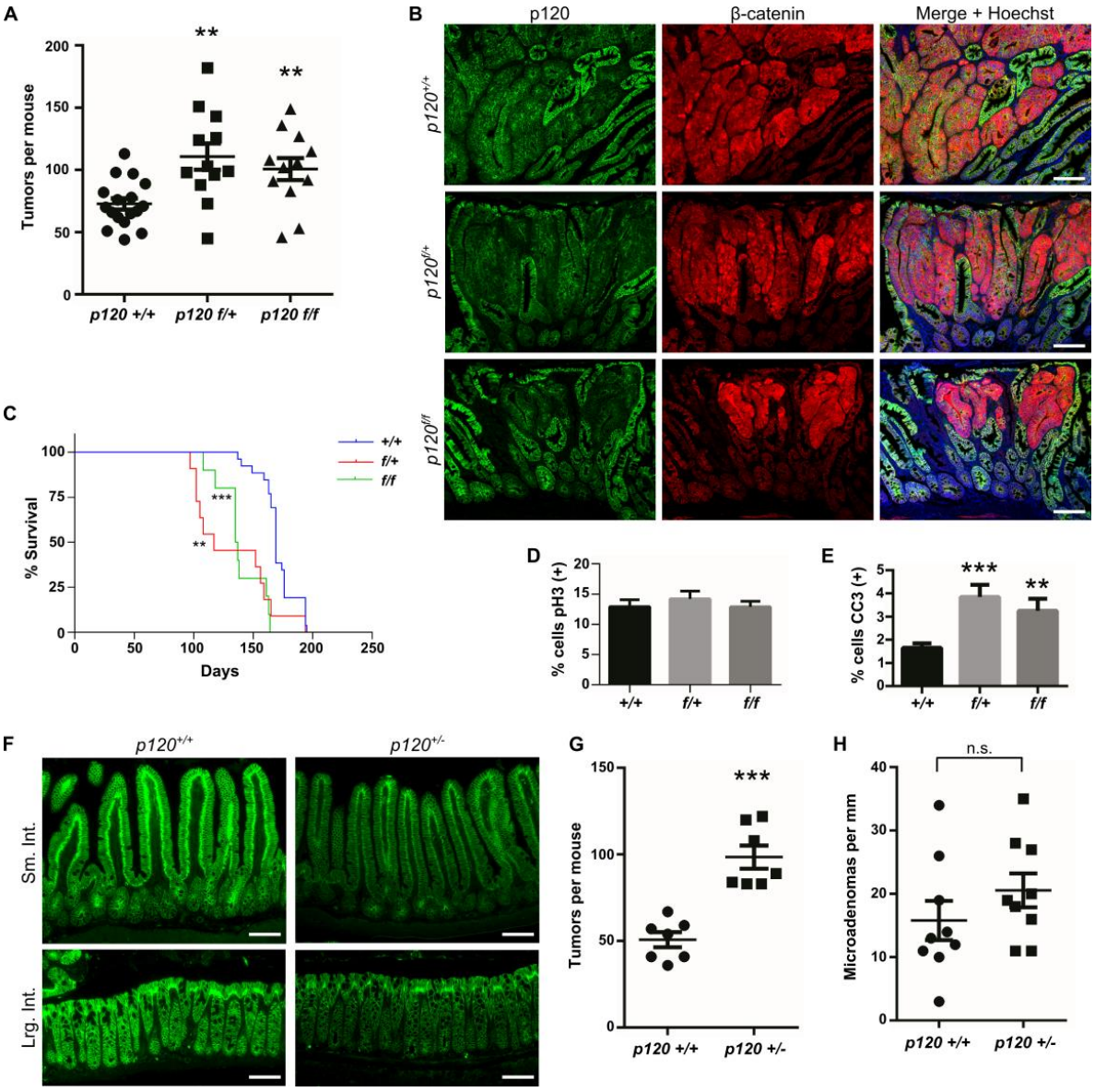

Figure 6. p120 is a haploinsufficient tumor suppressor in the intestine. (A) A similar increase in tumor multiplicity is seen in both *p120f/+* (110.7±11.6) and *p120f/f* (100.1±11) *ApcMin* cohorts as compared to *p120+/+* controls (72.8±5.1, **P < 0.01, Mann-Whitney test). Difference between *p120f/+* and *p120f/f* groups is non-significant (B) Representative tumors from each genotype stained for p120 (green) and β-catenin (red). (C) Decreased survival observed in both in *p120f/+* (**P < 0.01) and *p120f/f* cohorts (***P < 0.001, Log-rank test) as compared to WT. (D) No change in tumor proliferation measured by phospho-histone H3 staining. (E) Increased apoptotic index was seen by cleaved-caspase 3 staining in *p120f/+* and *p120f/f* tumors (***P < 0.001, **P < 0.01, Student's t test). (F). Global p120 heterozygous (*p120+/-*) mice show decreased p120 expression in both small (top panels) and large (bottom panels) intestine. All scale bars 100μm (G) *p120+/-; ApcMin* mice display 2-fold increase in tumor number over littermate controls (98.3±6.6 vs. 50.7±4.3, ***P < 0.001, Mann-Whitney test). (H) p120 heterozygousity does not affect microadenoma number (n=9 per group). (ns, Mann-Whitney test). Error bars on all graphs represent SEM.

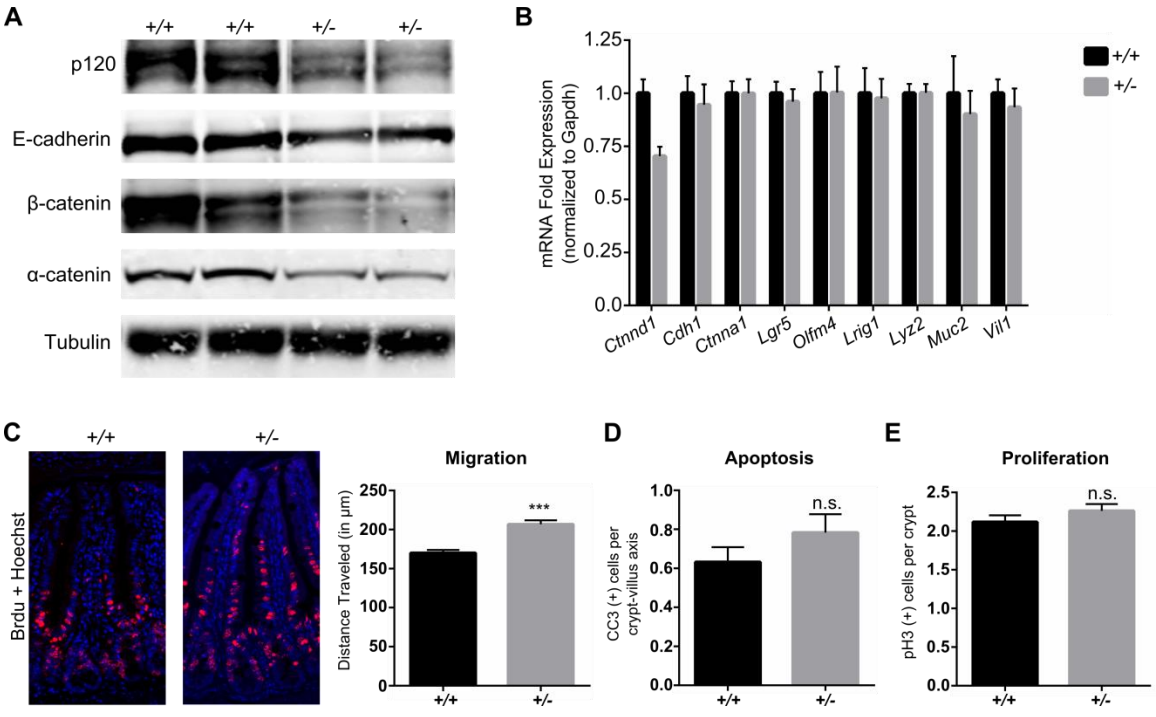

Figure 7. Characterization of p120 heterozygous mice. (A) Western blot of small intestinal tissue shows decreased expression for p120, E-cadherin, β-catenin, and α-catenin. Tubulin used as loading control. (B) mRNA analysis of whole intestine shows decreased p120 message, but no change in other stem cell or linage markers. (C) p120 WT and heterozygous mice were injected with BrdU 30 hours prior to sacrifice. p120 heterozygous mice show increased cell migration by analyzing position of BrdU positive cells (red) (170.2±3.7 vs. 206.3±5, ***P < 0.001, Mann-Whitney test). Quantification on right. Error bars represent SEM. (D) No change in apoptosis as measured by cleaved-caspase 3 staining. (E) No change in proliferation as measured by phospho-histone H3 staining.

The effect of p120 heterozygousity was then examined in the ApcMin background as a means of re-visiting potential p120 haploinsufficiency in the absence of all other variables. Importantly, the data showed that heterozygous p120 behaves in a manner that is essentially indistinguishable from the "limited (*ApcMin*) p120 ablation" model (compare Figure 6A to Figure 6G). Thus, it appears that the effects on tumor number seen in previous *ApcMin* and *Apc1638* tumor studies are indeed due to p120 haploinsufficiency, and cannot be attributed to a requirement for microenvironmental side effects of the limited ablation model.

To distinguish between tumor initiation and tumor progression, the ileums from 4-week-old *ApcMin; p120*+/- and *ApcMin; p120*+/+ mice were analyzed by β-catenin staining for the presence of microadenomas. While significant variation was seen in tumor number in general, Figure 6H shows little overall difference in the average number of microadenomas. Thus, it appears that the effect of monoallelic p120 loss manifests predominately downstream of *Apc* LOH without appreciably affecting the rate of tumor initiation. Furthermore, these data argue against significant roles for inflammatory or microenvironmental effects, as overall *Apc* mutation rates appear unchanged.

p120 is essential for *Apc*-induced tumorigenicity in the intestine

Throughout these studies, outright p120 loss was never observed in adenomas unless acutely forced (Figure 8). Areas of complete p120 ablation were often seen in close proximity to adenomatous tissue, but could be easily distinguished as WT by H&E and lack of β-catenin upregulation (Figure 8A, area enclosed by white dashed line). Strikingly, no instance of true p120 KO was found in any tumors analyzed from either the *Apc1638* (52 tumors) or *ApcMin* (191 tumors) limited p120 ablation tumor models (Figure 8B). However, these were long-term studies. To better understand the apparent incompatibility of p120 loss and tumor formation, we examined the immediate fate of tumor cells following tamoxifen-induced p120 ablation in 3-month-old *ApcMin* mice with numerous established tumors. Tumors were analyzed 2 days-, 1 week-, or 1 month-post induction (Figure 8B). Unlike the long-term tumor studies, short-term results show areas of complete p120 KO as small foci in adenoma tissues (Figure 8C, white boxes). These areas were

detected at days 2 and 7 post-TAM, but were never present at one month, indicating that the p120 null areas are lost altogether within 2-4 weeks. Exactly how these cells are cleared is unknown, as no differences in apoptosis were observed (Figure 8D) and there was no defect in proliferation (Figure 8E). Together without our *ApcMin* and *Apc1638* tumors studies, these observations indicate (1) that monoallelic p120 ablation increases tumor multiplicity and (2) that total p120 ablation is well tolerated in WT intestinal epithelium, but selectively incompatible with tumor cells leading to consistent retention of 1 allele.

p120 is dispensable for Kaiso expression and canonical Wnt signaling

The BTB/POZ transcription factor Kaiso can directly interact with p120 and has been suggested to strongly suppress canonical Wnt signaling in a manner alleviated by p120-dependent nuclear export (Daniel & Reynolds, 1999; Kelly et al, 2004; Park et al, 2005; Spring et al, 2005). To examine these relationships and potential feedback loops that might explain the rapid elimination of p120-ablated tumor cells *in vivo*, we characterized the expression of Kaiso and p120 in the small intestine and colon by immunofluorescence staining of FFPE tissue (Figure 9). Notably, staining intensities of Kaiso and p120 were inversely correlated in the small and large intestine (Figure 4A, Figure 9A), and Kaiso upregulation in the crypt, for example, coincided with reduced p120 staining. Conversely, Kaiso is extinguished as cells enter the villus, whereas p120 relocated to AJs and staining increased. In the large intestine, Kaiso and p120 formed vertical gradients oriented in opposite directions along the crypt axis (middle panels). The third set of panels show a representative *ApcMin* adenoma co-immunostained for β-catenin and Kaiso, where Kaiso staining sharply delineates the adenoma. Interestingly, strong expression of Kaiso protein and mRNA in samples from the small intestine coincided with areas of active Wnt signaling, such as the crypt, adenoma, and any area of the intestine after *Apc* ablation (Figure 9A and 9B). However, despite indications that p120's interaction with Kaiso might serve to physically remove it from the nucleus, Kaiso expression patterns in the colon were not obviously affected by p120 status in crypts expressing 0, 1, or both p120 alleles (Figure 9C). Thus, the effect of p120 loss on tumor cell viability is not mediated through Kaiso or its ability to modulate Wnt signaling.

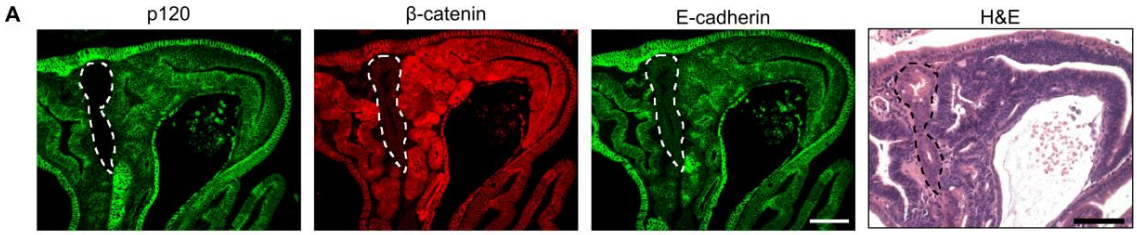

B

Background	TAM Tx	Age at Tx	Age past Tx	Tumor # analyzed	Tumors w/KO
Apc^{1638N}	3 day	1 month	8 months	52	0
Apc$^{Min/+}$	3 day	1 month	4 months	191	0
Apc$^{Min/+}$	5 day	3 months	2 days	127	37
Apc$^{Min/+}$	3 day	3 months	7 days	126	16
Apc$^{Min/+}$	3 day	3 months	1 month	93	0

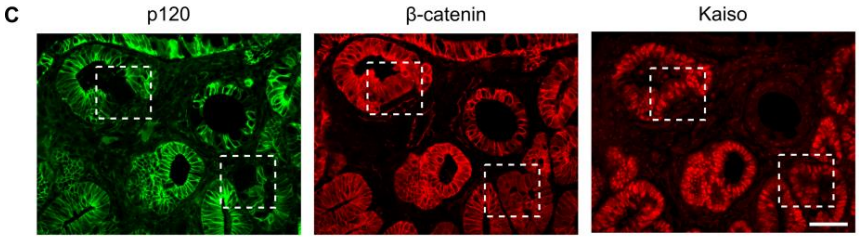

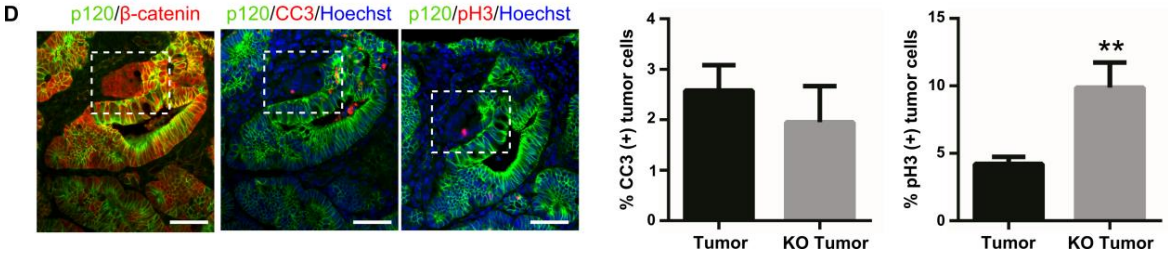

Figure 8. Tumor-specific requirement for p120 in *ApcMin* adenomas. (A) p120 KO is absent from adenomas. Analysis of 191 tumors from ApcMin p120 KO mice reveals total p120 loss was often seen near tumor tissue (dotted line), but was never adenomatous. Scale bars 100μm. (B) Forced p120 KO in established tumors results in rapid loss of null foci. In contrast to previous *Apc1638* and *ApcMin* studies, small areas of p120 KO were observed within adenoma tissue 2-7 days post TAM, yet these areas were invariably lost within 1 month. (C) Representative image shows p120 KO within adenoma tissue (boxes) with increased β-catenin and Kaiso staining, indicating adenoma tissue. Scale bar 50μm. (D) p120 KO cells are not lost due to increased apoptosis (cleaved-caspase 3) or decreased proliferation (phospho-histone H3). Staining quantified on right. Error bars represent SEM.

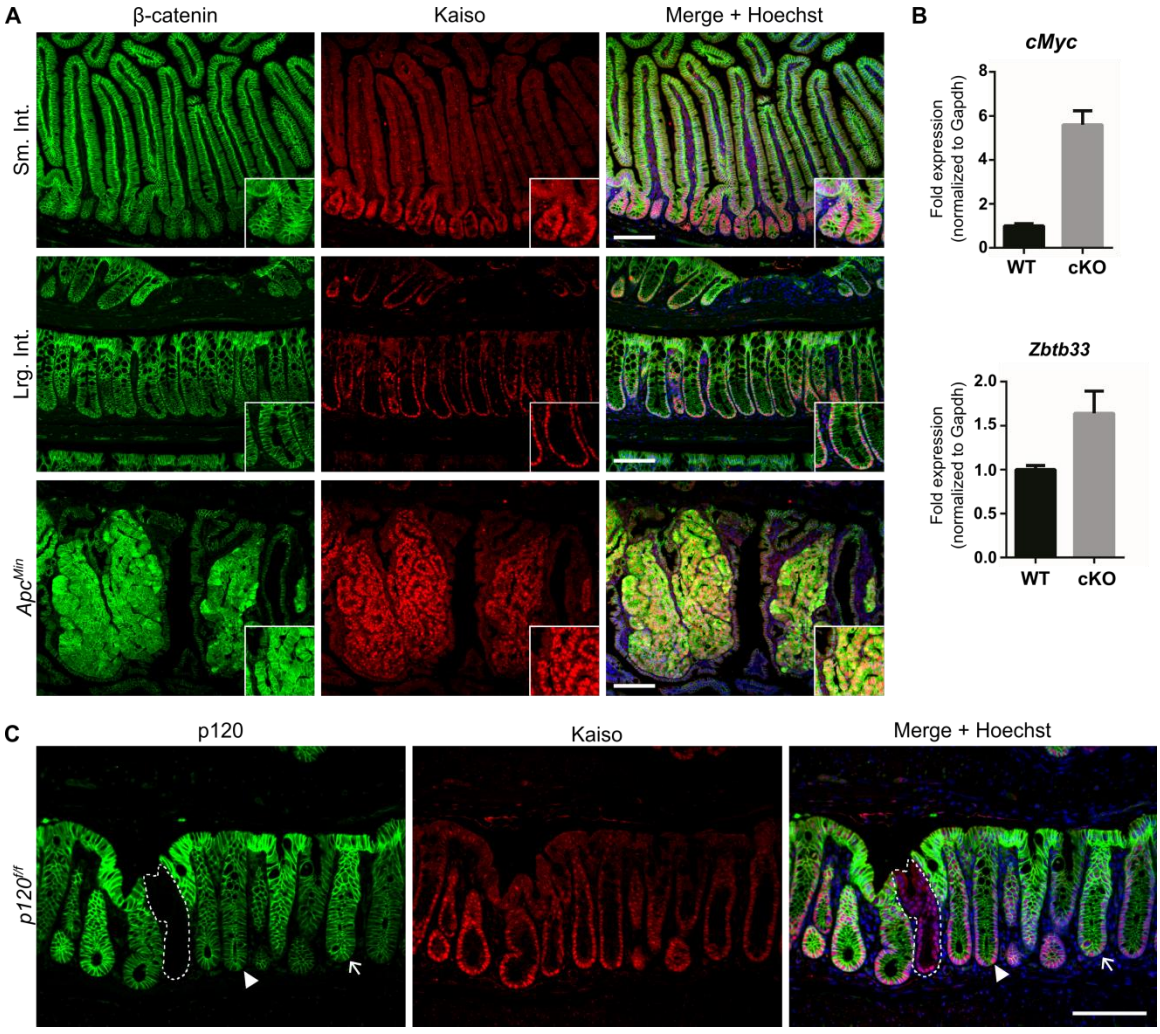

Figure 9. Kaiso staining correlates with Wnt activation irrespective of p120 expression. (A) Kaiso expression (red) is seen in the crypts of the small (top) and large intestine (middle) and overlays with high β-catenin staining (green) in *ApcMin* adenomas.(B) Kaiso (*Zbtb33*) mRNA increases following *Apc* loss in samples from day 5 *Lrig1-Cre; Apc cKO* mice. *c-Myc* = positive control (n=5 mice per group). (C) Kaiso expression remains constant despite changes in p120 levels. Representative section from limited p120 KO mouse shows Kaiso staining in the context of WT p120 (2 alleles, arrow), reduced p120 (1 allele, arrowhead), and p120 KO (outline). All scale bars 100μm.

Most proteins linked physically or functionally to p120 are tumor suppressors or oncogenes (e.g. Src, Receptor Tyrosine Kinases, E-cadherin, Rac, RhoA, chronic inflammation), thus p120 loss may dysregulate numerous growth and/or tumor associated pathways. To determine if any of these pathways or other cell death programs could explain the rapid loss of p120 null adenoma cells, extensive immunohistochemical studies were performed (Figure 10). Interestingly, common readouts for growth factor receptor activation, phos-AKT, phos-ERK, and phos-cJun, showed similar staining patterns in p120 WT and null adenoma cells. While p120 loss completely disrupts cell polarity in many cell culture and organ systems, these markers in the intestine (Crumbs3 and NaK ATPase) illustrate that p120 null adenoma cells are able to preserve normal polarity. Moreover, p120 loss was not found to induce cellular senescence by upregulation of p16, p19 or p21, nor autophagy (measured by ATG5 and LCA3). p120 loss not responsible for increased DNA damage and DNA double strand breaks (phos-H2AX), nor did it's short term loss induce the effects of chronic inflammation found in long-term p120 limited ablation models, and the short-term time points did not appear to be sufficient to induced neutrophil recruitment or Cox2 expression. Thus, the mechanism behind p120's requirement for adenoma cell viability remains unclear.

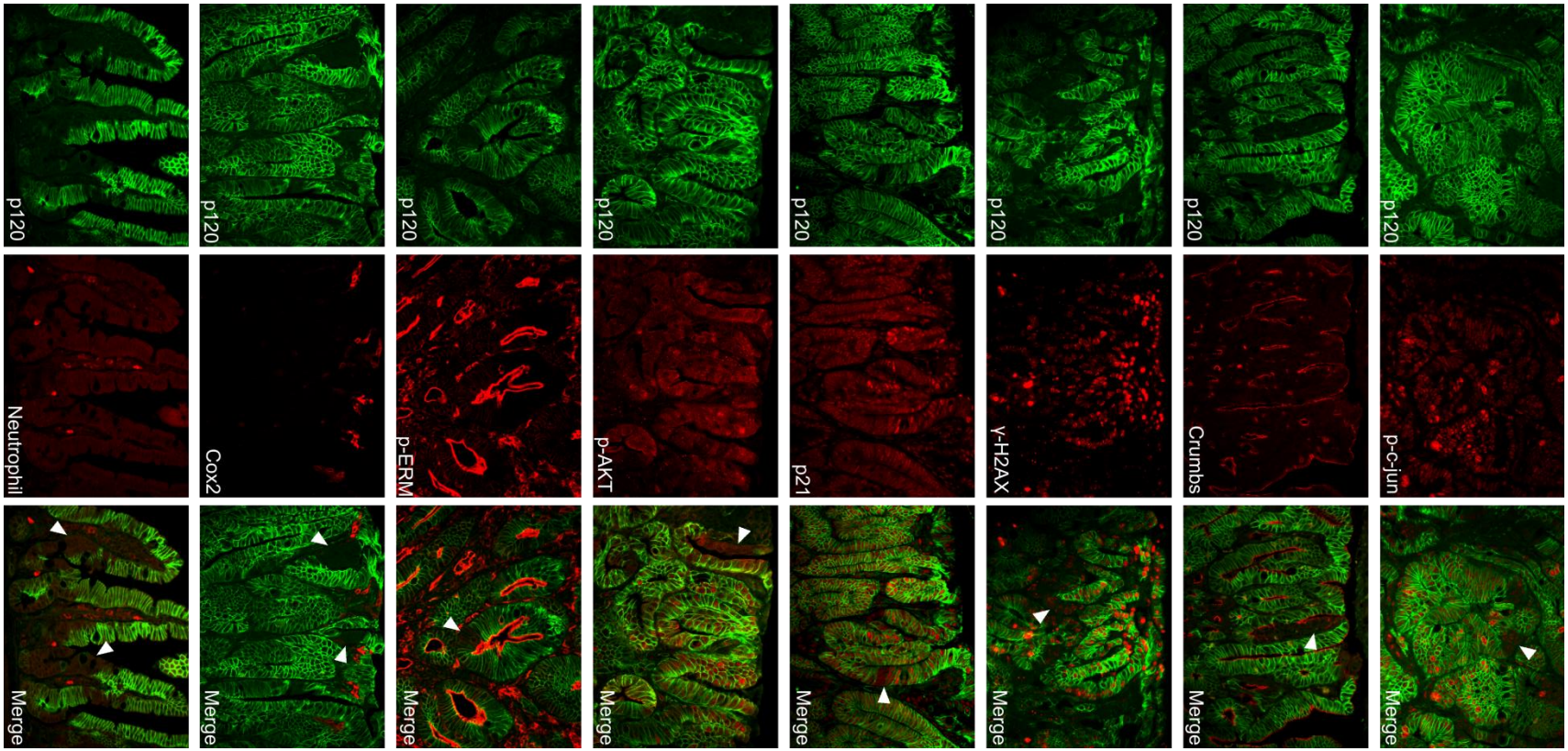

Figure 10. p120 null adenoma cells show no change in common pathway markers. Small clonal patches of p120 KO were analyzed by immunofluorescent staining. Representative images of p120 KO tumor cells (arrowheads) show p120 (green) costained with (from top to bottom) phospho-cJun, Crumbs3, phospho-H2AX, p21, phos-AKT, phospho-ERM, and Cox2. Bottom panel shows normal intestine stained with a neutrophil marker. Images show no defect in polarity or growth factor signaling specific to adenoma cells with p120 loss. Also note no increase in DNA damage, senescence, or immune cell recruitment to these areas.

Dysregulation at the level of the cadherin complex is a common denominator in intestinal tumorigenesis

p120 levels are known to determine cadherin levels via a direct binding mechanism required for cadherin stability, and α- and β-catenins are stabilized via binding to E-cadherin (Davis et al, 2003; Ireton et al, 2002). Thus, p120 ablation is typically accompanied by rapid degradation of α- & β-catenins, along with E-cadherin, which culminates with reduced cell-cell adhesion. Previously, we found reduced p120 staining in the crypt and adenoma, although this reduction is not due to a quantifiable drop in p120 levels. Furthermore, we found no change in E-cadherin or α-catenin protein, and in fact the cadherin complex appears to remain bound as determined by PLA analysis. To further characterize the relationship between p120 and cadherin complex proteins, *ApcMin* tumors and Apc cKO intestines were stained for α-catenin, β-catenin, and E-cadherin (Figure 11). While β-catenin is the obvious outlier owing to loss of APC and the subsequent inhibition of the β-catenin destruction complex, α-catenin and E-cadherin continued to track precisely with p120. Taken together with the biochemical data in Figure 4, these data suggest p120 is repositioned along with the cadherin complex in a manner that is underrepresented by fluorescent labeling methods. It is further likely that this reflects a physical and/or mechanistic change in status of the cadherin complex itself which functions as the mechanistic driver behind p120's phenotypes *in vivo*.

These experiments were originally based on the notion that p120 ablation was likely to recapitulate some or all phenotypes known to associate with loss of E-cadherin. An obvious question, particularly given p120's role in the complex, is whether the haploinsufficient phenotype reflects a role unique to p120, or a phenotype in fact dependent on the E-cadherin complex as an intact functional unit. Indeed, each of the core positions in the cadherin complex is essentially indispensable for adhesion.

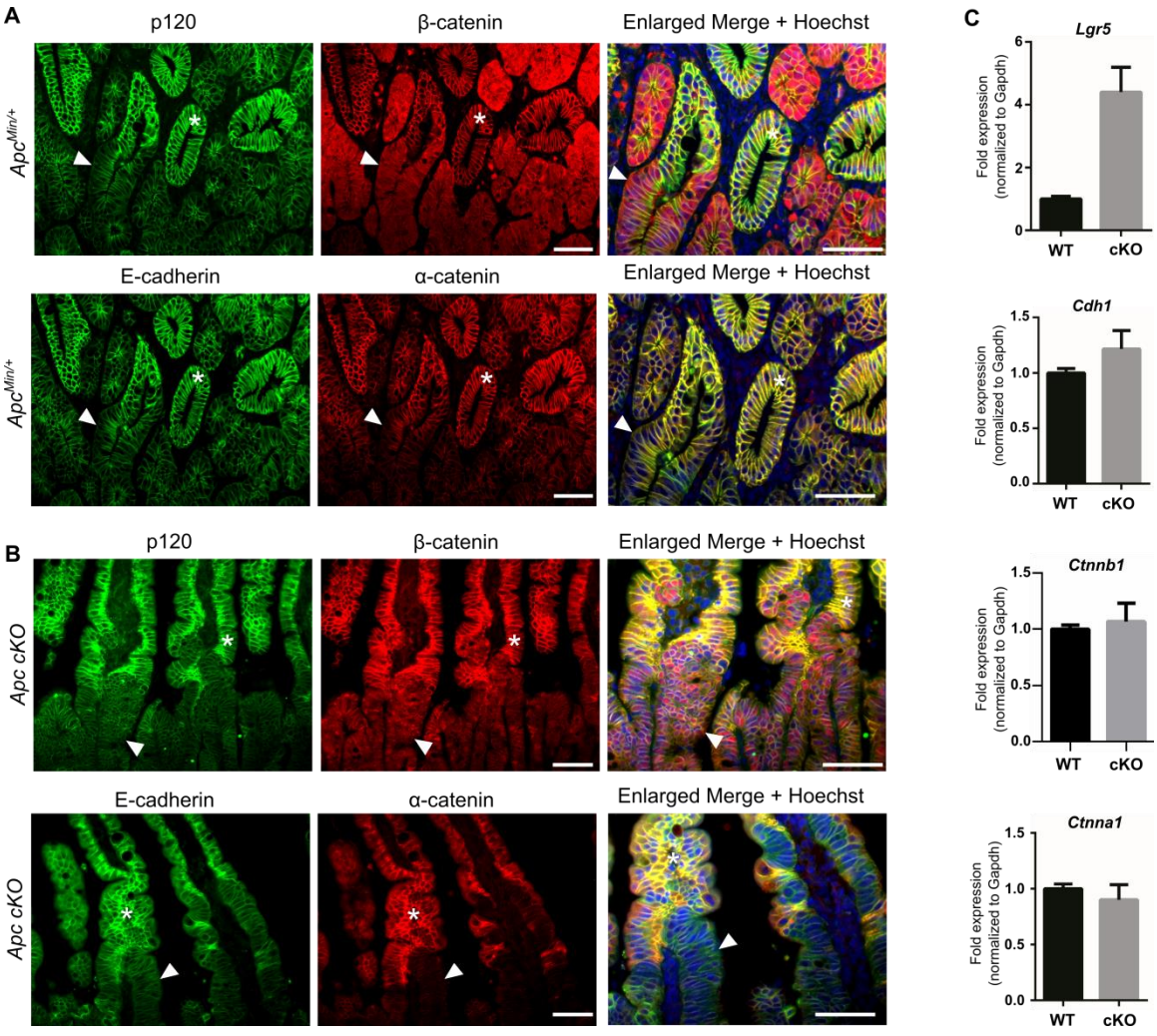

Figure 11. p120, E-cadherin, and α-catenin track together following *Apc* loss. E- cadherin and α-catenin staining is decreased along with p120 in (A) *ApcMin* tumors and (B) *Apc cKO* intestine as compared to WT tissue (asterisks). *Apc* null and tumor tissue are characterized by upregulated and/or mislocalized β-catenin (arrowhead). Scale bars 50μm. (C) Unchanged mRNA expression is seen for in all members of the cadherin complex in *Apc* cKO intestine, although the Wnt target *Lgr5* increases as expected. (n=5 mice per group). Error bars represent SEM**.** .

To address the question as directly as possible we turned to the Sleeping Beauty transposon system optimized recently by Copeland and Jenkins, and in particular, a series of SB screens targeted to the mouse intestine and conducted in the four major backgrounds predisposing toward human colon cancer. (i.e. mutant forms of *Apc*, *K-Ras*, *Smad4*, and *p53*). The system itself has been described recently in detail (Dupuy et al, 2006; Dupuy et al, 2009; Mann et al, 2012; Mann et al, 2014; March et al, 2011). Figure 12A is a schematic illustrating the transposon and a simplified summary of the mechanism(s) underlying its ability to generate both gain- and loss-of-function mutations throughout the genome by insertional mutagenesis. A manuscript describing the global analysis of these four screens is in preparation as a separate report (Neal Copeland, personal communication). Here, we extracted the relevant data for E-cadherin (*Cdh1*), p120 (*Ctnnd1*), α-catenin (*Ctnna1*), β-catenin (*Ctnnb1*) and plakoglobin (*Jub*) from all screens. Figure 12B shows raw hit data for *Apc*, *Ctnnd1* and *Ctnna1*. Genomic structures are shown in green across the center. Blue bars are individual hits and show location of mutations across the gene, and on each allele (above and below gene). In line with its role in initiation of human CRC, *Apc* was by far the most frequently hit gene in most screens (*Smad4* screen is a notable exception). Notably, the insertion patterns on *Ctnnd1* and *Ctnna1* are consistent with gene inactivation, as hits are distributed randomly across both alleles. Remarkably, the *Apc* hit map generated by SB (top panel) is all but indistinguishable from its real human counterpart, including the signature near absence of mutations on the 5' half of the upper allele. The result is a striking example of the efficacy of SB at recapitulating tumor progression with a very similar mode of action relative to forces driving human tumor progression.

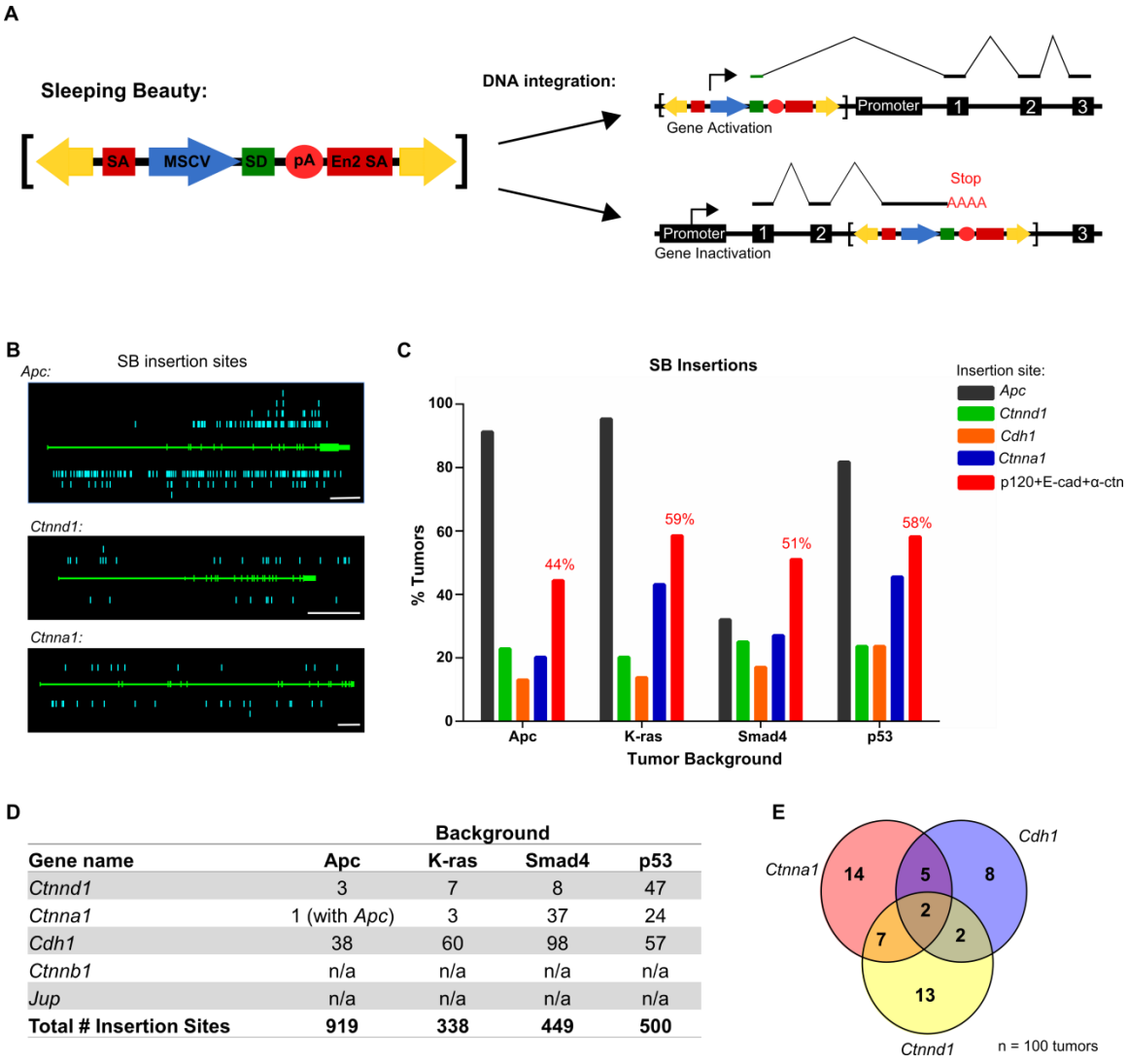

Figure 12. Dysregulation of the cadherin complex in multiple drivers of intestinal tumorigenesis. (A) Schematic of the T2Onc2 Sleeping Beauty transposon. The transposon yields "gain of function" mutations by driving transcription of nearby genes through an MSCV-driven splice donor. Insertion within a gene leads to "loss of function" by terminating transcription through a birectional-polyA signal. (B) Raw insertion sites for *Apc* compiled from all 4 genetic backgrounds (*ApcMin*, *KrasG12D*, *Smad4f/+*, and *p53R175H*) closely mimic human mutation patterns. Insertion sites for *Ctnnd1* (middle) and *Ctnna1* (bottom) in the *Smad4* SB background are consistent with gene inactivation. Scale bar 10Kb. (C) CIS analysis shows a high percentage of tumors with mutations in p120 (*Ctnnd1*), E-cadherin (*Cdh1*), and α-catenin (*Ctnna1*) in all genetic backgrounds. Collectively, mutations that target the cadherin complex (p120, E-cadherin, and α-catenin combined) were observed in close to 60% of all intestinal tumors. (D) Overall rankings for insertions of *Ctnnd1*, *Ctnna1*, *Cdh1*, *Ctnnb1*, and *Jub* in each SB genetic background. Total CISs identified in each background are shown at bottom. (E) Cadherin complex mutations were not mutually exclusive, as seen by overlapping insertions in *Smad4* SB tumors.

Key data are summarized in Figure 12C. The four screens are organized by genetic background, each of which constitutes an independently conducted screen. For each screen, hit frequencies are shown for *Apc* (black), *Ctnnd1* (green), *Cdh1* (orange), and *Ctnna1* (blue). Figure 12D shows overall rankings for each member of the complex as a function of their place in the field out of ~400 drivers identified. Because loss-of-function at any one of the three positions (i.e. p120, E-cadherin, α-catenin) inactivates the entire complex, the true impact of these mutations may be best represented by the sum of hits to these three components. This is indicated by the red bars in each set (red, Figure 12C), which show the non-overlapping sum of *Ctnnd1*, *Cdh1*, and *Ctnna1* gene insertions. The magnitude of these numbers – 44, 59, 51, and 58%, respectively for the different backgrounds, means that about half of all tumors, irrespective of genetic initiator, sustained a quantifiable tumor-promoting hit to the E-cadherin complex. While one hit should be sufficient to inactivate the cadherin complex, Figure 12E, shows that mutations to different complex components in the same tumor were not necessarily mutually exclusive, which be due to tumor heterogeneity and high selection rates in separate clonal populations. The combination of haploinsufficiency and actionable hit frequencies in roughly 50% of all tumors is extraordinary, and the mutation rate at the level of the cadherin complex is second only to major gatekeeper mutations, such as *Apc*, in each background.

Discussion

Although E-cadherin downregulation is typically viewed as a late event in intestinal tumor progression, new evidence presented here suggests that the integrity of the E-cadherin complex may be targeted/breached early and more often in the course of tumorigenesis than previously suspected. Focusing first on p120, we show here for the first time that p120 functions as an obligatory haploinsufficient tumor suppressor in the context of *Apc* LOH. Monoallelic p120 loss in an *Apc1638* background, for example, results in a 10-fold increase in tumor multiplicity, although retention of one allele appears to be a requirement for tumor growth. An obvious question, particularly given p120's cadherin stabilizing role, is whether the haploinsufficient phenotype reflects a role unique to p120, or a phenotype dependent on the E-cadherin complex as an intact functional unit. To address the question we turned to the Sleeping Beauty transposon system and a series of SB screens targeted to the mouse intestine and conducted in four major CRC predisposing backgrounds (i.e. mutant forms of *Apc*, *K-Ras*, *Smad4*, *p53*). Remarkably, p120, α-catenin and E-cadherin are consistently among the highest ranked hits, objectively highlighting the E-cadherin complex as a key mediator of tumor early progression.

The work described here was originally motivated by the notion that p120 ablation was likely to influence intestinal tumorigenesis through cell-cell adhesion defects and associated inflammation. Interestingly, both etiologies are associated with inflammatory diseases of the intestine, including Crohn's colitis and ulcerative colitis, which over time can predispose to colon cancer. Indeed, previously we found that limited p120 KO in the intestine by itself was sufficient to generate tumors in 45% of the animals (Smalley-Freed et al, 2011). While none of these tumors were null for p120, local inflammatory effects were clearly generated by p120 null tissues, which appeared to account for increased mutation and tumorigenesis. Indeed, p120 clearly has a cell autonomous role in controlling inflammation, and in some tissues, such as the esophagus, inflammation induced by p120 ablation is capable of generating invasive tumors (Stairs et al, 2011). Nonetheless, the contribution of p120 loss to inflammation seems to vary widely according to tissue and its role in intestinal tumorigenesis remains ill-defined.

To clarify the contribution of p120 to intestinal tumor development, we turn to well-established mouse models of intestinal tumorigenesis (Fodde et al, 1994; Moser et al, 1990). Here, we report that limited p120 ablation in *Apc1638* mice containing floxed p120 alleles (*p120 f/f*) resulted in a 10-fold increase in tumor multiplicity. As tumors were found to be monoallelic for p120, we suggest a haploinsufficient tumor suppressor role. Surprisingly, inflammation does not seem to play a major role in driving the increase in tumor multiplicity in these studies. By substituting a p120 heterozygous mouse for the *p120f/f* mouse required for outright ablation, local inflammation induced by p120 negative areas was eliminated altogether. In these cases, an essentially identical increase in tumor multiplicity (relative to controls) was observed despite the absence of p120 ablation. Loss of one p120 allele being the only remaining variable, it appears that the haploinsufficient phenotype is a direct function of monoallelic loss and cannot be significantly dependent on inflammation or potential unknown derivatives of the p120 null microenvironment.

In our limited p120 KO tumor studies, loss of the second allele was never observed within the tumor tissue and turns out to be selectively incompatible with tumor viability. The outright absence of p120 null cells in the context of the adenoma is striking, and holds true for all tumors analyzed to-date. Interestingly, p120 null foci can be induced transiently by tamoxifen and are readily detectable in tumors harvested early (1 week post TAM), but not late (1 month). Thus, it appears that the tumor cells are selectively dependent on p120 for survival and those without are rapidly eliminated. These findings reveal an obligatory haploinsufficient tumor suppressor role for p120, as loss of one p120 allele strongly promotes tumorigenesis yet retention of the second allele is likely a process of selection given that the cells are dependent on it to survive. The phenomenon was recently termed “nononcogenic addiction” after the better known “oncogenic addiction”, reflecting the potential therapeutic window of opportunity afforded by the tumor-specific requirement for p120 (Luo et al, 2009; Solimini et al, 2007). Interestingly, this is not the first time we have encountered a transformation-specific requirement for p120. While its KD is normally well tolerated, p120 is essential for tumorigenesis (i.e., anchorage independent cell growth) in MDCK cells transformed by Src- and Rac1- but not H-Ras (Dohn et al, 2009). Thus, Apc, Src and Rac1 all appear to require p120 for tumorigenic transformation.

Further analyses of SB insertional mutagenesis screens provide strong support for a haploinsufficient tumor suppressor role for p120, as well as α-catenin and E-cadherin. Strikingly, 40-60% of all intestinal tumors generated by SB contained at least one inactivated allele of p120, α-catenin or E-cadherin, irrespective of the initiating genetic background. Thus, our evidence strongly suggests that the integrity of the E-cadherin complex is breached early and often in the course of intestinal mutagenesis, such that monoallelic loss at any of these three loci is sufficient to substantially accelerate tumor progression. Moreover, previously published studies from both Fodde and Noda provide strong independent support for obligatory haploinsufficiency as the mode of action for these proteins (Shibata et al, 2007; Smits et al, 2000). Indeed, E-cadherin heterozygousity in the *Apc1638* model leads to an almost identical increase as reported in Figure 5, and α-catenin is likewise shown to be required for tumorigenesis in *Apc* mutant mice.

Importantly, the SB system vastly accelerates the random accumulation of mutations genome-wide in a fashion that closely approximates the forces at work in human tumors. Tumorigenic events are self-selecting in that they promote tumors, thus more efficient tumor promoting mutations are found more frequently. The final tally of drivers emanating from each screen, therefore, is effectively a top to bottom quantitatively-significant ranking of tumorigenic potency. Remarkably, in the field out of >400 drivers identified, α-catenin and p120 are ranked 2nd and 3rd in the *Apc*-sensitized background, with E-cadherin still in the top 4% (March et al, 2011). These results were relatively consistent in all backgrounds tested. Given that appear to be obligatory haploinsufficient, it seems that their impact on tumorigenesis/progression is mediated at the level of the E-cadherin and best represented by the sum of their hits. Remarkably, the collective hits to p120, E-cadherin, and α-catenin are second only to the primary gatekeepers and suggest an important role for the cadherin complex in early tumorigenesis directly downstream of tumor initiation.

While just one mutation should serve to inactivate the cadherin complex, mutations to different complex components in the same tumor are not mutually exclusive. However, the data returned by SB is in the form of hits per gene per tumor, and thus it cannot distinguish separate hits in two different cells in a tumor (i.e. haploinsufficiency) from hits on both alleles in the same cell (i.e. classic tumor suppressor mechanism). Interestingly, our finding of obligatory haploinsufficiency for p120 is key to interpreting this data, as we establish that hits to both p120 alleles is not tolerated following *Apc* LOH. This leaves haploinsufficiency as the only option available to SB for p120, α-catenin, and E-cadherin. Accordingly, the E-cadherin complex can be inactivated by single hits on either of two alleles for each of these three genes, as all six alleles inactivate the same complex.

Although E-cadherin downregulation is typically viewed as a late event in intestinal tumor progression, new evidence presented here suggests that the integrity of the E-cadherin complex is among the earliest and most important barriers breached in the course of intestinal tumorigenesis. Given that several components of the same complex have roughly equivalent monoallelic phenotypes, we suggest that the activity of the cadherin complex *en toto* is the functional unit of selection for Sleeping Beauty and the ultimate mechanism behind the tumor-promoting effects observed in p120 tumor models. Late stage alterations to the cadherin complex are well characterized and often mark a definitive transition to malignancy. Our data suggest that the E-cadherin complex is compromised both early and late over the course of tumor progression and highlight the global importance of their collective tumor suppressor roles.

CHAPTER IV

POTENTIAL ROLES FOR KAISO IN INTESTINAL HOMEOSTASIS AND CANCER

Introduction

Colorectal cancer (CRC) is the third leading cause of cancer-related deaths in the United States, estimated to cause over 50,000 deaths in 2014 (Siegel et al, 2014). Strikingly, almost 80% of spontaneous CRCs appear to be initiated by mutations in a single gene, the Adenomatous Polyposis Coli tumor suppressor gene (*APC*) (2012; Fearon & Vogelstein, 1990). The protein product of this gene, APC, negatively regulates the Wnt pathway by degrading excess cellular β-catenin as part of a large protein complex with AXIN1, GSK3β, CK1α, and β-TrCP (reviewed in (Clevers & Nusse, 2012)). Under normal Wnt ligand-induced activation, this complex is inhibited, which permits the accumulation and nuclear translocation of β-catenin, where it binds to TCF/LEF transcription factors to initiate transcription. In the intestine, active Wnt signaling is necessary to maintain the intestinal stem cell population (ISCs) by controlling powerful regulators of proliferation, differentiation, and stemness, such as *c-Myc*, *CyclinD1*, *Ascl2*, and *Lgr5* (reviewed in (Schepers & Clevers, 2012)). Importantly, loss of APC inactivates the β-catenin destruction complex, leading to constitutive activation of the Wnt pathway, unchecked proliferation, and rapid cell transformation (Sansom et al, 2004).

Originally identified as a binding partner of p120-catenin (p120), Kaiso (ZBTB33) is a member of the BTB/POZ-ZF (broadcomplex, tramtrack, bric-a-brac/poxvirus and zinc finger) subfamily of transcription factors (Daniel & Reynolds, 1999). Historically, Kaiso has been shown to bind both an unmethylated consensus sequence (KBS) and methylated CGCG motifs (Buck-Koehntop et al, 2012b; Daniel et al, 2002; Prokhortchouk et al, 2001; Ruzov et al, 2004), and is thought represses such genes as *MMP7* (matrilysin), *BCL6*, *CDKN2A* (p16), *Wnt11*, and *CyclinD1* through both KBS- and CGCG-mediated mechanisms (Donaldson et al, 2012; Kim et al, 2004; Koh et al, 2013; Lopes et al, 2008; Spring et al, 2005). Interestingly, Kaiso's methyl-binding ability is rather unique, as the Kaiso family proteins (Kaiso,

ZBTB4, and ZBTB38) are one of only 3 protein groups known to bind methylated DNA. Thus Kaiso and its family are suspected to have broad roles in chromatin maintenance and epigenetic regulation (Defossez & Stancheva, 2011; Fournier et al, 2012; Sasai et al, 2010a).

Kaiso's repressor function is further mediated by its protein binding partners. Kaiso has been shown to form repressive complexes with N-CoR, HDAC1, and MTG16, and is able to modulate function of CTCF (Barrett et al, 2012; Defossez et al, 2005; Iioka et al, 2009; Yoon et al, 2003). However, despite being the first Kaiso-binding partner identified, p120's interaction with Kaiso is still poorly understood. p120 has long been thought to inhibit Kaiso's transcriptional roles, as all three zinc fingers are required for p120 binding which would preclude simultaneous binding to DNA (Daniel & Reynolds, 1999). Functional studies have since shown p120 can indeed mediate Kaiso-induced transcriptional changes, either by competitive binding or by inhibiting Kaiso through cytoplasmic sequestration (Kelly et al, 2004; Kim et al, 2004; Park et al, 2006; Spring et al, 2005). Interestingly, Kaiso has also been reported to bind p120 family member δ- catenin and appears particularly important to neural development (Rodova et al, 2004).

Importantly, over the past decade Kaiso has been implicated in canonical Wnt signaling through multiple mechanisms. Kaiso is thought to directly regulates canonical Wnt targets such as *c-Myc*, *c-Fos*, *Siamois*, and *CyclinD1* (Donaldson et al, 2012; Park et al, 2005), as well as mitigate Wnt-dependent transcription through interactions with TCF3/TCF4 which disrupts their interactions with β-catenin and/or target promoters (Park et al, 2005; Ruzov et al, 2009). While most studies are in agreement that Kaiso functions to negatively regulate of Wnt signaling, others have shown more pleiotropic roles. Interestingly, studies from Iioka et al. demonstrate that Kaiso is able to regulate Wnt in a bi-modal fashion, and can activate or inhibit the pathway based on Kaiso amount and context (Iioka et al, 2009). Thus, broad conclusions about Kaiso's precise role in Wnt signaling may be premature, yet a functional interaction between the two pathways is well-supported.

Interestingly, as opposed to the negative role reported in the majority of cell culture models, *in vivo* and pathology studies mostly suggest a positive role for Kaiso in Wnt and protumorigenic signaling. In mice, global Kaiso knockout is apparently well tolerated and Kaiso null mice show no discernable differences from their WT littermates. However, when combined with the *ApcMin* tumor model, Kaiso loss mediates a protective phenotype, which delayed tumorigenesis and extended survival (Prokhortchouk et al, 2006). Conversely, Kaiso overexpression leads to dramatic alterations in tissue structure and cell differentiation (Chaudhary et al, 2013). Furthermore, increased Kaiso expression has also been reported in tumors from the breast, lung, and prostate, and is often associated with aggressiveness and decreased prognosis (Dai et al, 2009; Jones et al, 2014; Jones et al, 2012; Vermeulen et al, 2012). Thus, these studies point to a tumor promoting role for Kaiso, and furthermore a relevance to cancer formation and progression in a variety of tissues.

In addition to the Wnt pathway, Kaiso has other reported functions that may contribute to its protumorigenic effect. For example, Kaiso has been linked to p53, apoptosis, and DNA damage responses, and a study by the Melnick group found that Kaiso loss sensitizes CRC cells to chemotherapy by allowing expression of methylated tumor suppressors such as *CDKN2A* (Lopes et al, 2008). Importantly, this function in DNA methylation may be particularly relevant to CRC. While virtually all colon tumors display abnormally methylated genes, a unique molecular subgroup displays a CpG island methylator phenotype (CIMP) with an unusually high rate of gene methylation. (Lao & Grady, 2011). The putative Kaiso target gene, *CDKN2A*, is one such gene commonly silenced in CIMP (+) tumors. Taken together, these studies suggest many opportunities for Kaiso to influence CRC progression and therapeutic strategies, although its exact contribution to intestinal tumorigenesis is yet unknown.

Here, we describe for the first time Kaiso expression and localization in normal and transformed intestinal epithelium. Interestingly, these results show Kaiso is most highly expressed in areas dependent on robust Wnt activation (i.e. crypt and adenoma). While this observation makes Kaiso a likely target of Wnt gene induction, cell culture experiments fail to show a direct correlation between Wnt activation and Kaiso expression. Furthermore, in spite of numerous studies to the contrary, Kaiso itself did not dramatically alter downstream Wnt signaling as measured by either TOPFlash or Wnt target induction in CRC cell lines.

However, we found that Kaiso may contribute to Wnt regulation through inhibition of BMP signaling. To gain better insight into Kaiso's role in tumor formation and identify CRC-relevant target genes, we queried a large ChIP-seq dataset publically available through the Encyclopedia of DNA Elements (ENCODE) database. Surprisingly, these studies resulted in the identification of a new consensus site for Kaiso binding (eKBS), and we verified two such targets, HNRNPK and BANP, as likely targets of Kaiso repression in the intestine. Thus, while Kaiso's role in tumorigenesis is still unknown, these data add new complexity to the Kaiso literature while high-lighting Kaiso's context-specific nature.

Results

Kaiso has been implicated in multiple pathways relevant to tumorigenesis, including transcriptional control of tumor suppressors, Wnt signaling, apoptosis, proliferation, and invasion. Furthermore, Kaiso expression is often increased in epithelial cancers, and this expression correlates with increased tumor aggressiveness and poor prognosis. However, Kaiso's exact contribution to tumorigenesis is poorly understood and whether it represents a potential therapeutic target in CRC is still unknown.

Kaiso is expressed in proliferative zones in the intestine

To study Kaiso in the context of the intestine, we first characterized its expression in both normal and transformed tissues (Figure 13). As the majority of studies to-date which link Kaiso to the Wnt pathway has suggested an inhibitory role, we were surprised to see that Kaiso is predominantly expressed in nuclei of the crypt region. A decrease in staining is observed at the crypt neck, and thus Kaiso loss appears to correlate with the transition to differentiation and quiescence (Figure 13A). However, Kaiso expression is not solely limited to proliferative cells, as seen in Figure 13B. While Ki67 staining marks proliferating cells, mostly found in the transit amplifying region, nuclear Kaiso expression can be seen in every crypt cell regardless of proliferative status. Nor is Kaiso limited to undifferentiated cells, and expression is clearly seen in terminally-differentiated Paneth and CBCs. Kaiso expression was highly elevated in transformed cells, and expression is readily apparent in adenomas from both *ApcMin* and

Apc1638 mouse models (Figure 13A,). Interestingly, Kaiso appears to be an immediate consequence of transformation and robust staining can be noted even in the smallest microadenomas, as seen in Figure 13C.

To determine if the change in Kaiso staining reflected alterations at the protein and/or mRNA level, homozygous *Apc* floxed mice were crossed with an *Lrig1-CreER* driver (*Apcf/f; Lrig1-CreER,* aka Apc cKO) to allow synchronous *Apc* ablation and cell transformation across the entire intestinal epithelium (Powell et al, 2012; Shibata et al, 1997). Western blot and qRT-PCR analysis from this tissue reveal increased Kaiso expression in both protein (Figure 13D) and mRNA (Figure 13E). Interestingly, this expression pattern is highly suggestive of Wnt-driven transcriptional upregulation.

To determine if Kaiso expression was likewise increased in human intestinal tumors, a set of 151 small polyp samples was obtained through the Vanderbilt Translational Pathology Shared resource and serial sections were stained for Kaiso and β-catenin (Figure 14). Because staining in murine tumors was almost exclusively nuclear, we were surprised to see increased Kaiso expression with both cytoplasmic (Figure 14A) and nuclear localizations (Figure 14B). Indeed, both staining patterns occurred at similar frequencies (Figure 14C) and most often both localization patters were found in different areas of the same tissue sample. All told, Kaiso appeared to be upregulated in the epithelial cells of ~68% of polyp samples, suggesting early human tumors shows a similar phenotype as found in our *Apc* mutant mouse models. Interestingly, a subset of these samples also showed clear Kaiso staining in the infiltrating immune cell populations (Figure 14B, arrowhead), although the significance of this expression is unknown.

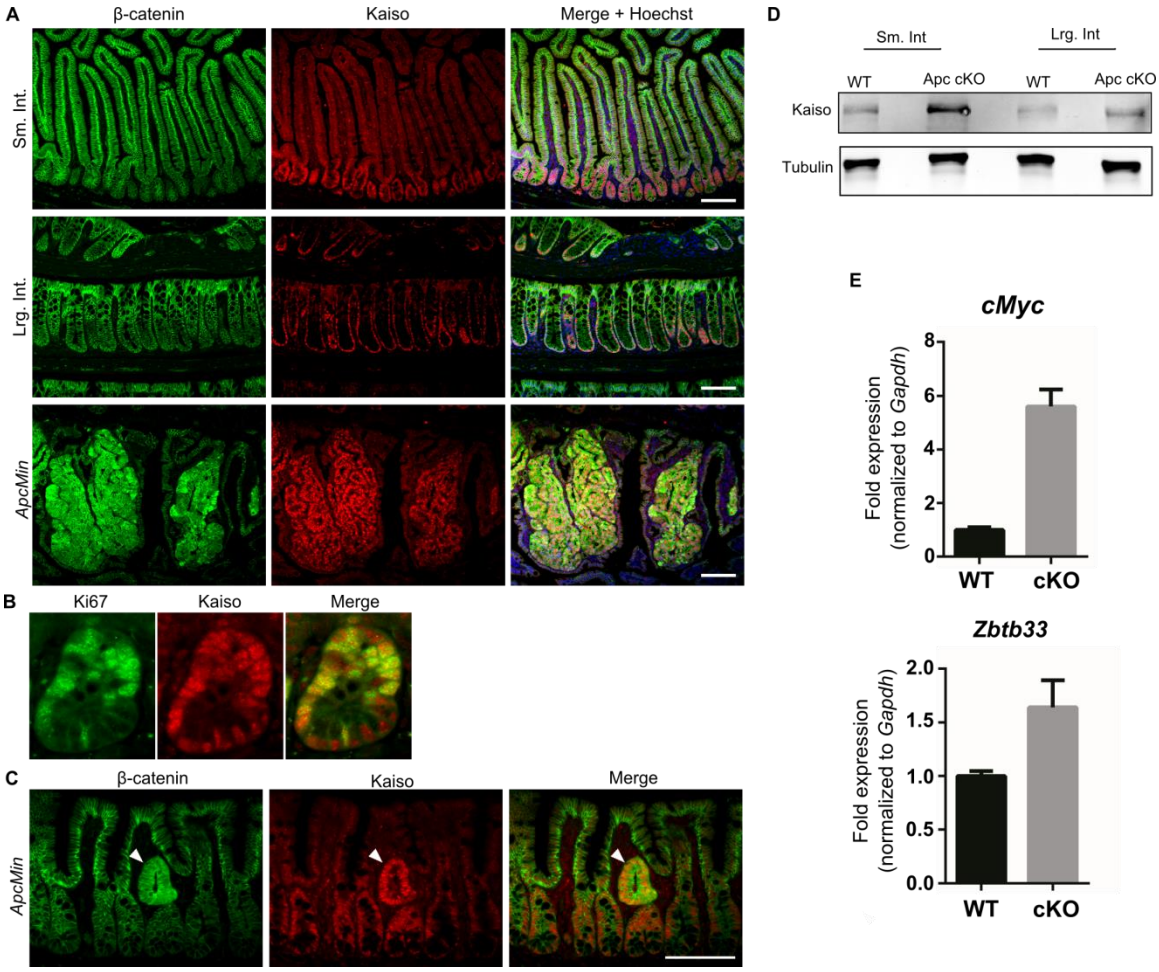

Figure 13. Kaiso is highly expressed in areas of Wnt activation in the intestine. (A) Sections of WT small intestine (top), large intestine (middle), and *ApcMin* adenoma (bottom) were analyzed by fluorescent immunohistochemistry for Kaiso (red) and β-catenin (green). (B) Single intestinal crypt stained for Ki67 (green) and Kaiso (red) (C) Microadenoma (arrow) shows concurrent increase in β-catenin (green) and Kaiso (red) expression. All scale bars = 100μm (D) Protein lysates from *Apc* null intestine show increased Kaiso protein by WB. Tubulin was used as a loading control. (E) mRNA analysis of *Apc* null intestine shows increased expression of *c-Myc* (positive control) and *ZBTB33*.

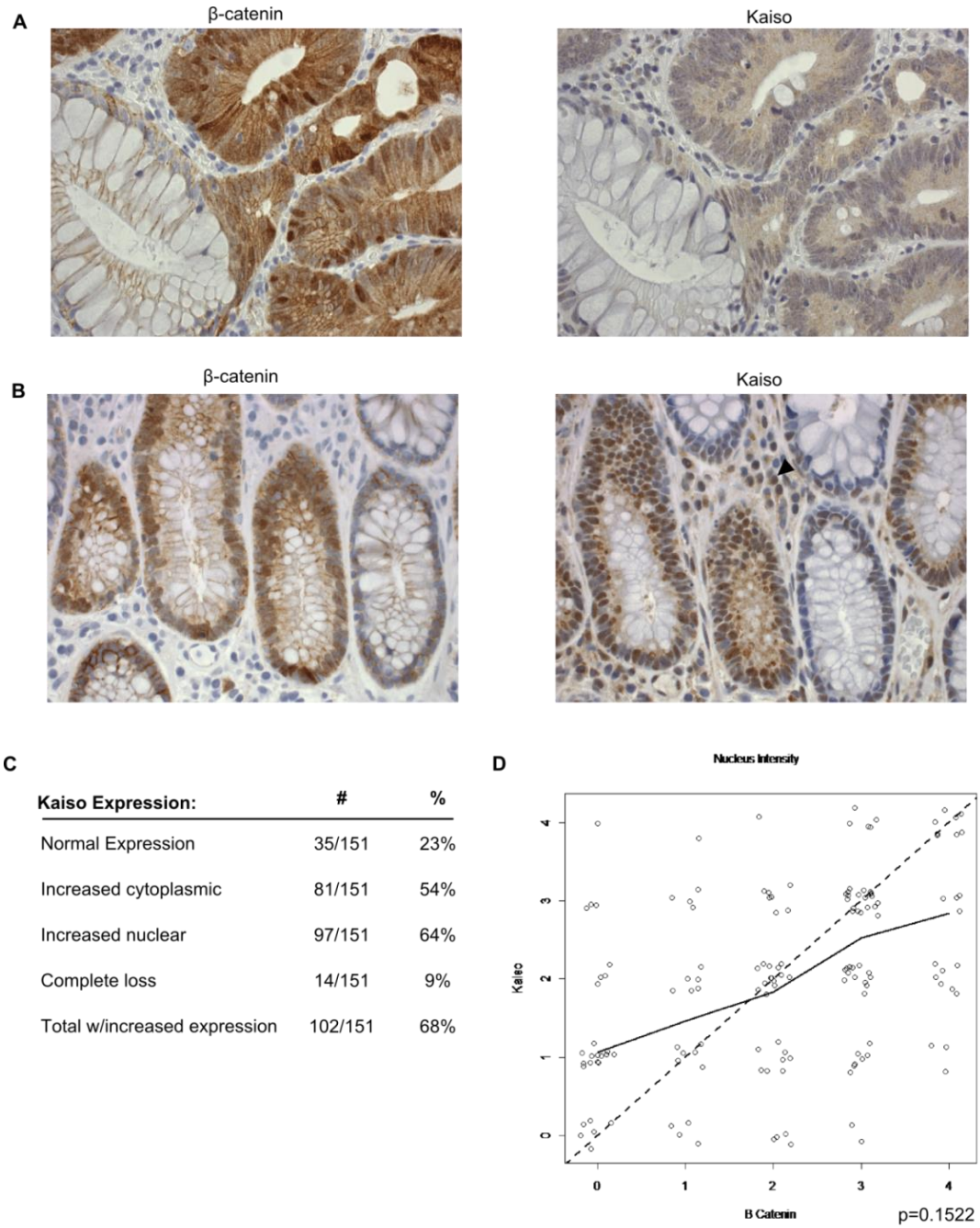

Kaiso Expression:	#	%
Normal Expression	35/151	23%
Increased cytoplasmic	81/151	54%
Increased nuclear	97/151	64%
Complete loss	14/151	9%
Total w/increased expression	102/151	68%

Figure 14. Kaiso is increased in human small adenoma samples. Serial sections from 151 small adenoma samples were stained for β-catenin and Kaiso. Kaiso staining in the adenoma showed both (A) cytoplasmic and (B) nuclear expression. Staining could also be observed in infiltrating immune cells (arrow) in some samples. (C) Kaiso expression breakdown in all samples based on staining intensity and localization. (D) Agreement report between β-catenin and Kaiso nuclear intensities shows no direct correlation.

Interestingly, the above data suggest that Kaiso may be a direct transcriptional target of Wnt activation. To investigate this hypothesis more closely, the human IHC samples were scored on a 0-4 expression scale (0 = negative, 1 = faint expression, 2 = low expression, 3 = moderate expression, and 4 = high expression). As seen in Figure14D, agreement between Kaiso and β-catenin intensity scores was not significant. These results were also recapitulated at a single cell level through collaboration with GE and the use of MultiOmyx imaging analysis (data not shown). This technology is unique in that it allows sequential fluorescent staining of the same sample with numerous probes, allowing quantitative colocalization of multiple markers in a single cell analysis (Nelson et al, 2013). As seen with the standard IHC approach, while Kaiso expression correlated regionally with increased β-catenin, it was not dependent on nuclear beta catenin expression on a cell-by-cell basis (McCulloch, personal communication). Taken together these data suggest Kaiso expression may be dependent on Wnt activation, but is likely not a direct target.

Kaiso expression is not dependent on Wnt activation

Most mouse and human IHC studies broadly suggest that Kaiso expression is dependent on canonical Wnt pathway activation. To directly test for Wnt-based regulation of Kaiso transcription, a panel of CRC cell lines was used for *in vitro* analysis (Figure 15). Cells were utilized to represent much of the CRC progression spectrum, and included HEK293 (human embryonic kidney), IEC6 (normal rat intestine), HT29 (well-differentiated colorectal carcinoma), CaCo2 (moderately differentiated colorectal carcinoma), and HCT116 (poorly-differentiated colorectal carcinoma). Cell lines were treated with Wnt3a conditioned media for 24-72 hours and assayed for Kaiso and Wnt target-gene expression. While it is important to note than some of these cell lines are unresponsive to Wnt due to pathway mutation, none of the cell lines exhibited an increase in Kaiso protein. (Figure 15A). Kaiso mRNA levels also remain unchanged even after 3 days of continuous Wnt stimulation, despite clear induction of the Wnt target *AXIN2* (Figure 15B).

Conversely, to determine if Wnt inhibition could downregulate Kaiso expression, Wnt signaling was ablated through stable infection of a DN-TCF4 lentiviral construct in which the N-terminal activation domain has been removed (Fuerer & Nusse, 2010). In agreement with complete shut-down of TCF4 mediated transcription, *AXIN2* mRNA drops to almost undetectable levels, particularly in cell lines with constitutive Wnt pathway mutations. Again, no change in Kaiso expression was detected via protein or mRNA (Figure 15C and 15D). Interestingly, recent studies have shown that Notch activation is important for stem cell activity and may be a mechanism through which Paneth cells help to maintain the ISC population (reviewed in (Clevers & Bevins, 2013)). To determine if Notch signaling was able to modulate Kaiso expression, cells were treated with a γ-secretase inhibitor (DAPT), which inhibits Notch signaling by preventing the formation of the Notch C-terminal domain (NCID). As expected, treatment dramatically increases mRNA levels *ATOH1* and *SPDEF*, which are normally subject to Notch-base inhibition. However, only a subtle increase in Kaiso was observed (Figure 15E and 15F). Thus, despite Kaiso's high expression in areas of Wnt activation, it is unlikely that Kaiso is directly controlled by the Notch or Wnt signaling cascades, and thus the mechanism of its regulation remains unclear.

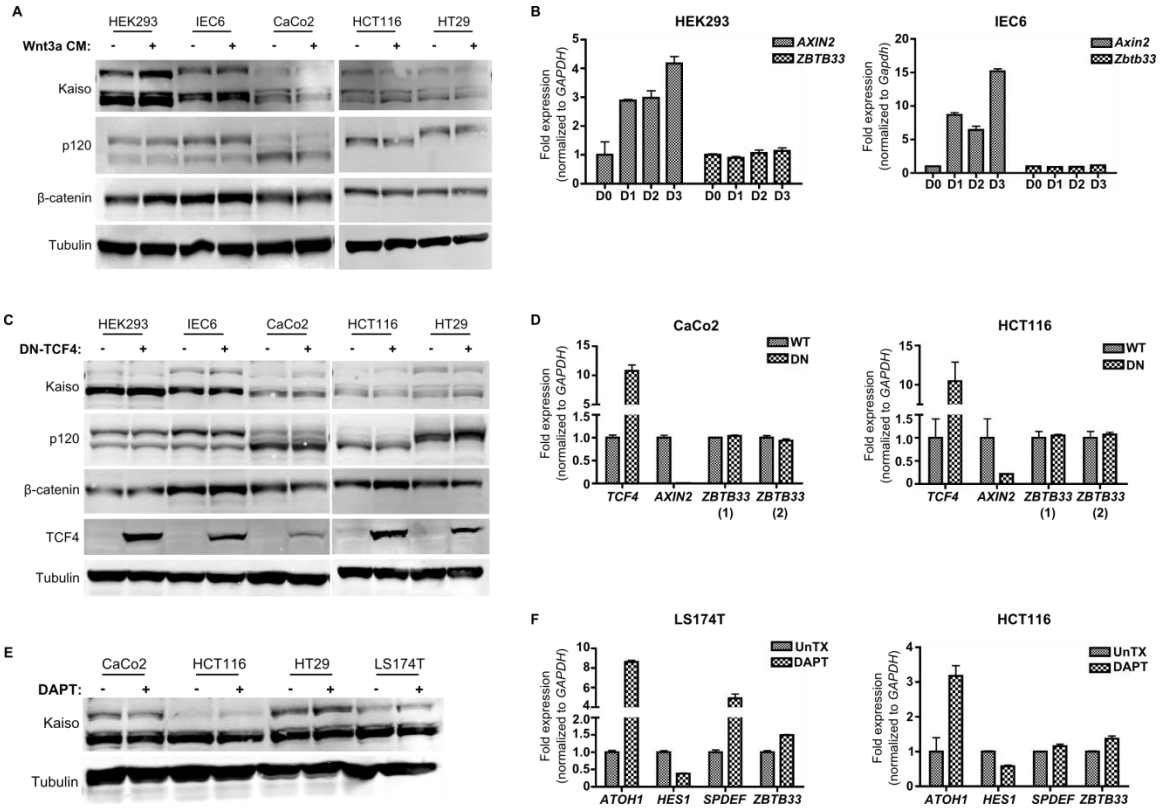

Figure 15. Wnt activity does not directly regulate Kaiso expression. Cell lines were treated with Wnt3a or control CM and analyzed after 24 hours for Kaiso (A) protein or (B) mRNA. Kaiso showed no change even though *AXIN2* mRNA was clearly induced. (C) Inactivating Wnt through expression of a dominant negative TCF4 (DN-TCF4) yields no change in Kaiso protein or (D) mRNA. Kaiso mRNA expression was queried with two separate qRT-PCR primer sets. (E) Cells were treated with 5μM DAPT or DMSO for 24 hours. Little change in protein or (F) mRNA levels.

Investigating Kaiso function in the intestinal epithelium

To begin to elucidate Kaiso function in the intestine, we developed a series of CRC cell lines with altered Kaiso expression through both shRNA-mediated knockdown and lentiviral overexpression (Figure 16). Interestingly, these modifications often yielded only modest changes in Kaiso protein (Figure 16A), and the results were highly variable between cell lines. As seen in Figure 16C and 16D, Kaiso overexpression in the SW480 line results in higher nuclear expression in almost all cells, while overexpression is barely detect in LS174T cells, if at all, despite cell growth during drug selection. An intermediate phenotype is illustrated by HCT116 cells, where overexpression results in both cytoplasmic and nuclear expression in a much smaller portion of cells.

Kaiso KD, while still variable, was more consistent. Five Sigma Mission shRNA constructs were tested, and one construct, #1539, consistently yielded the best knockdown results in almost all cell lines, followed by #2600 and #358. Thus, these constructs were designated shRNA-1, shRNA-2, and shRNA-3 respectively for use in future experiments. As seen in figure 16A, substantial knockdown could be obtained in HCT116, HT29, and SW480 cells. However, KD lines were attempted with CaCo2 cells and LS174T cells, but these attempts resulted in widespread cell death and no yielded no detectable KD in the puromycin-selected populations. It is tempting to speculate that these cells are somehow dependent on Kaiso expression. Thus, while useful to study the role of Kaiso in CRC, development of these tools further highlight the variability of Kaiso expression and regulation.

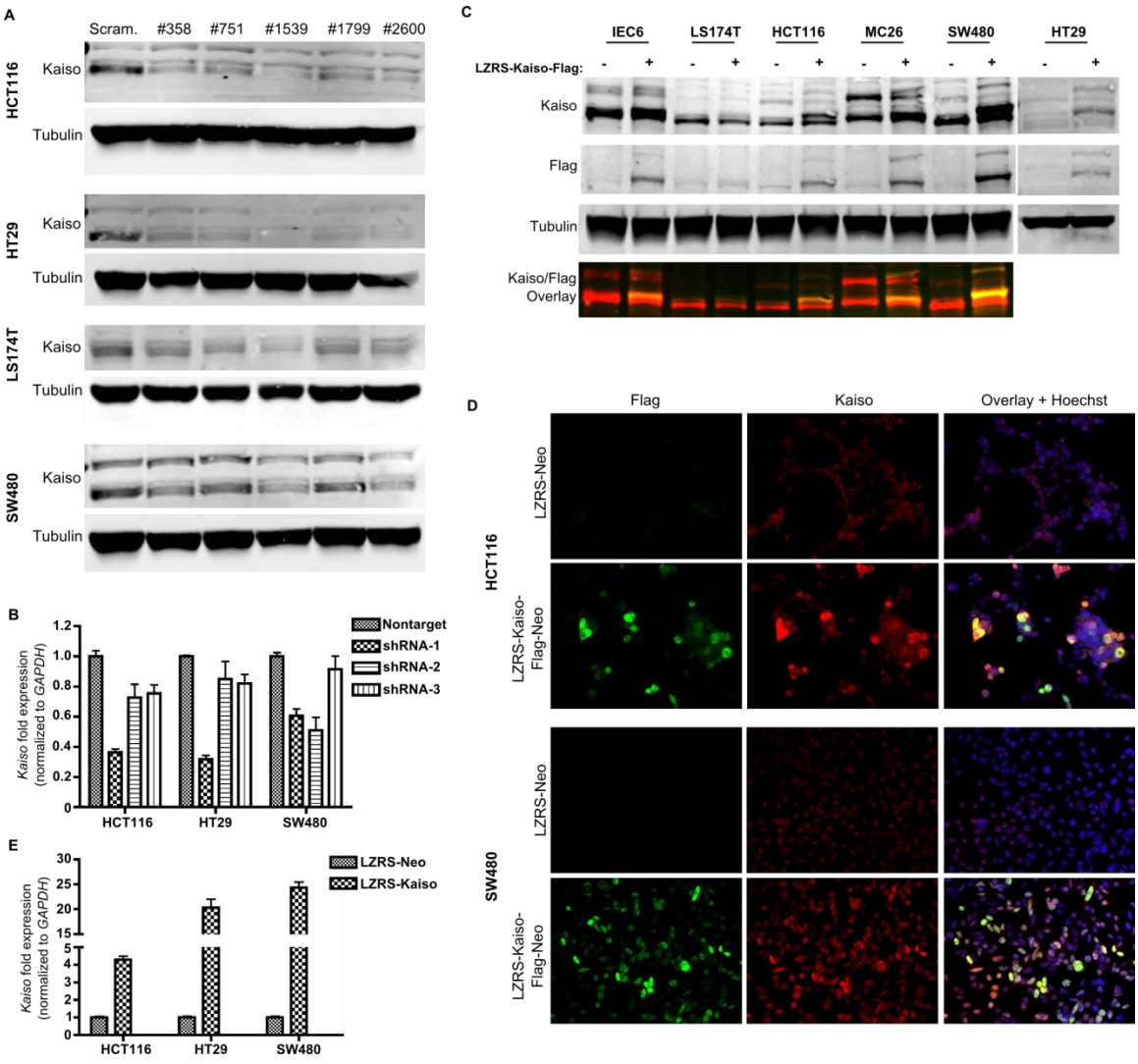

Figure 16. Development of Kaiso knockdown and overexpressing cell lines. (A) CRC cells were infected with 5 shRNA constructs to mediate Kaiso KD along with a scrambled, nontarget control. Protein expression after selection is shown via WB. (B) 3 best KD constructs analyzed for Kaiso mRNA. shRNA1 = #1539, shRNA2 = #2600, shRNA3 = #358. (C) Cell lines were infected with LZRS-Neo-Kaiso-Flag construct. Kaiso and Flag expression is analyzed by WB. Overlay clearly shows presence of Kaiso-flag protein in some cell lines. (D) Cells were stained for Flag tag (green) and Kaiso (red). Localization and amount of overexpressing cells varied between cell lines. (E) mRNA analysis of Kaiso overexpression.

Kaiso does not directly influence Wnt signaling transduction

Kaiso is consistently reported to attenuate Wnt signaling. To determine if Kaiso can inhibit Wnt in CRC cell lines, Kaiso KD and OE cells were tested for Wnt-responsiveness by functional and transcriptional readouts (Figure 17). TOPFlash experiments in RKO cells show no change in Wnt-based readouts upon Kaiso knockdown using either Wnt3a conditioned media or LiCl, which highly activates Wnt-mediated transcription by inhibiting GSK3β (Figure 17A). Likewise, Kaiso overexpression in IEC6 cells yields no change in *Axin2* induction over a 72 hour time-course. Interestingly, a subtle difference was noted in HCT116 cells. *AXIN2* transcription in this cell line consistently shows a gradual increase up to 48 hours, followed by a slight decrease at 72 hours. Kaiso OE cells appeared to shift the time-course, resulting in the highest *AXIN2* expression at an earlier time point than control cells. However, both cells lines returned to similar levels by 72 hours (Figure 17B). Thus, it is possible Kaiso plays a more subtle role in Wnt signaling than previously thought, fine-tuning the Wnt response in a context-specific manner as opposed to global regulation.

Kaiso loss increases tumor latency and increases survival time in the *ApcMin* mouse. As the authors reported no change in proliferation, apoptosis, or other tumor characteristic, the reason behind this delay is still unclear. In an attempt to delineate Kaiso's role in adenoma formation in a shorter time-frame, we crossed Kaiso null mice with our homozygous *Apc* floxed mice (Apc cKO) to yield *Kaiso null; Apcf/f; Lrig1-CreER* mice. Following tamoxifen (TAM) induction, *Apc* loss drives immediate transformation as evidenced by increased proliferation and altered migration. These cells are pushed up the villus in a consistent and time dependent fashion until death of the mouse at approximately 5-6 days post TAM. To analyze changes in these Kaiso and *Apc* double null cells, cohorts of Kaiso null and WT cKO mice were sac'd 5 days post induction. Changes in cell proliferation, apoptosis, migration, and survival were measured between littermates. Surprisingly, Kaiso loss showed no outright phenotype, and no changes in apoptosis, migration, or survival were observed (Figure 17C). It is worth noting that Kaiso loss does induce a small, but statistically significant decrease in proliferation; however whether this change is physiologically relevant remains to be determined. Taken together, these data suggest a minor role for Kaiso in Wnt-signaling, and suggest that Kaiso is not a robust contributor to tumorigenesis or tumor progression in CRC.

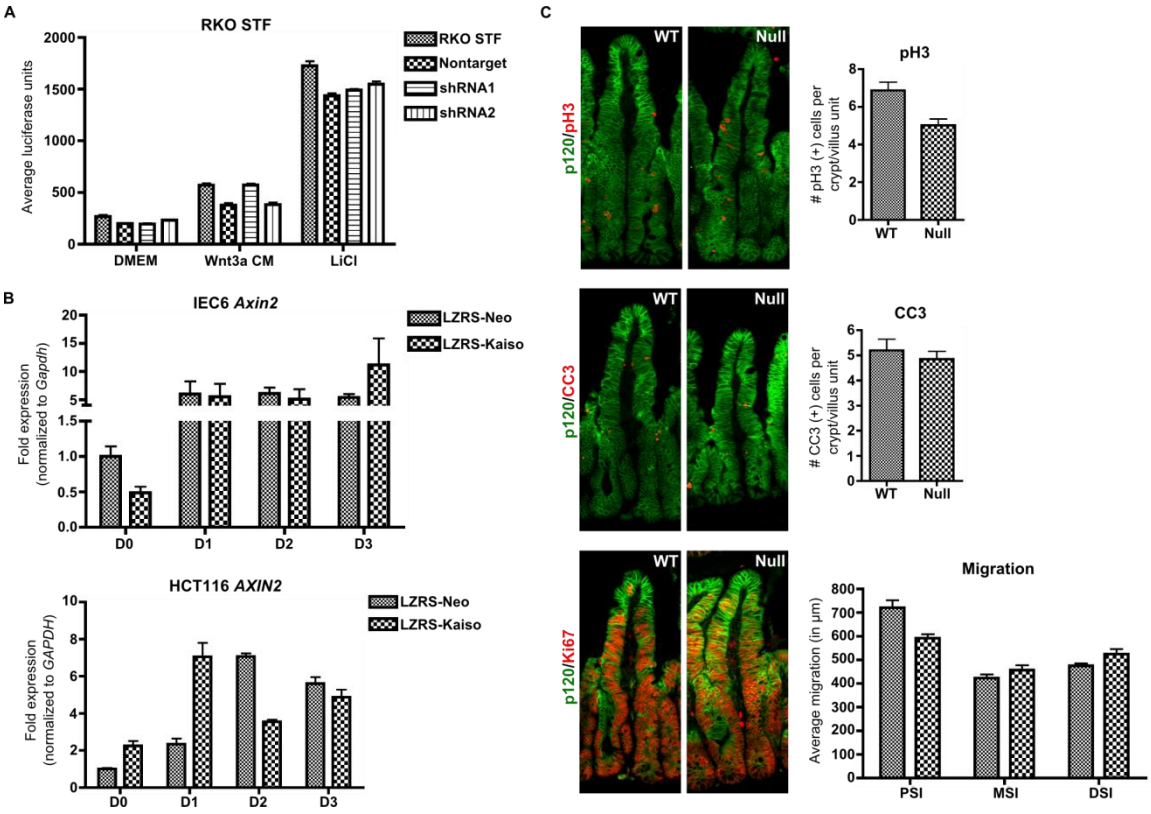

Figure 17. Kaiso does not alter Wnt activation *in vitro* or *in vivo*. (A) Kaiso was knocked down in RKO cells expressing a SuperTOPFlash reporter (STF). TOPFlash luciferase assays were completed after 24 hour stimulation with Wnt3a CM or 5µM LiCl. (B) LZRS-Kaiso and LZRS-Neo control IEC6 and Hct116 cells were treated with Wnt3a for up to 72 hours and analyzed for Wnt activation by *AXIN2* expression. (C) Synchronous *Apc* loss induced was in mice with or without Kaiso expression. Proliferation was measured by phospho-histone H3 (top), apoptosis by cleaved caspase 3 (middle) and distance travelled by Ki67 (+) transformed cells (bottom) at 5 days post TAM. Because migration can vary between intestinal segments, migration data was collected separately for proximal (PSI), middle (MSI), and distal intestine (DSI). p120 costain is in green and staining is quantified on the right.

Kaiso and p120 expression and localization are not codependent

p120 was Kaiso's first identified binding partner, and studies have suggested that p120 may inhibit Kaiso-mediated transcription by physically removing it from the nucleus. Importantly, intestinal adenomas from *Apc* mutant mouse lines show a striking decrease in p120 staining, which may be due to mislocalization. It is interesting to note that p120 staining is altered in the same cell population with high Kaiso expression, thus it seems likely that p120 may be mislocalized in an attempt to remove Kaiso from the nucleus in early tumor formation. We therefore stained both Kaiso WT and Kaiso null intestinal samples to determine if Kaiso expression could influence p120 localization. However, as seen in Figure 15, decreased p120 staining is still observed in the crypt (Figure 18A) and adenoma (Figure 18B) of Kaiso null mice, therefore it is unlikely that p120 mislocalization is a direct response to increased Kaiso protein levels. Conversely, to determine if p120 expression influences Kaiso localization, we stained intestinal samples with limited p120 ablation (Chapter 3) and mosaic p120 KO in approximately 10% of the intestinal epithelium (Smalley-Freed et al, 2011). It is quite clear from these studies that p120 loss has no appreciable effect on Kaiso localization. Figure 18C shows colon tissue with loss of 2 (dotted line) p120 alleles, 1 (arrowhead) p120 allele, and no p120 loss (arrow). As seen with p120, neither Kaiso localization nor expression levels change with varying levels of its binding partner. Therefore, while both proteins appear to play a role in CRC initiation, these roles are most likely separate. The context in which Kaiso and p120 interact *in vivo* is still unknown.

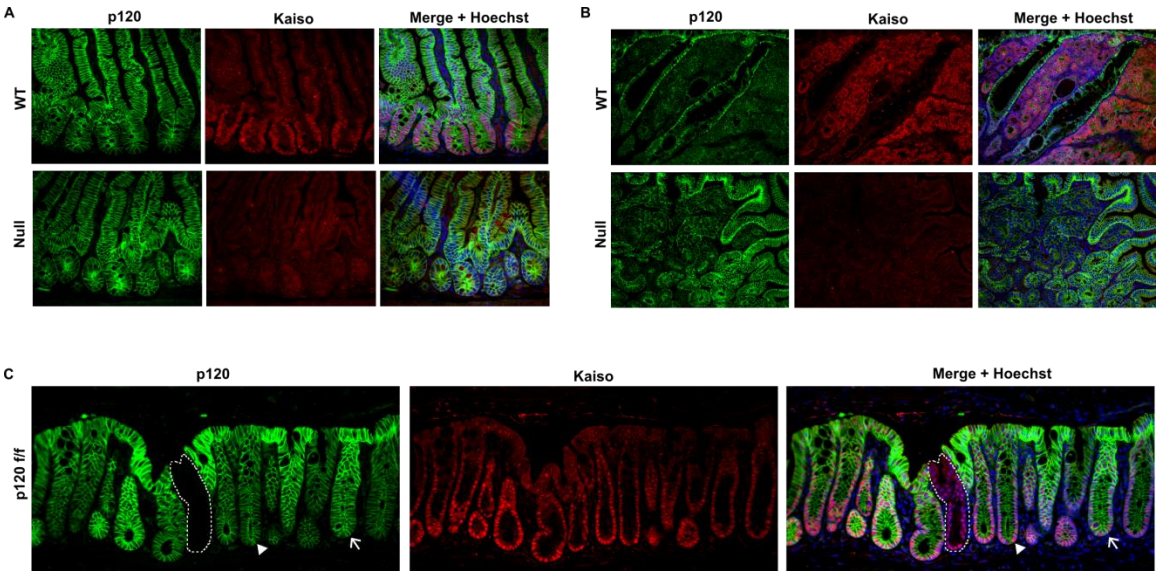

Figure 18. Localization and expression of p120 and Kaiso are not codependent. (A) Small intestine sections were stained for p120 (green) and Kaiso (red) in either WT (top panels) or Kaiso null mice (bottom panels). Decreased p120 staining in the crypts is still observed in Kaiso null mice. (B) Decreased p120 staining (green) is still seen in adenomas from both WT (top panels) and Kaiso null (bottom panels) *ApcMin* mice. (C) Colon tissue from p120 limited KO mice was stained for p120 (green) and Kaiso (red). Kaiso localization is similar in p120 null (dotted line), heterozygous (arrowhead), and WT (arrow) tissue.

A role for Kaiso in p53-mediated apoptosis

A final role for Kaiso as suggested by the literature which may contribute to CRC tumorigenesis and/or progression is Kaiso-mediated regulation of apoptosis and p53. Kaiso has been proposed to both inhibit and induce p53 activation as part of the apoptotic response (Koh et al, 2014; Lopes et al, 2008). While the Melnick group asserts that Kaiso loss sensitized cells to etoposide by alleviating repression of methylated tumor suppressor genes, studies from Koh and colleagues report that DNA damage is able to induce Kaiso expression and potentiate an apoptotic response. Importantly, these studies have major implications for chemosensitivity, and a heightened DNA damage response could offer a potential mechanism for the increased tumor latency observed in mouse models.

To determine the effect of Kaiso KD on apoptosis in CRC, cells were treated with 5μM etoposide for 48 hours and analyzed for Kaiso expression, p53 activation, and apoptosis (Figure 19). Interestingly, as reported by the Korean group, increased Kaiso is seen following etoposide treatment in the HCT116 cell line (Figure 19A). However, Kaiso induction is not seen in any other cell line tested, and while expression in SW480 cells is unchanged, Kaiso expression actually decreases following etoposide treatment in the HT29 line (Figure 19B and 19C). Furthermore, based on the model proposed by Koh et al., one would expect decreased apoptosis due to Kaiso loss. However, the opposite effect more often occurred and slight increases in cleaved caspase 3 staining are seen in all three KD lines. Most surprising, perhaps, was that Kaiso KD alone induced p53 expression and activation, as measured via phospho-p53, in SW480 cells (Figure 19C). This increase was only seen in the SW480 line, and furthermore the SW480 Kaiso KD lines did not display additional p53 activation following DNA damage. Oddly, SW480 cells also had the least reduction in Kaiso protein, thus a Kaiso-specific effect was somewhat surprising, but is a logical conclusion based on previous failed KD attempts in CaCo2 and LS174T lines. On the whole, these data do suggest cross talk between the Kaiso and p53 pathways, but once again highlight that Kaiso's role can be variable and highly contextual.

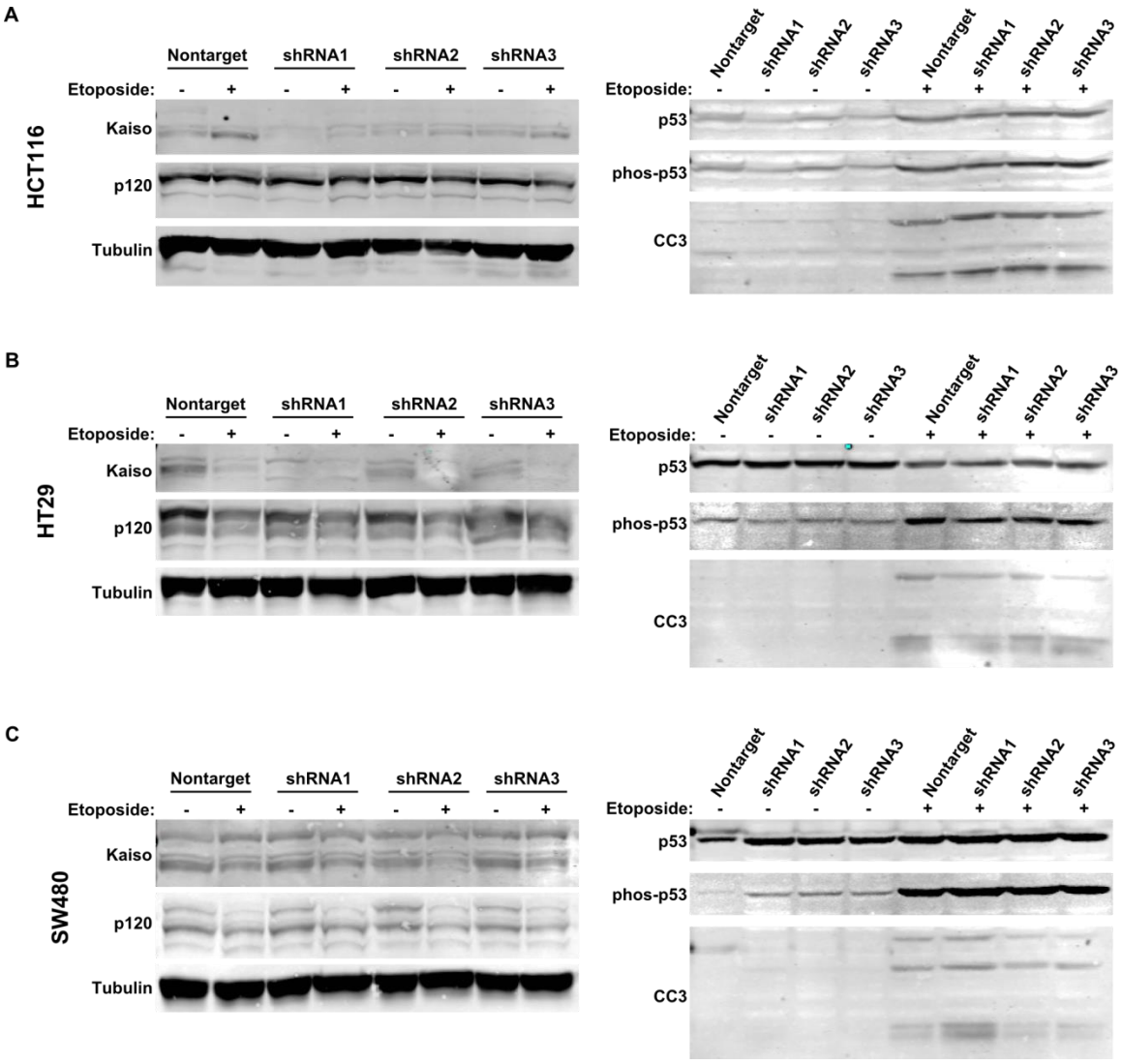

Figure 19. Kaiso influences p53 activation in CRC cell lines. Control and Kaiso KD CRC cells were treated with 5μM etoposide for 48 hours and analyze by WB for Kaiso, p120, p53, phosphorylated (activated) p53, and cleaved caspase 3 (CC3). (A) Etoposide treatment induced Kaiso only in HCT116 cells. (B) HT29 cells showed no difference with Kaiso KD. (C) SW480 cells show activated p53 following Kaiso KD. Tubulin was used as a loading control for all experiments.

Identification and validation of Kaiso ChIP-seq targets

Kaiso literature over the past decade has generated an extensive list of potential Kaiso target genes. Many of these genes, such as *CyclinD1*, and *CDKN2A*, are known tumor suppressors, yet Kaiso-mediated changes in gene expression have yet to be identified *in vivo*. Thus, to identify *bona fide* Kaiso target genes that may contribute to Kaiso's function in the intestinal tumorigenesis model, we turned to a recent ChIP-seq screen done by the Myers lab as a part of the Human Genome Project (HGP) and made publically available through the Encyclopedia of DNA Elements (ENCODE) database. This screen includes results from 4 different cell lines, HCT116, HepG2, GM12878, and K562. By this approach, we were able to generate a list of over 400 genes in which Kaiso binding peaks are apparent in multiple cell lines (see example Figure 20A).

To begin characterization and validation of these new target genes, we subjected this gene list to pathway and promoter analysis (Figure 20). Surprisingly, none of Kaiso's previously identified targets was confirmed by this screen, and subsequent promoter analysis only 5 identified genes (out of 405) which contained a full KBS site (Figure 20B). Instead, the top-rated gene set included genes regulated by a previously "unknown" binding motif (TMTCGCGANR) (Figure 20C). Unlike previously identified Kaiso targets, presence of this well-conserved motif is typically associated with transcriptional **activation** (Guo et al, 2008; Mikula et al, 2010; Wyrwicz et al, 2007; Yamashita et al, 2007). Interestingly, this gene set includes numerous protein production and mRNA translation genes with high levels of expression. Thus, Kaiso may mediate expression of genes responsible for maintaining continuous proliferation and would likely be transactivated to positively regulate these targets. Thus, while Kaiso clearly inhibits KBS-dependent reporter constructs, whether this scenario recapitulates Kaiso's true function is unclear.

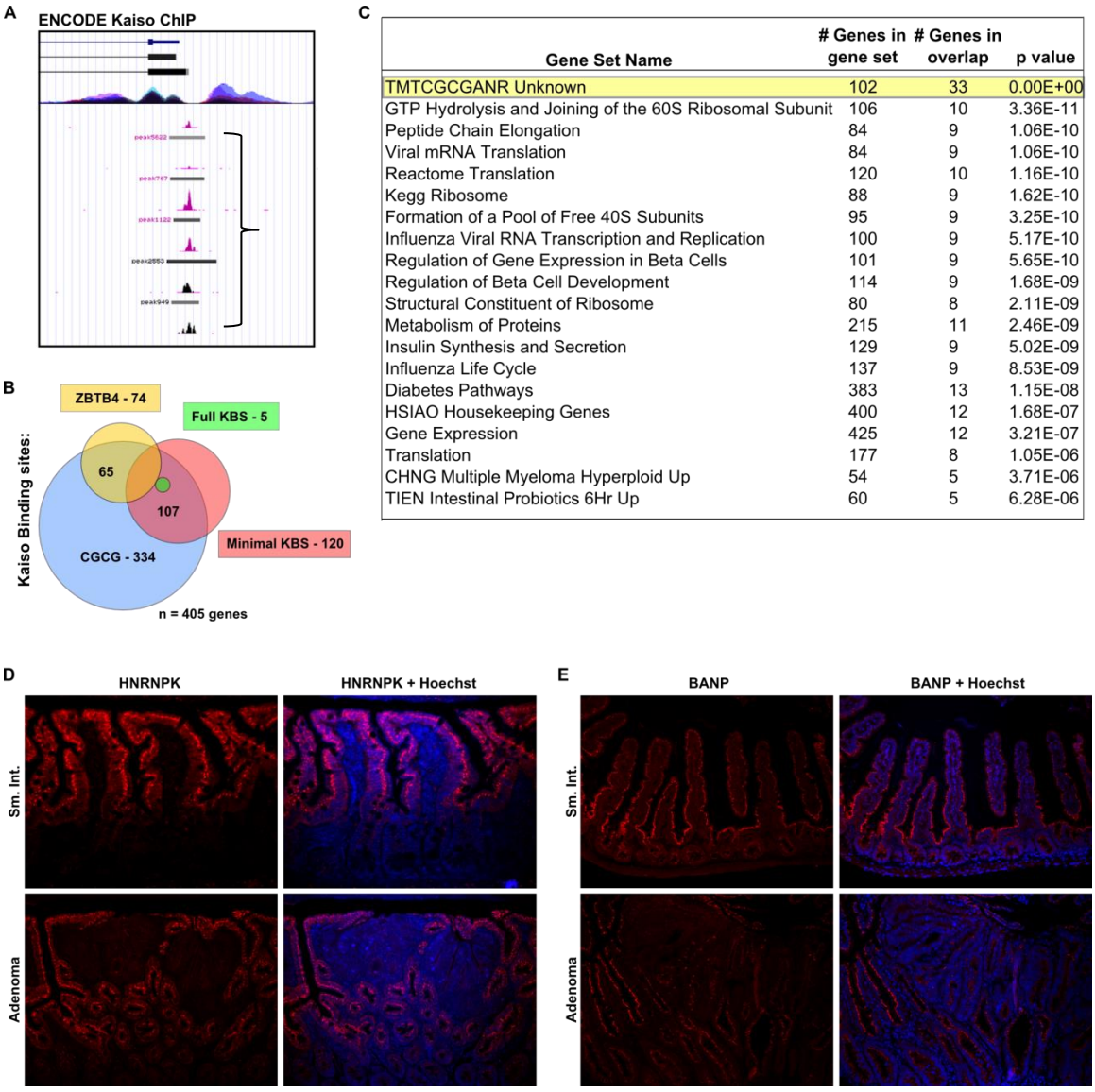

Gene Set Name	# Genes in gene set	# Genes in overlap	p value
TMTCGCGANR Unknown	102	33	0.00E+00
GTP Hydrolysis and Joining of the 60S Ribosomal Subunit	106	10	3.36E-11
Peptide Chain Elongation	84	9	1.06E-10
Viral mRNA Translation	84	9	1.06E-10
Reactome Translation	120	10	1.16E-10
Kegg Ribosome	88	9	1.62E-10
Formation of a Pool of Free 40S Subunits	95	9	3.25E-10
Influenza Viral RNA Transcription and Replication	100	9	5.17E-10
Regulation of Gene Expression in Beta Cells	101	9	5.65E-10
Regulation of Beta Cell Development	114	9	1.68E-09
Structural Constituent of Ribosome	80	8	2.11E-09
Metabolism of Proteins	215	11	2.46E-09
Insulin Synthesis and Secretion	129	9	5.02E-09
Influenza Life Cycle	137	9	8.53E-09
Diabetes Pathways	383	13	1.15E-08
HSIAO Housekeeping Genes	400	12	1.68E-07
Gene Expression	425	12	3.21E-07
Translation	177	8	1.05E-06
CHNG Multiple Myeloma Hyperploid Up	54	5	3.71E-06
TIEN Intestinal Probiotics 6Hr Up	60	5	6.28E-06

Figure 20. Identification of new Kaiso target genes through ENCODE analysis. Kaiso ChIP-seq results were queried from the ENCODE database. (A) Representative Kaiso binding peak. (B) Identification of known Kaiso binding sites by promoter sequence analysis. (C) Top 20 results from pathway analysis of 405 putative Kaiso target genes. "Unknown" motif gene set is highlighted. (D) WT intestine (top panels) and *ApcMin* adenoma (bottom panels) was stained for HNRNPK expression or (E) BANP.

Since the time of our analysis, other studies have been published which identify the new Kaiso binding site (ENDOCDE Kaiso binding site, or eKBS) and verify Kaiso binding by ChIP experiments (Raghav et al, 2012). However, no study to-date has shown Kaiso-mediated changes in eKBS target transcription. Thus, we examined expression of a subset of eKBS targets in Kaiso KD and OE cell lines, and those results are listed in Table 7. Interestingly, while there is generally little change in target gene mRNA, some of the greatest changes was noted in KD lines for HNRNPK and BANP. Therefore, these proteins were analyzed by fluorescent staining in the normal intestine and *ApcMin* adenomas (Figure20D and 20E). Surprisingly, in spite of data suggesting that Kaiso promotes expression of eKBS genes, both HNRNPK and BANP are expressed in an exact inverse pattern to Kaiso, showing decreased staining in the crypt and adenoma. While these data argue that Kaiso still likely functions primarily as a transcriptional repressor *in vivo*, the identification of new Kaiso target creates new avenues by which to explore Kaiso's function in this tissue.

A role for Kaiso in BMP signaling

In order to maintain homeostasis, tight control over Wnt signaling is necessary for proper regulation of proliferation and stemness. In the intestine, other morphogenic pathways, such as BMP, work in opposition to Wnt. While canonical Wnt signals serve to maintain an undifferentiated state in the intestinal crypt, BMP4 expression is highest in the villus where it promotes differentiation and inhibits Wnt-induced proliferation. We have previously established that Kaiso transcription is not responsive to Wnt or Notch, but it remains a possibility that Kaiso expression is instead due to negative regulation through a pathway such as BMP. To test if BMP-mediated signaling can influence Kaiso expression, mammary and CRC cell lines were treated with 100ng/mL BMP4 for 24 hours and assayed for *Kaiso* mRNA by qRT-PCR (Figure 21A and 21B). After 24 hours stimulation, increased transcription was readily seen in established BMP4 targets such as *ID1* and *SMAD6*, yet we observed no change in Kaiso. Thus, Kaiso regulation appears to be independent of all major developmental pathways influencing intestinal homeostasis.

	SW480			
	shRNA1	shRNA2	shRNA3	OE
ATF2	0.86482	0.87101	1.16139	0.95549
ATF4	0.74984	0.82211	1.44393	1.02474
ATF7	0.989	1.0984	1.25579	0.99573
BANP	0.00793	0.96132	1.5166	1.3728
BUB1B	0.84397	0.97586	1.01384	1.14534
CCNC	1.08352	0.09301	1.12869	1.21749
CDC20	0.76455	1.2575	0.98763	1.26657
CUL3	0.05458	1.24457	1.49485	1.09584
DDX20	0.90067	1.32366	1.13445	1.10262
DENR	0.71355	1.088	1.31746	1.06308
UHRF2	0.76327	0.73081	0.95304	1.05071
WDR77	1.07897	1.08987	1.01604	0.97076
DIDO1	0.92933	1.02424	1.29297	0.98357
MAD1L1	0.91352	0.86434	0.9961	1.00312
MAP3K7	0.54767	0.66267	0.75421	0.97314
MAPK14	1.50647	0.78667	0.96466	1.01089
MKL2	0.8262	0.66705	1.19066	1.08212
PDRG1	0.9344	1.00163	1.02399	1.03247
PHB	1.1958	0.90828	0.9798	1.18372
PRDX1	1.15945	0.94874	0.96132	1.21084
RPL26	0.9444	0.67312	0.53687	1.10889
SIRT4	2.14689	0.90493	1.34721	0.9241
UBE2D3	1.18573	0.92672	1.12919	1.03577
RPS11	1.36773	0.83443	1.07077	1.133
RPS15	1.20477	0.81569	1.09158	1.14508
RPS15A	1.15473	0.82046	0.89089	
RPS19	1.27914	0.81469	1.07817	
RPS2	1.12653	0.84519	1.21906	1.03629
RPS28	1.09482	0.97088	1.09666	
RPS3A	1.11776	0.72767	1.08416	1.15266
RPS6	1.19276	0.94492	1.17481	1.10449
RPS7	1.26285	0.86446	1.06366	1.08056
RPS9	1.11816	0.91045	1.03683	1.03231
XPC	0.75922	0.99816	1.17558	0.87133
ZBTB2	0.8757	1.07157	1.19305	0.9539

	HCT116			
	shRNA1	shRNA2	shRNA3	OE
ATF2	0.95982	1.12454	1.06307	1.1981
ATF4	0.96303	1.26843	1.07246	1.17265
ATF7	1.08702	1.38475	1.2155	1.06599
BANP	0.84519	2.62022	0.66908	1.37863
BUB1B	0.94936	1.45565	1.09562	1.34753
CCNC	1.08424	1.50603	1.19803	1.27219
CDC20	0.10564	1.22796	1.08989	1.06854
CUL3	0.78303	1.60363	0.42305	0.97526
DDX20	1.27941	1.47862	1.19182	0.97382
DENR	1.21963	1.57862	1.20338	0.97208
UHRF2	1.09273	0.70772	1.15195	0.81731
WDR77	1.39938	1.42927	1.26252	1.03868
DIDO1	1.0894	2.35647	1.42226	1.45684
MAD1L1	1.0848	1.83884	1.27623	1.16291
MAP3K7	1.17817	1.6119	0.88382	0.87943
MAPK14	1.49502	1.40687	1.05855	0.80722
MKL2	1.36772	1.77536	1.5834	1.04782
PDRG1	1.30141	1.68553	1.26601	1.00525
PHB	1.21412	1.56478	1.35525	1.05657
PRDX1	1.05439	1.48253	1.12482	0.98241
RPL26	0.9662	1.34012	1.32071	0.88907
SIRT4	0.82423	0.87044	0.99588	0.91408
UBE2D3	1.32278	1.21368	1.26324	0.96639
RPS11	1.22358	1.09124	1.18848	0.82451
RPS15	1.05552	1.46715	1.35443	1.18215
RPS15A	1.0545	1.32975	1.05643	
RPS19	0.8948	1.36991	1.14517	
RPS2	0.83209	1.10923	1.19115	1.08186
RPS28	0.87167	1.25818	1.07267	
RPS3A	0.97347	1.2861	1.14444	1.10977
RPS6	1.046	1.3589	1.32505	1.03079
RPS7	1.23223	1.18958	1.16399	0.9738
RPS9	0.89016	1.22222	1.27738	0.99007
XPC	0.9466	1.46334	1.35773	0.9723
ZBTB2	1.46451	1.59283	1.4178	0.86561

	HT29			
	shRNA1	shRNA2	shRNA3	OE
ATF2	1.23578	1.23521	1.49379	1.06285
ATF4	1.1223	1.68956	1.61635	1.28857
ATF7	1.83271	1.55234	1.7082	1.00773
BANP	2.19973	2.81403	2.21662	1.21614
BUB1B	1.39882	1.59594	1.45602	1.16233
CCNC	1.4488	1.29907	1.58873	1.14624
CDC20	1.31262	1.49039	1.33353	1.06534
CUL3	1.11364	1.27178	1.4536	1.05144
DDX20	1.6017	1.67425	1.64722	1.13083
DENR	1.38482	1.62073	1.68066	1.18232
UHRF2	1.35785	0.95341	1.40171	1.27199
WDR77	1.47588	1.25657	1.23349	1.19196
DIDO1	1.8584	2.10719	1.8211	1.4942
MAD1L1	1.93208	2.04208	1.65579	1.36657
MAP3K7	1.85398	2.00274	1.31013	0.96026
MAPK14	1.43416	1.19871	0.96738	1.04403
MKL2	1.24576	1.36911	1.4393	1.27155
PDRG1	2.01626	1.7414	1.59242	1.11246
PHB	1.61027	1.59506	1.62359	1.31059
PRDX1	1.63763	1.73727	1.54475	1.17233
RPL26	1.10514	1.52313	1.67583	0.96064
SIRT4	0.75022	0.74641	0.90512	0.8971
UBE2D3	1.35687	1.20503	1.36244	1.04306
RPS11	1.47172	1.20115	1.62739	1.09614
RPS15	1.50404	1.35939	1.55125	1.36005
RPS15A	1.16131	1.21219	1.38605	
RPS19	1.26755	1.32696	1.36722	
RPS2	1.10441	1.22335	1.35758	0.97114
RPS28	1.29745	1.43209	1.78839	
RPS3A	1.24328	1.23463	1.48592	1.06978
RPS6	1.11357	1.21541	1.61342	0.99459
RPS7	1.39216	1.16066	1.40172	1.05357
RPS9	1.29492	1.25627	1.55967	1.20205
XPC	1.22637	1.63881	1.42847	1.19795
ZBTB2	1.94393	1.54248	1.8957	1.40335

Table 7. mRNA expression of ENCODE Kaiso targets. SW480, HCT116, and HT29 cells with Kaiso KD or overexpression (OE) were analyzed for gene expression by qRT-PCR. Values are represented as fold change relative to control (control = 1) after normalization to GAPDH.

Interestingly, a subset of Kaiso eKBS targets (e.g. *DIDO1*, *MAD1L1*, and *MKL2)* has been implicated in BMP- and transforming growth factor β (TGFβ)-mediated signaling (Braig & Bosserhoff, 2013; Hein et al, 2011; Li et al, 2012a; Werner et al, 2001). To test whether Kaiso could indirectly mediate Wnt by regulating responses to BMP or TGFβ signaling, we treated both WT and Kaiso OE cells with BMP4 to determine if Kaiso could affect BMP-induced transcription. Surprisingly, Kaiso overexpression inhibited the induction of the established BMP target genes *ID1*, *SMAD6*, and *SMAD7*. Furthermore, *DIDO1*, *MAD1L1*, and *MKL2*, were all responsive to BMP signaling and displayed increased mRNA expression following BMP treatment. Importantly though, BMP-induced upregulation of these targets was inhibited with Kaiso overexpression, however this upregulation was abolished with Kaiso overexpression (Figure 21C). Taken together, these results suggest a novel role for Kaiso in the intestine through regulation of BMP signaling, which may begin to elucidate Kaiso's role in the intestine and intestinal tumorigenesis.

Discussion

Previous work has demonstrated a complex and multifaceted role for Kaiso in regulation of many important cellular pathways. These studies have shown that Kaiso is able to inhibit Wnt signaling through both protein-protein interactions and direct repression of Wnt target genes, regulate p53-mediated apoptosis, and broadly contribute to epigenetic regulation through transcriptional suppression of methylated DNA. Here, we investigate the pleiotropic roles of Kaiso as they pertain to intestinal tumorigenesis and progression. Unlike the majority of *in vitro* studies, we found that Kaiso most likely has a positive function in Wnt signaling *in vivo*, possibly due to inhibition of BMP signaling. We further illustrate a role for Kaiso in p53-mediated apoptosis of CRC cells, although these results vary greatly depending on the cell line tested and broader roles will need to be further elucidated in *in vivo* systems. Furthermore, we report results obtained by query of a large ChIP-seq screen to identify novel Kaiso target genes. Surprisingly, the ChIP-seq studies identified a new consensus Kaiso target site (eKBS), which is primarily found in genes required for mRNA translation and protein production. Together, these studies question much of the previous Kaiso literature, yet also highlight a highly contextual nature which may contribute to conflicting results regarding Kaiso function.

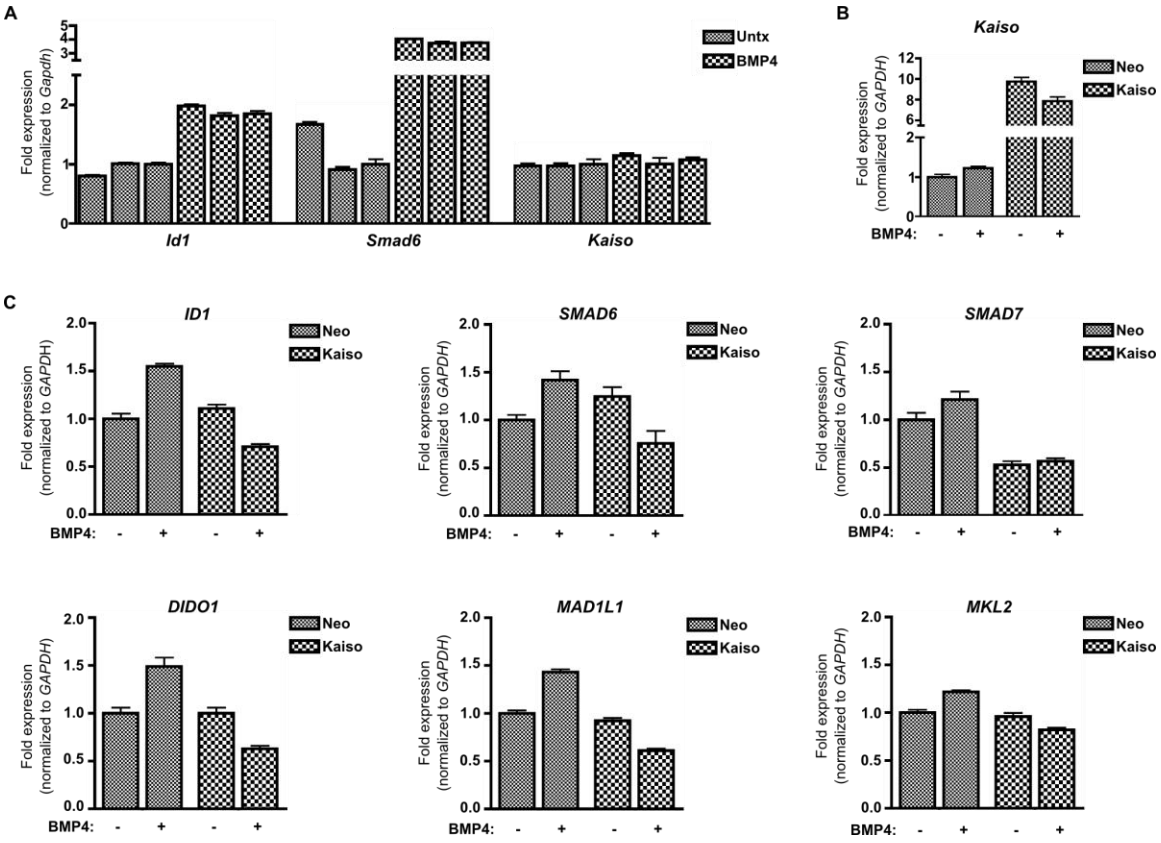

Figure 21. Kaiso inhibits BMP-mediated gene induction. (A) Mouse mammary tumor cell lines were treated with 100 ng/mL BMP4 and gene expression was analyzed by qRT-PCR. (B) Kaiso expression in HCT116 cell lines with (LZRS-Kaiso) and without (LZRS-Neo) Kaiso overexpression were treated with BMP4. No change in Kaiso expression was seen in either cell population. (C) Expression of BMP and Kaiso targets with and without BMP treatment. Kaiso overexpression inhibits induction of BMP targets *ID1*, *SMAD6*, *SMAD7*, and Kaiso targets *DIDO1*, *MAD1L1*, and *MKL2*.

In the intestine, Kaiso is highly expressed in the crypt region as well as transformed adenomatous tissue from all tumor models analyzed to-date (Figure 13). Both are highly proliferative, and similarities between the crypt and adenoma cells are well-established. Indeed, *Apc* loss is thought to confer a "crypt-progenitor phenotype" by constitutive Wnt activation, which drives a permanent replication program and blocks the differentiation cells normally undergo at the crypt shoulder (Sansom et al, 2004; van de Wetering et al, 2002). Thus, many properties of crypt cells are preserved or amplified following *Apc* loss, such as activated/nuclear β-catenin, EPHB2 expression, proliferation, and a lack of differentiation. Interestingly, Kaiso appears to be another such marker of the progenitor phenotype, as its normal crypt expression is maintained and possibly amplified in the adenoma. Importantly, other markers of Wnt activation, such as Wnt target genes (i.e. *Axin2*, *Lgr5*), are often not expressed at high enough levels to reliably detect by common IHC methods. Likewise, β-catenin upregulation and/or nuclear localization can be quite subtle at the earliest stages of tumorigenesis, particularly in tumor models that fail to display massive β-catenin upregulation (i.e. *Apc1638*). Kaiso, on the other hand, is a robust and striking marker of Wnt activation that is apparent at the earliest events in tumorigenesis (Figure 13C). Thus, Kaiso expression should be a welcomed and useful addition to the "toolbox" for studying intestinal tumor formation and allow early detection of *Apc* loss and microadenoma formation.

Kaiso's expression pattern *in vivo* is highly suggestive of Wnt-based regulation, yet we were unable to establish a connection between Wnt activation and Kaiso transcription (Figure 15). Kaiso was also not robustly regulated by other established developmental pathways in the intestine, namely Notch and BMP. However, other signaling pathways exist that may explain this expression pattern that have not yet been explored. For example, further ENCODE ChIP-seq studies have identified NFκB subunits bound at the Kaiso promoter, and epithelial NFκB activation has been observed both in the crypt and following *Apc* loss, where it is thought to contribute to stem cell maintenance and tumorigenesis (Myant et al, 2013; Schwitalla et al, 2013). Indeed, Kaiso expression may increase after certain types of cell stress, such as wound healing (Kondapalli et al, 2004). Furthermore, others have shown Kaiso transcription to be dependent on 3D morphology and signals derived from the extracellular matrix, which may suggest a role for the microenvironment in Kaiso regulation (Soubry et al, 2005). Thus, while the mechanism of Kaiso induction still remains unclear, and numerous avenues remain to be explored as the topic of future studies.

In spite of numerous studies which have shown repressive roles for Kaiso, our studies failed to find any Kaiso-mediated impact on Wnt activation either *in vivo* or *in vitro*. Instead, we report Kaiso to be highly expressed in areas with robust Wnt activity, a pattern more consistent with a positive role in this pathway. This conclusion is further supported by the previous reports from Kaiso transgenic and knockout mouse models, as Kaiso loss delays tumor formation in the *ApcMin* model and Kaiso transgenic mice show an expansion of the crypt compartment. In all, our data show the possibility of a subtle, positive role for Kaiso, as evidenced by a slight reduction in proliferation following *Apc* loss in Kaiso null mice, and by a shift in the *AXIN2* time-course in HCT116 cells. However, these results are likely too minor to account for the delayed onset of tumorigenesis in the *ApcMin; Kaiso null* study, or fully explain Kaiso's function in the crypt or adenoma.

Interestingly, cell culture studies suggest that Kaiso's most likely intersection with Wnt signaling is through its ability to attenuate responses to BMP stimulation. In the intestine, BMP suppresses Wnt to promote differentiation and inhibit proliferation, and ablation of BMP signaling through receptor KO or ectopic expression of Noggin results in Wnt target repression, *de novo* crypt formation, and a phenotype similar to Juvenile polyposis syndrome (Haramis et al, 2004; He et al, 2004). Furthermore, downstream BMP-effector SMAD4 has been shown to directly inhibit β-catenin at the transcription level, and *SMAD4* deletion increases tumorigenesis and transcription of Wnt target genes in *Apc1638* mice (Freeman et al, 2012). Here, we show that Kaiso overexpression can completely block BMP4-mediated upregulation of *ID1*, *SMAD6*, and *SMAD7* in HCT116 cells. *DIDO1*, *MAD1L1*, and *MKL2*, potential Kaiso targets identified by ChIP-seq, are also induced by BMP treatment in a Kaiso-dependent fashion. Thus, these genes are likely *bona fide* Kaiso targets and subject to Kaiso-mediated repression in the context of BMP. Interestingly, these genes have been shown to mediate downstream signals from TGF-β, a closely related morphogen which utilizes many of the same downstream effectors as BMP. While the role of TGF-β in intestinal homeostasis is not well understood, recent data from the TCGA identified a surprising number of TGF-β pathway mutations, which indicate a more extensive role in CRC than previously believed (2012). While it is still unclear if Kaiso-mediated repression of *DIDO1, MAD1L1*, and *MKL2* are also observed in the context of TGF-β stimulation, it is interesting to speculate that Kaiso may influence multiple aspects of CRC progression by modulation of both BMP and TGF-β activity.

Kaiso may also play a role in CRC development by regulation of inflammation and the immune response. The link between inflammation and cancer is well-established, and inflammatory bowel diseases, such as Crohn's colitis and ulcerative colitis, are a major risk factor for CRC. As seen in Figure 14, positive Kaiso staining is often seen in infiltrating immune cells in human colon polyps. Studies analyzing Kaiso KO in the spleen report splenomegaly and atypical germinal centers, possibly due to Kaiso-mediated transcriptional changes in *BCL-6*, a B-cell specific gene often deregulated in lymphomas (Koh et al, 2013). Furthermore, pathway analysis of eKBS target genes identifies gene sets necessary for B-cell development and function, as well as those upregulated following probiotic treatment in the intestine (Figure 20C). Knockout of Kaiso's binding partner, p120, has also been shown to generate an inflammatory response which has been causally linked to phenotypes in the skin, intestine, and the esophagus (Perez-Moreno et al, 2006). Thus regulation of inflammatory responses may be an outlet for functional interaction between p120 and Kaiso. Kaiso overexpression in the intestine leads to the development of several inflammatory features, such as increased neutrophil infiltration and activation, villi fusion, and crypt hyperplasia, although it is important to note that Kaiso expression in this model is restricted solely to epithelial cells, thus these particular changes are most likely regulated by non-cell autonomous mechanisms. However, taken together these data suggest Kaiso-mediated changes in inflammatory responses may be complex but broadly relevant to intestinal inflammation and tumorigenesis.

Kaiso has been previously characterized as a transcriptional repressor whether binding a non-methylated consensus site (KBS) or to di-methylated CGCG motifs. However, our analysis of Kaiso binding peaks in the ENCODE database failed to identify any previously reported target genes, and promoter sequence analysis revealed a full length KBS in only ~1% of the ChIP-seq identified genes. Thus, while Kaiso clearly modulates expression of KBS-based promoter constructs, these data do not support a biological relevance for the traditional KBS sequence. Surprisingly, gene pathway analysis of the ChIP-seq gene set identified a new binding motif (eKBS) that was previously characterized as an "orphan" motif with no known transcriptional regulators. Since our initial assessment, other groups have further validated the eKBS, further suggesting this site indeed is a *bona fide* Kaiso binding site (Raghav et al, 2012). The eKBS does include a core CGCG, and Kaiso binding *in vitro* is higher upon CGCG methylation. Together with the high rate of CGCG motifs in Kaiso target genes, these data are still consistent with Kaiso-mediated

repression of methylated DNA sequences. However, one important exception lies in work from the Farnham group, which used the Kaiso ENCODE genes and compared them with DNA methylation databases (Blattler et al, 2013). Here, eKBS-regulated Kaiso target genes were found to be some of the most actively transcribed genes in the genome and rarely methylated. Indeed, the eKBS motif appears to disproportionately regulate genes necessary for housekeeping, mRNA translation, and protein production, and Kaiso is often expressed in proliferative cell populations *in vivo*. Also, the eKBS sequence is known to be necessary for target gene activation, and mutation of the eKBS site in *HNRNPK* abolishes its transcription (Mikula et al, 2010). With these data, it is tempting to speculate that Kaiso primarily functions as a transcriptional activator in this gene set. However, here we show that protein from two such genes, HNRNPK and BANP, are expressed in an inverse pattern to Kaiso in the intestine and points back to transcriptional repression. Furthermore, it is important to note that Kaiso-mediated changes in eKBS target genes or eKBS reporter constructs have yet to be reported. Thus much work remains to be done on identifying both Kaiso target genes and the manner in which Kaiso contributes to their regulation.

Perhaps the most conclusive aspect of the data presented herein lies in the variability of Kaiso-mediated phenotypes. It is important to note the frequency of conflicting reports on Kaiso function throughout the current literature: Kaiso both inhibits and augments the Wnt response. Kaiso binds methylated and non-methylated genes. Kaiso induces and attenuates p53-mediated apoptosis. Indeed, gene expression changes induced by Kaiso were rarely consistent across the three different knockdown constructs (Table 7) or across the different CRC lines tested (e.g., BANP upregulation is seen in HCT116, but not SW480 KD lines). Response to etoposide treatment in Kaiso KD cells was surprisingly variable; for example Kaiso knockdown activated p53 solely in SW480 cells. Thus, it appears Kaiso may play a highly contextual role which may vary dramatically between different between tissue and organ systems. Furthermore, caution may be necessary in extrapolating data from Kaiso-focused studies, particularly in cell culture-based model systems, as Kaiso's exact function likely depends on tissue-specific changes in gene expression, available binding partners, and signaling pathways. Thus, much work remains to be done to fully understand Kaiso's contribution, not only to the intestine and CRC, but other tissues as well.

CHAPTER V

FUTURE DIRECTIONS

Introduction

Here, we show that p120, along with the E-cadherin complex, functions as a singular haploinsufficient entity in the context of *Apc* loss in the intestine. We further identify p120 as having obligatory haploinsufficiency, as loss of both p120 alleles was incompatible with adenoma growth despite being dispensable for WT tissue. Alterations to p120 and the cadherin complex appear to be a normal consequence of Wnt activation, as decreased p120 staining is observed in both the crypt and adenoma. Taken together, we suspect this is a product of a crypt-progenitor phenotype that functionally contributes to the rapidly expanding crypt and/or adenoma cells. These data were further extended to E-cadherin and α-catenin by observation of nearly identical results with IHC, Sleeping Beauty mutagenesis screens, and mouse tumor models as reported by the literature. Thus, the cadherin complex appears to be a discreet functional unit, and removal of only one component will inactivate the complex as a whole. By virtue of its high selection in the Sleeping Beauty mutagenesis screens, in conjunction with the pathology literature, we believe that inactivation of the cadherin complex constitutes a major functional roadblock to early tumor establishment and progression.

p120's binding partner Kaiso also likely contributes to tumorigenesis, although its functional contribution is still unknown. Here, we show Kaiso is dramatically upregulated in the Wnt-driven cells of the crypt and adenoma, and Kaiso expression is a robust and useful marker of *Apc* null cells. While numerous roles for Kaiso have been reported in Wnt signaling pathway regulation, our data suggest any effect of Kaiso on this pathway is quite subtle and not likely to account for the phenotype observed in the *ApcMin* line, where Kaiso loss delays tumorigenesis. Intriguingly, Kaiso may have a role modulating BMP signaling, which has multiple implications for intestinal homeostasis and CRC development. However, perhaps the most striking facet of Kaiso biology represented here lies in the identification of a new Kaiso binding site (eKBS), through query of publically available ChIP-seq screens. While literature suggests the eKBS mediates transcriptional activation, IHC studies of eKBS targets still imply that Kaiso functions as a transcriptional repressor, at least in the intestine. These studies have only just begun, and there are still many questions to be answered in order to fully understand p120 and Kaiso's function in intestinal tumorigenesis and how this relates to human CRC development and progression.

Contribution of the cadherin complex to intestinal tumorigenesis

While we show that p120's contribution as a haploinsufficient tumor suppressor is most likely at the level of the cadherin complex, how the cadherin complex functionally contributes to tumorigenesis is still unknown. A number of molecular interactions exist which could explain these results. For example, inactivation of the cadherin complex has been shown to augment canonical Wnt signaling under a variety of scenarios by releasing membrane-associated β-catenin to participate in the Wnt cascade (Fagotto et al, 1996; Heasman et al, 1994; Kuphal & Behrens, 2006). Indeed, aberrant Wnt activation was presented by the Fodde group as a possible mechanism for the effects of E-cadherin reduction on *Apc1638* tumor formation (Smits et al, 2000). However, our studies have failed to generate any supportive evidence for a Wnt-dependent mechanism. Indeed, in the p120 null and *p120+/-* intestine and *p120+/-* enteroid culture, proliferation and cellular differentiation remain largely unaffected (Chapter 3, Appendix A). Surprisingly, mRNA analysis from these samples has often shown downregulation of Wnt target expression, rather than a p120-dependent increase. Moreover, analysis of aged *p120+/-* mice has found that, at baseline, these mice

are not predisposed to tumor formation and still require an initiating mutation for the tumorigenic effects described herein (data not shown). However, it is important to note that these results still cannot rule out a Wnt/cadherin-driven mechanism. Further experiments to conclusively address this scenario include mouse crosses with Wnt-reporter mice (e.g. *Axin2 lacz*), Wnt-reporter (i.e. TOPFlash) experiments *in vitro* or *ex vivo*, or further characterization of *ex vivo* enteroid cultures (e.g. plating efficiency, stem-spheroid formation, R-spondin dependency).

The cadherin complex may also contribute to tumorigenesis by mediating RTK growth factor signaling pathways. Indeed, many have shown that cadherins and RTKs are able to colocalize, and in many systems cadherins suppress RTK activation and signaling (Qian et al, 2004; Takahashi & Suzuki, 1996). *In vitro*, cadherin-based inhibition of RTKs is associated with contact-inhibition of cell growth, where generation of cell-cell contacts shuts down proliferation upon monolayer confluence (Takahashi & Suzuki, 1996). Contact inhibition is further dependent on the HIPPO pathway and its associated proteins, YAP1 and Merlin, both of which have been shown to interact with the cadherin complex and its members (Curto et al, 2007; Hamaratoglu et al, 2006; Kim et al, 2011). Because staining for cadherin complex members shows alterations in areas of active proliferation in the intestine (i.e. crypt and adenoma), it is tempting to speculate that this may serve to mediate a form of contact-inhibition *in vivo*, and the cadherin is recruited back to the membrane at the villus to aid the transition to differentiation and cell quiescence. However, these data are not consistent with similar rates in proliferation and growth factor pathway activation (e.g. phos-AKT, phos-ERK, phos-YAP1) in *p120+/-* intestines or enteroids. Further mRNA analysis on TEAD/YAP1 dependent targets, such as *Cdk6*, may shed light on whether increased signaling through this pathway may help to mediate effects of p120 heterozygousity. Also, attempts to analyze phosphorylated EGFR levels by western blot have not yet been successful, but would be important to clearly establish the level of RTK activation in these models.

On the other hand, it is entirely possible that the decreased staining seen in the crypt and adenoma may not be functionally relevant to intestinal biology. Indeed, differences in cell size and morphology have been known to influence staining intensities. For example, the concentration of glucose transporters in adipocytes cells decreases with increased cell size, although the total number of transporters remains constant in the larger plasma membrane (Karnieli et al, 1986). A similar effect could serve to mediate the immunofluorescent intensities shown here. No data to-date has suggested a decrease in p120 protein or questioned its localization on the membrane, and even PLA studies show similar numbers of E-cadherin/p120 complexes in both normal villus and tumor samples. However, both the crypt and adenoma cells are morphologically distinct from villi cells, which maintain more extensive cell-cell contacts. Therefore, the possibility remains that the decrease in staining is due to a similar number of cadherin complexes spread along a larger cell surface as opposed to its normal restriction at the lateral membranes. Testing this hypothesis would require further biochemical experiments, such as cell fractionations from the normal crypt, villi, and *Apc* KO intestine, as well as high resolution confocal microscopy.

While the use of *in vitro* methods could help investigate the role of the cadherin complex at a molecular level, the alterations observed in p120 are not reproducible in any CRC cell lines tested to date. However, recent advances have described *ex vivo* culture methods, allowing the culture of 3D crypt-like organoids from primary mouse intestine (Sato et al, 2011a; Sato et al, 2009). Importantly, viral-mediated genetic manipulation is possible, and these protocols have been used successfully (Koo et al, 2011)(Appendix B). Therefore, future studies should be able to tease apart the contribution of the cadherin complex on cell growth, growth factor responsiveness, and Wnt activation in a biologically relevant model system. Furthermore, while clearly suggested by previous literature and the SB data, whether phenotypes due E-cadherin and α-catenin loss are truly identical to p120 is still unclear. For example, phenotypes associated with α-catenin loss *in vivo* are frequently more severe than that of E-cadherin in epithelial tissues, suggesting α-catenin may mediate non-cadherin associated roles in addition to its classical role at the membrane (Vasioukhin et al, 2001). The *ex vivo* system could allow for knockdown or overexpression studies with individual cadherin complex members or binding deficient mutants to clearly define functional similarities.

Interestingly, most phenotypes for p120 loss *in vivo* have been ultimately attributed to loss of cell-cell adhesion. While limited p120 loss or p120 heterozygousity in the intestine shows little phenotype, both p120 heterozygous enteroid and tumoroid cultures show increased branching and morphological defects when cultured *ex vivo* (Appendix A). Whether this represents a functional manifestation of *in vivo* roles is not yet clear. However, this phenotype, with cell sloughing, ductal occlusion, and aberrant ductal growth, mirror many *in vivo* phenotypes in other systems. Thus, while the ultimate mechanism by which adhesion can influence tumorigenesis is still unknown, it is likely that the true phenotype behind loss of p120 and the cadherin complex in the intestine can be attributed to loss of cell-cell adhesion.

p120's requirement in CRC

p120 loss was incompatible with adenoma growth despite being quite well tolerated in the intestinal crypt. Yet how and why these cells are lost from the tumor is still unclear. Interestingly, because p120 null crypts can persist long-term for the life of the animal, p120 is clearly not an absolute requirement for Wnt signaling or proliferation *per se*. Unfortunately, extensive investigation through IHC studies have to-date found no alterations in p120 null *ApcMin* adenoma cells that could account for their rapid loss. As identification of p120 null cells necessitates coimmunofluorescent staining approaches, further studies in this system are limited by quality antibodies that are reliable for fluorescent IHC.

As shown in Appendix A, the requirement for p120 in *ApcMin* adenomas was further addressed by tumoroid 3D culture. Tumors from *ApcMin; Vil-CreER; p120f/f* and *ApcMin; Lgr5-CreER; p120f/f* mice were isolated and p120 KO was induced in culture by treatment with 4-hydroxy-tamoxifen (4-OH TAM). While it was originally our hope to generate widespread p120 KO for easier analysis, these cultures completely recapitulated the *in vivo* effects. Complete p120 KO was rarely seen, and the limited number of p120 KO cells found in the tumoroids did not commonly express the apoptosis marker, cleaved caspase 3, although numerous cleaved caspase 3-positive cells were found extruding from the epithelial layer in both control and 4-OH TAM-treated cultures. Furthermore, TAM-treated *ApcMin* tumoroids show extensive cell sloughing and shrinking over time (Appendix A, Figure X). This phenotype, combined with the limited

number of p120 KO cells and the rate of cell extrusion in these cultures in general, make likely that the size reduction and sloughing observed in treated enteroids could be due to adhesion-dependent loss of p120 KO cells into tumoroid lumen. Whether these cells are still viable at extrusion is unclear, but on the whole these data suggest the requirement for p120, mediated by the cadherin complex, could easily be due to alterations in cell-cell adhesion.

The intestine is a highly dynamic environment, with a continuous process of proliferation, migration, and sloughing into the intestinal lumen. This phenomenon can also be observed in the tumors, and cells (both apoptotic and viable) can often be seen in the middle of adenomatous crypts. As described above, this may provide a mechanism for loss of p120 KO cells due to lack of adhesion and the ability to participate in collective migration. In human CRC, complete p120 null cells are not found in early stage tumors, but have been reported in late-stage CRCs. One possibility for this observation could be that mutation in a particular pathway (e.g. p53) may alleviate a "requirement" for p120, as p120 has been shown *in vitro* to be necessary for transformation by both Src and Rac, but not H-Ras (Dohn et al, 2009). With the establishment of the *ex vivo* tumoroid system, this can be tested by lentiviral-based expression of different oncogenes in the context of p120 loss. However, it is also possible that this retention is due to instead to the process of dedifferentiation and the loss of crypt/lumen structures for p120 null cells to be lost into. Support for this hypothesis also comes from work done on the requirement for p120 in the mammary gland. In the developing mammary gland, p120 null cells are lost and are likely sloughed into the ductal lumen due to defects in collective migration (Kurley et al, 2012). However, tumors from the Polyoma Virus middle T (PyVT) mouse model, which have no luminal access and appear as a tightly packed cellular mass, are able to retain p120 KO cells. Metastases from these tumors, which must travel the vasculature to a secondary site, are invariably positive for p120 (ABR unpublished data). Thus, whether p120 is truly required for viability *per se* and whether this depends more on mutation or morphology remains to be determined.

The role of Kaiso in intestinal tumorigenesis

To-date, our studies on Kaiso have been inconclusive, and no direct function in the intestine has been found despite investigation of many tumor suppressing and promoting roles that have been reported in the literature. However, our *in vitro* studies suggest Kaiso may mediate the response to BMP signaling in the intestine, implicating a role for Kaiso in regulating a major pathway responsible for maintaining intestinal homeostasis. However, these studies have not yet been verified *in vivo*, for example by analysis of BMP target genes in Kaiso null and overexpressing mice. To-date, Kaiso null cultures have not been established in the *ex vivo* enteroid system, which could be utilized to determine more subtle phenotypic differences between Kaiso null, Kaiso OE, and Kaiso WT intestines. Furthermore, the BMP inhibitor Noggin is a required growth factor for enteroid culture. Modulating amount of Noggin could more clearly establish if any phenotypes are in fact due to alterations in BMP signaling or responsiveness.

Here, we identify a new Kaiso binding site and have generated an extensive list of potential Kaiso target genes by query of a publically available ChIP-seq database. While other groups have published results that further link Kaiso to the eKBS site, validation of these genes as *bona fide*, Kaiso-responsive targets has not yet been done. Thus, it is crucial to determine which genes are consistently regulated by Kaiso both *in vitro* and *in vivo*, as well as the manner of Kaiso's effect on gene transcription. While literature on the eKBS itself suggests this sequence is primarily responsible for mediating transcriptional activation (Guo et al, 2008; Mikula et al, 2010; Wyrwicz et al, 2007), our IHC studies suggest that, at least in the intestine, this may not be the case. One possibility is that Kaiso differentially regulates these genes depending on the organ and tissue systems. Interestingly, Kaiso is also highly upregulated in mammary tumors from PyVT mice, and concurrent studies on Kaiso target genes in the mammary and intestinal systems may help elucidate context- and tissue-dependent roles.

Clinical Relevance

Extensive pathology literature reports p120 downregulation or mislocalization in various stages of human CRCs. Furthermore, our analysis of the TCGA data shows p120 is downregulated in at the mRNA level in a majority of colon adenocarcinomas. Thus, alterations to p120 appear to be widely applicable to human CRCs, although its use as a prognostic marker has been disputed.

Here, we show that a functional cadherin complex is an early factor in the development of intestinal tumors, thus it may be widely applicable to CRC cancers. While p120 itself is a poor drug target due to its requirement for cell homeostasis, many of the pathways p120 and the cadherin complex interface with can be reliably targeted. Therefore, elucidating the mechanism behind p120's role in early tumor establishment may yield treatment or preventative measures in the clinic. It would also be interesting to know if the requirement for cadherin inactivation is the same in non-spontaneous CRCs, such as colitis associated cancers or hereditary nonpolyposis colorectal cancer (Lynch syndrome). While these tumors commonly rely on initiating mutations other than *APC* (Chaubert et al, 1994; Fishel et al, 1993; Papadopoulos et al, 1994), we have no reason to suspect the role for p120 and the cadherin complex are not widely applicable based on the similarities in pathology and IHC studies across cancers from multiple tissue systems.

REFERENCES

(2012) Comprehensive molecular characterization of human colon and rectal cancer. *Nature* **487:** 330-337

Aberle H, Bauer A, Stappert J, Kispert A, Kemler R (1997) beta-catenin is a target for the ubiquitin-proteasome pathway. *Embo J* **16:** 3797-3804

Albuquerque C, Breukel C, van der Luijt R, Fidalgo P, Lage P, Slors FJ, Leitao CN, Fodde R, Smits R (2002) The 'just-right' signaling model: APC somatic mutations are selected based on a specific level of activation of the beta-catenin signaling cascade. *Human molecular genetics* **11:** 1549-1560

Anastasiadis PZ (2007) p120-ctn: A nexus for contextual signaling via Rho GTPases. *Biochim Biophys Acta* **1773:** 34-46

Anastasiadis PZ, Moon SY, Thoreson MA, Mariner DJ, Crawford HC, Zheng Y, Reynolds AB (2000) Inhibition of RhoA by p120 catenin. *Nat Cell Biol* **2:** 637-644

Anastasiadis PZ, Reynolds AB (2000) The p120 catenin family: complex roles in adhesion, signaling and cancer. *Journal of Cell Science* **113:** 1319-1334

Azzolin L, Panciera T, Soligo S, Enzo E, Bicciato S, Dupont S, Bresolin S, Frasson C, Basso G, Guzzardo V, Fassina A, Cordenonsi M, Piccolo S (2014) YAP/TAZ incorporation in the beta-catenin destruction complex orchestrates the Wnt response. *Cell* **158:** 157-170

Barker N, Clevers H (2007) Tracking down the stem cells of the intestine: strategies to identify adult stem cells. *Gastroenterology* **133:** 1755-1760

Barker N, van Es JH, Kuipers J, Kujala P, van den Born M, Cozijnsen M, Haegebarth A, Korving J, Begthel H, Peters PJ, Clevers H (2007) Identification of stem cells in small intestine and colon by marker gene Lgr5. *Nature* **449:** 1003-1007

Barker N, van Oudenaarden A, Clevers H (2012) Identifying the stem cell of the intestinal crypt: strategies and pitfalls. *Cell Stem Cell* **11:** 452-460

Barrett CW, Smith JJ, Lu LC, Markham N, Stengel KR, Short SP, Zhang B, Hunt AA, Fingleton BM, Carnahan RH, Engel ME, Chen X, Beauchamp RD, Wilson KT, Hiebert SW, Reynolds AB, Williams CS (2012) Kaiso

directs the transcriptional corepressor MTG16 to the Kaiso binding site in target promoters. *PloS one* **7:** e51205

Barry ER, Morikawa T, Butler BL, Shrestha K, de la Rosa R, Yan KS, Fuchs CS, Magness ST, Smits R, Ogino S, Kuo CJ, Camargo FD (2013) Restriction of intestinal stem cell expansion and the regenerative response by YAP. *Nature* **493:** 106-110

Bartlett JD, Dobeck JM, Tye CE, Perez-Moreno M, Stokes N, Reynolds AB, Fuchs E, Skobe Z (2010) Targeted p120-Catenin Ablation Disrupts Dental Enamel Development. *PLoS ONE* **5:** e12703

Batlle E, Henderson JT, Beghtel H, van den Born MM, Sancho E, Huls G, Meeldijk J, Robertson J, van de Wetering M, Pawson T, Clevers H (2002) Beta-catenin and TCF mediate cell positioning in the intestinal epithelium by controlling the expression of EphB/ephrinB. *Cell* **111:** 251-263

Behrens J, von Kries JP, Kuhl M, Bruhn L, Wedlich D, Grosschedl R, Birchmeier W (1996) Functional interaction of beta-catenin with the transcription factor LEF-1. *Nature* **382:** 638-642

Bellovin DI, Bates RC, Muzikansky A, Rimm DL, Mercurio AM (2005) Altered localization of p120 catenin during epithelial to mesenchymal transition of colon carcinoma is prognostic for aggressive disease. *Cancer Res* **65:** 10938-10945

Berx G, Cleton-Jansen AM, Nollet F, de Leeuw WJ, van de Vijver M, Cornelisse C, van Roy F (1995) E-cadherin is a tumour/invasion suppressor gene mutated in human lobular breast cancers. *Embo J* **14:** 6107-6115

Berx G, Nollet F, van Roy F (1998) Dysregulation of the E-cadherin/catenin complex by irreversible mutations in human carcinomas. *Cell Adhes Commun* **6:** 171-184

Birchmeier W, Behrens J (1994) Cadherin expression in carcinomas: role in the formation of cell junctions and the prevention of invasiveness. *Biochim Biophys Acta* **1198:** 11-26

Blache P, van de Wetering M, Duluc I, Domon C, Berta P, Freund JN, Clevers H, Jay P (2004) SOX9 is an intestine crypt transcription factor, is regulated by the Wnt pathway, and represses the CDX2 and MUC2 genes. *The Journal of cell biology* **166:** 37-47

Blattler A, Yao L, Wang Y, Ye Z, Jin VX, Farnham PJ (2013) ZBTB33 binds unmethylated regions of the genome associated with actively expressed genes. *Epigenetics Chromatin* **6:** 13

Bolos V, Peinado H, Perez-Moreno MA, Fraga MF, Esteller M, Cano A (2003) The transcription factor Slug represses E-cadherin expression and induces epithelial to mesenchymal transitions: a comparison with Snail and E47 repressors. *Journal of cell science* **116:** 499-511

Bondi J, Bukholm G, Nesland JM, Bakka A, Bukholm IR (2006) An increase in the number of adhesion proteins with altered expression is associated with an increased risk of cancer death for colon carcinoma patients. *Int J Colorectal Dis* **21:** 231-237

Braig S, Bosserhoff AK (2013) Death inducer-obliterator 1 (Dido1) is a BMP target gene and promotes BMP-induced melanoma progression. *Oncogene* **32:** 837-848

Buck-Koehntop BA, Martinez-Yamout MA, Dyson HJ, Wright PE (2012a) Kaiso uses all three zinc fingers and adjacent sequence motifs for high affinity binding to sequence-specific and methyl-CpG DNA targets. *FEBS Lett* **586:** 734-739

Buck-Koehntop BA, Stanfield RL, Ekiert DC, Martinez-Yamout MA, Dyson HJ, Wilson IA, Wright PE (2012b) Molecular basis for recognition of methylated and specific DNA sequences by the zinc finger protein Kaiso. *Proc Natl Acad Sci U S A* **109:** 15229-15234

Cai J, Zhang N, Zheng Y, de Wilde RF, Maitra A, Pan D (2010) The Hippo signaling pathway restricts the oncogenic potential of an intestinal regeneration program. *Genes Dev* **24:** 2383-2388

Camargo FD, Gokhale S, Johnnidis JB, Fu D, Bell GW, Jaenisch R, Brummelkamp TR (2007) YAP1 increases organ size and expands undifferentiated progenitor cells. *Curr Biol* **17:** 2054-2060

Cano A, Perez-Moreno MA, Rodrigo I, Locascio A, Blanco MJ, del Barrio MG, Portillo F, Nieto MA (2000) The transcription factor snail controls epithelial-mesenchymal transitions by repressing E-cadherin expression. *Nature cell biology* **2:** 76-83

Carnahan RH, Rokas A, Gaucher EA, Reynolds AB (2010) The Molecular Evolution of the p120-Catenin Subfamily and Its Functional Associations. *PLoS ONE* **5:** e15747

Castano J, Solanas G, Casagolda D, Raurell I, Villagrasa P, Bustelo XR, Garcia de Herreros A, Dunach M (2007) Specific phosphorylation of p120-catenin regulatory domain differently modulates its binding to RhoA. *Mol Cell Biol* **27:** 1745-1757

Cavallo RA, Cox RT, Moline MM, Roose J, Polevoy GA, Clevers H, Peifer M, Bejsovec A (1998) Drosophila Tcf and Groucho interact to repress Wingless signalling activity. *Nature* **395:** 604-608

Chaubert P, Benhattar J, Saraga E, Costa J (1994) K-ras mutations and p53 alterations in neoplastic and nonneoplastic lesions associated with longstanding ulcerative colitis. *Am J Pathol* **144:** 767-775

Chaudhary R, Pierre CC, Nanan K, Wojtal D, Morone S, Pinelli C, Wood GA, Robine S, Daniel JM (2013) The POZ-ZF transcription factor Kaiso (ZBTB33) induces inflammation and progenitor cell differentiation in the murine intestine. *PloS one* **8:** e74160

Cheng H, Leblond CP (1974) Origin, differentiation and renewal of the four main epithelial cell types in the mouse small intestine. V. Unitarian Theory of the origin of the four epithelial cell types. *Am J Anat* **141:** 537-561

Cheung AF, Carter AM, Kostova KK, Woodruff JF, Crowley D, Bronson RT, Haigis KM, Jacks T (2010) Complete deletion of Apc results in severe polyposis in mice. *Oncogene* **29:** 1857-1864

Cheung LW, Mak AS, Cheung AN, Ngan HY, Leung PC, Wong AS (2011) P-cadherin cooperates with insulin-like growth factor-1 receptor to promote metastatic signaling of gonadotropin-releasing hormone in ovarian cancer via p120 catenin. *Oncogene* **30:** 2964-2974

Clevers H, Batlle E (2013) SnapShot: the intestinal crypt. *Cell* **152:** 1198-1198 e1192

Clevers H, Nusse R (2012) Wnt/beta-catenin signaling and disease. *Cell* **149:** 1192-1205

Clevers HC, Bevins CL (2013) Paneth cells: maestros of the small intestinal crypts. *Annu Rev Physiol* **75:** 289-311

Creamer B, Shorter RG, Bamforth J (1961) The turnover and shedding of epithelial cells. I. The turnover in the gastro-intestinal tract. *Gut* **2:** 110-118

Crepaldi T, Pollack AL, Prat M, Zborek A, Mostov K, Comoglio PM (1994) Targeting of the SF/HGF receptor to the basolateral domain of polarized epithelial cells. *The Journal of cell biology* **125:** 313-320

Curto M, Cole BK, Lallemand D, Liu CH, McClatchey AI (2007) Contact-dependent inhibition of EGFR signaling by Nf2/Merlin. *The Journal of cell biology* **177:** 893-903

Curto M, McClatchey AI (2008) Nf2/Merlin: a coordinator of receptor signalling and intercellular contact. *British journal of cancer* **98:** 256-262

Dai SD, Wang Y, Miao Y, Zhao Y, Zhang Y, Jiang GY, Zhang PX, Yang ZQ, Wang EH (2009) Cytoplasmic Kaiso is associated with poor prognosis in non-small cell lung cancer. *BMC Cancer* **9:** 178

Daniel JM (2007) Dancing in and out of the nucleus: p120(ctn) and the transcription factor Kaiso. *Biochim Biophys Acta* **1773:** 59-68

Daniel JM, Reynolds AB (1995) The tyrosine kinase substrate p120cas binds directly to E-cadherin but not to the adenomatous polyposis coli protein or alpha-catenin. *Mol Cell Biol* **15:** 4819-4824

Daniel JM, Reynolds AB (1999) The catenin p120(ctn) interacts with Kaiso, a novel BTB/POZ domain zinc finger transcription factor. *Mol Cell Biol* **19:** 3614-3623

Daniel JM, Spring CM, Crawford HC, Reynolds AB, Baig A (2002) The p120(ctn)-binding partner Kaiso is a bi-modal DNA-binding protein that recognizes both a sequence-specific consensus and methylated CpG dinucleotides. *Nucleic Acids Res* **30:** 2911-2919

Davis MA, Ireton RC, Reynolds AB (2003) A core function for p120-catenin in cadherin turnover. *The Journal of Cell Biology* **163:** 525-534

Davis MA, Reynolds AB (2006) Blocked Acinar Development, E-Cadherin Reduction, and Intraepithelial Neoplasia upon Ablation of p120-Catenin in the Mouse Salivary Gland. *Dev Cell* **10:** 21-31

de Lau W, Barker N, Low TY, Koo BK, Li VS, Teunissen H, Kujala P, Haegebarth A, Peters PJ, van de Wetering M, Stange DE, van Es JE, Guardavaccaro D, Schasfoort RB, Mohri Y, Nishimori K, Mohammed S, Heck AJ, Clevers H (2011) Lgr5 homologues associate with Wnt receptors and mediate R-spondin signalling. *Nature* **476:** 293-297

Defossez PA, Kelly KF, Filion GJ, Perez-Torrado R, Magdinier F, Menoni H, Nordgaard CL, Daniel JM, Gilson E (2005) The human enhancer blocker CTC-binding factor interacts with the transcription factor Kaiso. *J Biol Chem* **280:** 43017-43023

Defossez PA, Stancheva I (2011) Biological functions of methyl-CpG-binding proteins. *Prog Mol Biol Transl Sci* **101:** 377-398

Dogan A, Wang ZD, Spencer J (1995) E-cadherin expression in intestinal epithelium. *J Clin Pathol* **48:** 143-146

Dohn MR, Brown MV, Reynolds AB (2009) An essential role for p120-catenin in Src- and Rac1-mediated anchorage-independent cell growth. *The Journal of Cell Biology* **184:** 437-450

Donaldson NS, Pierre CC, Anstey MI, Robinson SC, Weerawardane SM, Daniel JM (2012) Kaiso represses the cell cycle gene cyclin D1 via sequence-specific and methyl-CpG-dependent mechanisms. *PloS one* **7:** e50398

Dupuy AJ, Jenkins NA, Copeland NG (2006) Sleeping beauty: a novel cancer gene discovery tool. *Human molecular genetics* **15 Spec No 1:** R75-79

Dupuy AJ, Rogers LM, Kim J, Nannapaneni K, Starr TK, Liu P, Largaespada DA, Scheetz TE, Jenkins NA, Copeland NG (2009) A modified sleeping beauty transposon system that can be used to model a wide variety of human cancers in mice. *Cancer Res* **69:** 8150-8156

el Marjou F, Janssen KP, Chang BH, Li M, Hindie V, Chan L, Louvard D, Chambon P, Metzger D, Robine S (2004) Tissue-specific and inducible Cre-mediated recombination in the gut epithelium. *Genesis* **39:** 186-193

Elia LP, Yamamoto M, Zang K, Reichardt LF (2006) p120 catenin regulates dendritic spine and synapse development through Rho-family GTPases and cadherins. *Neuron* **51:** 43-56

Escaffit F, Perreault N, Jean D, Francoeur C, Herring E, Rancourt C, Rivard N, Vachon PH, Pare F, Boucher MP, Auclair J, Beaulieu JF (2005) Repressed E-cadherin expression in the lower crypt of human small intestine: a cell marker of functional relevance. *Experimental cell research* **302:** 206-220

Fagotto F, Funayama N, Gluck U, Gumbiner BM (1996) Binding to cadherins antagonizes the signaling activity of beta-catenin during axis formation in Xenopus. *The Journal of cell biology* **132:** 1105-1114

Fagotto F, Gluck U, Gumbiner BM (1998) Nuclear localization signal-independent and importin/karyopherin-independent nuclear import of beta-catenin. *Curr Biol* **8:** 181-190

Farin HF, Van Es JH, Clevers H (2012) Redundant sources of Wnt regulate intestinal stem cells and promote formation of Paneth cells. *Gastroenterology* **143:** 1518-1529 e1517

Fearon ER, Vogelstein B (1990) A genetic model for colorectal tumorigenesis. *Cell* **61:** 759-767

Filion GJ, Zhenilo S, Salozhin S, Yamada D, Prokhortchouk E, Defossez PA (2006) A family of human zinc finger proteins that bind methylated DNA and repress transcription. *Mol Cell Biol* **26:** 169-181

Fishel R, Lescoe MK, Rao MR, Copeland NG, Jenkins NA, Garber J, Kane M, Kolodner R (1993) The human mutator gene homolog MSH2 and its association with hereditary nonpolyposis colon cancer. *Cell* **75:** 1027-1038

Fodde R, Edelmann W, Yang K, van Leeuwen C, Carlson C, Renault B, Breukel C, Alt E, Lipkin M, Khan PM, et al. (1994) A targeted chain-termination mutation in the mouse Apc gene results in multiple intestinal tumors. *Proc Natl Acad Sci U S A* **91:** 8969-8973

Fournier A, Sasai N, Nakao M, Defossez PA (2012) The role of methyl-binding proteins in chromatin organization and epigenome maintenance. *Brief Funct Genomics* **11:** 251-264

Fre S, Huyghe M, Mourikis P, Robine S, Louvard D, Artavanis-Tsakonas S (2005) Notch signals control the fate of immature progenitor cells in the intestine. *Nature* **435:** 964-968

Freeman TJ, Smith JJ, Chen X, Washington MK, Roland JT, Means AL, Eschrich SA, Yeatman TJ, Deane NG, Beauchamp RD (2012) Smad4-mediated signaling inhibits intestinal neoplasia by inhibiting expression of beta-catenin. *Gastroenterology* **142:** 562-571 e562

Friedl P (2004) Prespecification and plasticity: shifting mechanisms of cell migration. *Current opinion in cell biology* **16:** 14-23

Friedl P, Hegerfeldt Y, Tusch M (2004) Collective cell migration in morphogenesis and cancer. *Int J Dev Biol* **48:** 441-449

Fuerer C, Nusse R (2010) Lentiviral vectors to probe and manipulate the Wnt signaling pathway. *PLoS ONE* **5:** e9370

Giovannini M, Robanus-Maandag E, Niwa-Kawakita M, van der Valk M, Woodruff JM, Goutebroze L, Merel P, Berns A, Thomas G (1999) Schwann cell hyperplasia and tumors in transgenic mice expressing a naturally occurring mutant NF2 protein. *Genes Dev* **13:** 978-986

Gold JS, Reynolds AB, Rimm DL (1998) Loss of p120ctn in human colorectal cancer predicts metastasis and poor survival. *Cancer Letters* **132:** 193-201

Goodwin M, Kovacs EM, Thoreson MA, Reynolds AB, Yap AS (2003) Minimal Mutation of the Cytoplasmic Tail Inhibits the Ability of E-cadherin to Activate Rac but Not Phosphatidylinositol 3-Kinase. *Journal of Biological Chemistry* **278:** 20533-20539

Gottardi CJ, Wong E, Gumbiner BM (2001) E-cadherin suppresses cellular transformation by inhibiting beta-catenin signaling in an adhesion-independent manner. *The Journal of cell biology* **153:** 1049-1060

Graff JR, Herman JG, Lapidus RG, Chopra H, Xu R, Jarrard DF, Isaacs WB, Pitha PM, Davidson NE, Baylin SB (1995) E-cadherin expression is silenced by DNA hypermethylation in human breast and prostate carcinomas. *Cancer Res* **55:** 5195-5199

Gumbiner BM (2005) Regulation of cadherin-mediated adhesion in morphogenesis. *Nat Rev Mol Cell Biol* **6:** 622-634

Guo G, Bauer S, Hecht J, Schulz MH, Busche A, Robinson PN (2008) A short ultraconserved sequence drives transcription from an alternate FBN1 promoter. *Int J Biochem Cell Biol* **40:** 638-650

Hagemann RF, Sigdestad CP, Lesher S (1970) A quantitative description of the intestinal epithelium of the mouse. *Am J Anat* **129:** 41-51

Hamaratoglu F, Willecke M, Kango-Singh M, Nolo R, Hyun E, Tao C, Jafar-Nejad H, Halder G (2006) The tumour-suppressor genes NF2/Merlin and Expanded act through Hippo signalling to regulate cell proliferation and apoptosis. *Nature cell biology* **8:** 27-36

Haramis AP, Begthel H, van den Born M, van Es J, Jonkheer S, Offerhaus GJ, Clevers H (2004) De novo crypt formation and juvenile polyposis on BMP inhibition in mouse intestine. *Science* **303:** 1684-1686

He TC, Sparks AB, Rago C, Hermeking H, Zawel L, da Costa LT, Morin PJ, Vogelstein B, Kinzler KW (1998) Identification of c-MYC as a target of the APC pathway. *Science* **281:** 1509-1512

He XC, Zhang J, Tong WG, Tawfik O, Ross J, Scoville DH, Tian Q, Zeng X, He X, Wiedemann LM, Mishina Y, Li L (2004) BMP signaling inhibits intestinal stem cell self-renewal through suppression of Wnt-beta-catenin signaling. *Nature genetics* **36:** 1117-1121

Heasman J, Crawford A, Goldstone K, Garner-Hamrick P, Gumbiner B, McCrea P, Kintner C, Noro CY, Wylie C (1994) Overexpression of cadherins and underexpression of beta-catenin inhibit dorsal mesoderm induction in early Xenopus embryos. *Cell* **79:** 791-803

Hein N, Jiang K, Cornelissen C, Luscher B (2011) TGFbeta1 enhances MAD1 expression and stimulates promoter-bound Pol II phosphorylation: basic functions of C/EBP, SP and SMAD3 transcription factors. *BMC Mol Biol* **12:** 9

Henderson P, van Limbergen JE, Schwarze J, Wilson DC (2011) Function of the intestinal epithelium and its dysregulation in inflammatory bowel disease. *Inflamm Bowel Dis* **17:** 382-395

Hermiston ML, Gordon JI (1995) Inflammatory bowel disease and adenomas in mice expressing a dominant negative N-cadherin. *Science* **270:** 1203-1207

Hermiston ML, Wong MH, Gordon JI (1996) Forced expression of E-cadherin in the mouse intestinal epithelium slows cell migration and provides evidence for nonautonomous regulation of cell fate in a self-renewing system. *Genes Dev* **10:** 985-996

Herzig M, Savarese F, Novatchkova M, Semb H, Christofori G (2007) Tumor progression induced by the loss of E-cadherin independent of beta-catenin/Tcf-mediated Wnt signaling. *Oncogene* **26:** 2290-2298

Hoschuetzky H, Aberle H, Kemler R (1994) Beta-catenin mediates the interaction of the cadherin-catenin complex with epidermal growth factor receptor. *The Journal of cell biology* **127:** 1375-1380

Huber O, Korn R, McLaughlin J, Ohsugi M, Herrmann BG, Kemler R (1996) Nuclear localization of beta-catenin by interaction with transcription factor LEF-1. *Mech Dev* **59:** 3-10

Hulpiau P, van Roy F (2009) Molecular evolution of the cadherin superfamily. *Int J Biochem Cell Biol* **41:** 349-369

Iioka H, Doerner SK, Tamai K (2009) Kaiso is a bimodal modulator for Wnt/beta-catenin signaling. *FEBS Lett* **583:** 627-632

Ireton RC, Davis MA, van Hengel J, Mariner DJ, Barnes K, Thoreson MA, Anastasiadis PZ, Matrisian L, Bundy LM, Sealy L, Gilbert B, van Roy F, Reynolds AB (2002) A novel role for p120 catenin in E-cadherin function. *The Journal of Cell Biology* **159:** 465-476

Jaffe AB, Hall A (2005) Rho GTPases: biochemistry and biology. *Annu Rev Cell Dev Biol* **21:** 247-269

Johnson E, Seachrist DD, DeLeon-Rodriguez CM, Lozada KL, Miedler J, Abdul-Karim FW, Keri RA (2010) HER2/ErbB2-induced breast cancer cell migration and invasion require p120 catenin activation of Rac1 and Cdc42. *J Biol Chem* **285:** 29491-29501

Jones J, Wang H, Karanam B, Theodore S, Dean-Colomb W, Welch DR, Grizzle W, Yates C (2014) Nuclear localization of Kaiso promotes the poorly differentiated phenotype and EMT in infiltrating ductal carcinomas. *Clin Exp Metastasis*

Jones J, Wang H, Zhou J, Hardy S, Turner T, Austin D, He Q, Wells A, Grizzle WE, Yates C (2012) Nuclear Kaiso indicates aggressive prostate cancers and promotes migration and invasiveness of prostate cancer cells. *Am J Pathol* **181:** 1836-1846

Kalluri R, Weinberg RA (2009) The basics of epithelial-mesenchymal transition. *J Clin Invest* **119:** 1420-1428

Karatzas G, Karayiannakis AJ, Syrigos KN, Chatzigianni E, Papanikolaou S, Riza F, Papanikolaou D (1999) E-cadherin expression correlates with tumor differentiation in colorectal cancer. *Hepatogastroenterology* **46:** 232-235

Karnieli E, Barzilai A, Rafaeloff R, Armoni M (1986) Distribution of glucose transporters in membrane fractions isolated from human adipose cells. Relation to cell size. *J Clin Invest* **78**:1051-1055

Keirsebilck A, Bonne S, Staes K, van Hengel J, Nollet F, Reynolds A, van Roy F (1998) Molecular cloning of the human p120ctn catenin gene (CTNND1): expression of multiple alternatively spliced isoforms. *Genomics* **50:** 129-146

Kelly KF, Spring CM, Otchere AA, Daniel JM (2004) NLS-dependent nuclear localization of p120ctn is necessary to relieve Kaiso-mediated transcriptional repression. *Journal of Cell Science* **117:** 2675-2686

Kim NG, Koh E, Chen X, Gumbiner BM (2011) E-cadherin mediates contact inhibition of proliferation through Hippo signaling-pathway components. *Proc Natl Acad Sci U S A* **108:** 11930-11935

Kim SW, Park JI, Spring CM, Sater AK, Ji H, Otchere AA, Daniel JM, McCrea PD (2004) Non-canonical Wnt signals are modulated by the Kaiso transcriptional repressor and p120-catenin. *Nature cell biology* **6:** 1212-1220

Kinzler KW, Nilbert MC, Vogelstein B, Bryan TM, Levy DB, Smith KJ, Preisinger AC, Hamilton SR, Hedge P, Markham A, et al. (1991) Identification of a gene located at chromosome 5q21 that is mutated in colorectal cancers. *Science* **251:** 1366-1370

Kinzler KW, Vogelstein B (1996) Lessons from hereditary colorectal cancer. *Cell* **87:** 159-170

Kitagawa M, Hatakeyama S, Shirane M, Matsumoto M, Ishida N, Hattori K, Nakamichi I, Kikuchi A, Nakayama K (1999) An F-box protein, FWD1, mediates ubiquitin-dependent proteolysis of beta-catenin. *Embo J* **18:** 2401-2410

Koh DI, Han D, Ryu H, Choi WI, Jeon BN, Kim MK, Kim Y, Kim JY, Parry L, Clarke AR, Reynolds AB, Hur MW (2014) KAISO, a critical regulator of p53-mediated transcription of CDKN1A and apoptotic genes. *Proc Natl Acad Sci U S A* **111:** 15078-15083

Koh DI, Yoon JH, Kim MK, An H, Kim MY, Hur MW (2013) Kaiso is a key regulator of spleen germinal center formation by repressing Bcl6 expression in splenocytes. *Biochem Biophys Res Commun* **442:** 177-182

Kondapalli J, Flozak AS, Albuquerque ML (2004) Laminar shear stress differentially modulates gene expression of p120 catenin, Kaiso transcription factor, and vascular endothelial cadherin in human coronary artery endothelial cells. *J Biol Chem* **279:** 11417-11424

Koo BK, Stange DE, Sato T, Karthaus W, Farin HF, Huch M, van Es JH, Clevers H (2011) Controlled gene expression in primary Lgr5 organoid cultures. *Nat Methods*

Kosinski C, Stange DE, Xu C, Chan AS, Ho C, Yuen ST, Mifflin RC, Powell DW, Clevers H, Leung SY, Chen X (2010) Indian hedgehog regulates intestinal stem cell fate through epithelial-mesenchymal interactions during development. *Gastroenterology* **139:** 893-903

Kuhnert F, Davis CR, Wang HT, Chu P, Lee M, Yuan J, Nusse R, Kuo CJ (2004) Essential requirement for Wnt signaling in proliferation of adult small intestine and colon revealed by adenoviral expression of Dickkopf-1. *Proc Natl Acad Sci U S A* **101:** 266-271

Kuphal F, Behrens J (2006) E-cadherin modulates Wnt-dependent transcription in colorectal cancer cells but does not alter Wnt-independent gene expression in fibroblasts. *Experimental cell research* **312:** 457-467

Kuraguchi M, Wang XP, Bronson RT, Rothenberg R, Ohene-Baah NY, Lund JJ, Kucherlapati M, Maas RL, Kucherlapati R (2006) Adenomatous polyposis coli (APC) is required for normal development of skin and thymus. *PLoS genetics* **2:** e146

Kurley SJ, Bierie B, Carnahan RH, Lobdell NA, Davis MA, Hofmann I, Moses HL, Muller WJ, Reynolds AB (2012) p120-catenin is essential for terminal end bud function and mammary morphogenesis. *Development* **139:** 1754-1764

Lao VV, Grady WM (2011) Epigenetics and colorectal cancer. *Nat Rev Gastroenterol Hepatol* **8:** 686-700

Laprise P, Langlois MJ, Boucher MJ, Jobin C, Rivard N (2004) Down-regulation of MEK/ERK signaling by E-cadherin-dependent PI3K/Akt pathway in differentiating intestinal epithelial cells. *J Cell Physiol* **199:** 32-39

Lee D, Yu M, Lee E, Kim H, Yang Y, Kim K, Pannicia C, Kurie JM, Threadgill DW (2009) Tumor-specific apoptosis caused by deletion of the ERBB3 pseudo-kinase in mouse intestinal epithelium. *J Clin Invest* **119:** 2702-2713

Lei QY, Zhang H, Zhao B, Zha ZY, Bai F, Pei XH, Zhao S, Xiong Y, Guan KL (2008) TAZ promotes cell proliferation and epithelial-mesenchymal transition and is inhibited by the hippo pathway. *Mol Cell Biol* **28:** 2426-2436

Li J, Bowens N, Cheng L, Zhu X, Chen M, Hannenhalli S, Cappola TP, Parmacek MS (2012a) Myocardin-like protein 2 regulates TGFbeta signaling in embryonic stem cells and the developing vasculature. *Development* **139:** 3531-3542

Li VS, Ng SS, Boersema PJ, Low TY, Karthaus WR, Gerlach JP, Mohammed S, Heck AJ, Maurice MM, Mahmoudi T, Clevers H (2012b) Wnt signaling through inhibition of beta-catenin degradation in an intact Axin1 complex. *Cell* **149:** 1245-1256

Libusova L, Stemmler MP, Hierholzer A, Schwarz H, Kemler R (2010) N-cadherin can structurally substitute for E-cadherin during intestinal development but leads to polyp formation. *Development* **137:** 2297-2305

Lien WH, Klezovitch O, Fernandez TE, Delrow J, Vasioukhin V (2006) alphaE-catenin controls cerebral cortical size by regulating the hedgehog signaling pathway. *Science* **311:** 1609-1612

Liu C, Li Y, Semenov M, Han C, Baeg GH, Tan Y, Zhang Z, Lin X, He X (2002) Control of beta-catenin phosphorylation/degradation by a dual-kinase mechanism. *Cell* **108:** 837-847

Lopes EC, Valls E, Figueroa ME, Mazur A, Meng FG, Chiosis G, Laird PW, Schreiber-Agus N, Greally JM, Prokhortchouk E, Melnick A (2008) Kaiso contributes to DNA methylation-dependent silencing of tumor suppressor genes in colon cancer cell lines. *Cancer Res* **68:** 7258-7263

Luo J, Solimini NL, Elledge SJ (2009) Principles of cancer therapy: oncogene and non-oncogene addiction. *Cell* **136:** 823-837

Ma L, Young J, Prabhala H, Pan E, Mestdagh P, Muth D, Teruya-Feldstein J, Reinhardt F, Onder TT, Valastyan S, Westermann F, Speleman F, Vandesompele J, Weinberg RA (2010) miR-9, a MYC/MYCN-activated microRNA, regulates E-cadherin and cancer metastasis. *Nature cell biology* **12:** 247-256

Machado JC, Soares P, Carneiro F, Rocha A, Beck S, Blin N, Berx G, Sobrinho-Simoes M (1999) E-cadherin gene mutations provide a genetic basis for the phenotypic divergence of mixed gastric carcinomas. *Laboratory investigation; a journal of technical methods and pathology* **79:** 459-465

Mahe MM, Aihara E, Schumacher MA, Zavros Y, Montrose MH, Helmrath MA, Sato T, Shroyer NF (2013) Establishment of gastrointestinal epithelial organoids. *Curr Protoc Mouse Biol* **3:** 217-240

Mann KM, Ward JM, Yew CC, Kovochich A, Dawson DW, Black MA, Brett BT, Sheetz TE, Dupuy AJ, Chang DK, Biankin AV, Waddell N, Kassahn KS, Grimmond SM, Rust AG, Adams DJ, Jenkins NA, Copeland NG (2012) Sleeping Beauty mutagenesis reveals cooperating mutations and pathways in pancreatic adenocarcinoma. *Proc Natl Acad Sci U S A* **109:** 5934-5941

Mann MB, Jenkins NA, Copeland NG, Mann KM (2014) Sleeping Beauty mutagenesis: exploiting forward genetic screens for cancer gene discovery. *Curr Opin Genet Dev* **24C:** 16-22

March HN, Rust AG, Wright NA, Ten Hoeve J, de Ridder J, Eldridge M, van der Weyden L, Berns A, Gadiot J, Uren A, Kemp R, Arends MJ, Wessels LF, Winton DJ, Adams DJ (2011) Insertional mutagenesis identifies multiple networks of cooperating genes driving intestinal tumorigenesis. *Nature genetics* **43:** 1202-1209

Marciano DK, Brakeman PR, Lee CZ, Spivak N, Eastburn DJ, Bryant DM, Beaudoin GM, 3rd, Hofmann I, Mostov KE, Reichardt LF (2011) p120 catenin is required for normal renal tubulogenesis and glomerulogenesis. *Development* **138:** 2099-2109

Maretzky T, Reiss K, Ludwig A, Buchholz J, Scholz F, Proksch E, de Strooper B, Hartmann D, Saftig P (2005) ADAM10 mediates E-cadherin shedding and regulates epithelial cell-cell adhesion, migration, and beta-catenin translocation. *Proc Natl Acad Sci U S A* **102:** 9182-9187

Mariner DJ, Davis MA, Reynolds AB (2004) EGFR signaling to p120-catenin through phosphorylation at Y228. *Journal of Cell Science* **117:** 1339-1350

Marshman E, Booth C, Potten CS (2002) The intestinal epithelial stem cell. *Bioessays* **24:** 91-98

McClatchey AI, Saotome I, Mercer K, Crowley D, Gusella JF, Bronson RT, Jacks T (1998) Mice heterozygous for a mutation at the Nf2 tumor suppressor locus develop a range of highly metastatic tumors. *Genes Dev* **12:** 1121-1133

Medema JP, Vermeulen L (2011) Microenvironmental regulation of stem cells in intestinal homeostasis and cancer. *Nature* **474:** 318-326

Mikula M, Gaj P, Dzwonek K, Rubel T, Karczmarski J, Paziewska A, Dzwonek A, Bragoszewski P, Dadlez M, Ostrowski J (2010) Comprehensive analysis of the palindromic motif TCTCGCGAGA: a regulatory element of the HNRNPK promoter. *DNA Res* **17:** 245-260

Miyashita Y, Ozawa M (2007) Increased internalization of p120-uncoupled E-cadherin and a requirement for a dileucine motif in the cytoplasmic domain for endocytosis of the protein. *J Biol Chem* **282:** 11540-11548

Mo Y-Y, Reynolds AB (1996) Identification of Murine p120cas Isoforms and Heterogeneous Expression of p120cas Isoforms in Human Tumor Cell Lines. *Cancer Res* **56:** 2633-2640

Molenaar M, van de Wetering M, Oosterwegel M, Peterson-Maduro J, Godsave S, Korinek V, Roose J, Destree O, Clevers H (1996) XTcf-3 transcription factor mediates beta-catenin-induced axis formation in Xenopus embryos. *Cell* **86:** 391-399

Moll R, Mitze M, Frixen UH, Birchmeier W (1993) Differential loss of E-cadherin expression in infiltrating ductal and lobular breast carcinomas. *Am J Pathol* **143:** 1731-1742

Montgomery RK, Carlone DL, Richmond CA, Farilla L, Kranendonk ME, Henderson DE, Baffour-Awuah NY, Ambruzs DM, Fogli LK, Algra S, Breault DT (2011) Mouse telomerase reverse transcriptase (mTert) expression marks slowly cycling intestinal stem cells. *Proc Natl Acad Sci U S A* **108:** 179-184

Mooseker MS (1985) Organization, chemistry, and assembly of the cytoskeletal apparatus of the intestinal brush border. *Annu Rev Cell Biol* **1:** 209-241

Morali OG, Delmas V, Moore R, Jeanney C, Thiery JP, Larue L (2001) IGF-II induces rapid beta-catenin relocation to the nucleus during epithelium to mesenchyme transition. *Oncogene* **20:** 4942-4950

Moser AR, Pitot HC, Dove WF (1990) A dominant mutation that predisposes to multiple intestinal neoplasia in the mouse. *Science* **247:** 322-324

Muncan V, Sansom OJ, Tertoolen L, Phesse TJ, Begthel H, Sancho E, Cole AM, Gregorieff A, de Alboran IM, Clevers H, Clarke AR (2006) Rapid loss of intestinal crypts upon conditional deletion of the Wnt/Tcf-4 target gene c-Myc. *Mol Cell Biol* **26:** 8418-8426

Myant KB, Cammareri P, McGhee EJ, Ridgway RA, Huels DJ, Cordero JB, Schwitalla S, Kalna G, Ogg EL, Athineos D, Timpson P, Vidal M, Murray GI, Greten FR, Anderson KI, Sansom OJ (2013) ROS production and NF-kappaB activation triggered by RAC1 facilitate WNT-driven intestinal stem cell proliferation and colorectal cancer initiation. *Cell Stem Cell* **12:** 761-773

Nakamura Y, Nishisho I, Kinzler KW, Vogelstein B, Miyoshi Y, Miki Y, Ando H, Horii A (1992) Mutations of the APC (adenomatous polyposis coli) gene in FAP (familial polyposis coli) patients and in sporadic colorectal tumors. *Tohoku J Exp Med* **168:** 141-147

Nelson DA, Manhardt C, Kamath V, Sui Y, Santamaria-Pang A, Can A, Bello M, Corwin A, Dinn SR, Lazare M, Gervais EM, Sequeira SJ, Peters SB, Ginty F, Gerdes MJ, Larsen M (2013) Quantitative single cell analysis of cell population dynamics during submandibular salivary gland development and differentiation. *Biol Open* **2:** 439-447

Nimnual AS, Taylor LJ, Bar-Sagi D (2003) Redox-dependent downregulation of Rho by Rac. *Nature cell biology* **5:** 236-241

Nishisho I, Nakamura Y, Miyoshi Y, Miki Y, Ando H, Horii A, Koyama K, Utsunomiya J, Baba S, Hedge P (1991) Mutations of chromosome 5q21 genes in FAP and colorectal cancer patients. *Science* **253:** 665-669

Noah TK, Donahue B, Shroyer NF (2011) Intestinal development and differentiation. *Experimental cell research* **317:** 2702-2710

Noren NK, Liu BP, Burridge K, Kreft B (2000) p120 catenin regulates the actin cytoskeleton via Rho family GTPases. *The Journal of Cell Biology* **150:** 567-580

Nusse R, Varmus HE (1992) Wnt genes. *Cell* **69:** 1073-1087

Oas RG, Xiao K, Summers S, Wittich KB, Chiasson CM, Martin WD, Grossniklaus HE, Vincent PA, Reynolds AB, Kowalczyk AP (2010) p120-Catenin Is Required for Mouse Vascular Development. *Circ Res* **106:** 941-951

Oshima M, Oshima H, Kitagawa K, Kobayashi M, Itakura C, Taketo M (1995) Loss of Apc heterozygosity and abnormal tissue building in nascent intestinal polyps in mice carrying a truncated Apc gene. *Proc Natl Acad Sci U S A* **92:** 4482-4486

Ota M, Sasaki H (2008) Mammalian Tead proteins regulate cell proliferation and contact inhibition as transcriptional mediators of Hippo signaling. *Development* **135:** 4059-4069

Palacios J, Sarrio D, Garcia-Macias MC, Bryant B, Sobel ME, Merino MJ (2003) Frequent E-cadherin gene inactivation by loss of heterozygosity in pleomorphic lobular carcinoma of the breast. *Modern pathology : an official journal of the United States and Canadian Academy of Pathology, Inc* **16:** 674-678

Pan D (2010) The hippo signaling pathway in development and cancer. *Dev Cell* **19:** 491-505

Papadopoulos N, Nicolaides NC, Wei YF, Ruben SM, Carter KC, Rosen CA, Haseltine WA, Fleischmann RD, Fraser CM, Adams MD, et al. (1994) Mutation of a mutL homolog in hereditary colon cancer. *Science* **263:** 1625-1629

Park JI, Ji H, Jun S, Gu D, Hikasa H, Li L, Sokol SY, McCrea PD (2006) Frodo links Dishevelled to the p120-catenin/Kaiso pathway: distinct catenin subfamilies promote Wnt signals. *Dev Cell* **11:** 683-695

Park JI, Kim SW, Lyons JP, Ji H, Nguyen TT, Cho K, Barton MC, Deroo T, Vleminckx K, Moon RT, McCrea PD (2005) Kaiso/p120-catenin and TCF/beta-catenin complexes coordinately regulate canonical Wnt gene targets. *Dev Cell* **8:** 843-854

Pece S, Gutkind JS (2000) Signaling from E-cadherins to the MAPK pathway by the recruitment and activation of epidermal growth factor receptors upon cell-cell contact formation. *J Biol Chem* **275:** 41227-41233

Perez-Moreno M, Davis MA, Wong E, Pasolli HA, Reynolds AB, Fuchs E (2006) p120-Catenin Mediates Inflammatory Responses in the Skin. *Cell* **124:** 631-644

Perl AK, Wilgenbus P, Dahl U, Semb H, Christofori G (1998) A causal role for E-cadherin in the transition from adenoma to carcinoma. *Nature* **392:** 190-193

Peterson LW, Artis D (2014) Intestinal epithelial cells: regulators of barrier function and immune homeostasis. *Nat Rev Immunol* **14:** 141-153

Pieters T, van Roy F, van Hengel J (2012) Functions of p120ctn isoforms in cell-cell adhesion and intracellular signaling. *Front Biosci (Landmark Ed)* **17:** 1669-1694

Pinto D, Gregorieff A, Begthel H, Clevers H (2003) Canonical Wnt signals are essential for homeostasis of the intestinal epithelium. *Genes Dev* **17:** 1709-1713

Potten CS (1977) Extreme sensitivity of some intestinal crypt cells to X and gamma irradiation. *Nature* **269:** 518-521

Powell AE, Wang Y, Li Y, Poulin EJ, Means AL, Washington MK, Higginbotham JN, Juchheim A, Prasad N, Levy SE, Guo Y, Shyr Y, Aronow BJ, Haigis KM, Franklin JL, Coffey RJ (2012) The pan-ErbB negative regulator Lrig1 is an intestinal stem cell marker that functions as a tumor suppressor. *Cell* **149:** 146-158

Prokhortchouk A, Hendrich B, Jorgensen H, Ruzov A, Wilm M, Georgiev G, Bird A, Prokhortchouk E (2001) The p120 catenin partner Kaiso is a DNA methylation-dependent transcriptional repressor. *Genes Dev* **15:** 1613-1618

Prokhortchouk A, Sansom O, Selfridge J, Caballero IM, Salozhin S, Aithozhina D, Cerchietti L, Meng FG, Augenlicht LH, Mariadason JM, Hendrich B, Melnick A, Prokhortchouk E, Clarke A, Bird A (2006) Kaiso-deficient mice show resistance to intestinal cancer. *Mol Cell Biol* **26:** 199-208

Qian X, Karpova T, Sheppard AM, McNally J, Lowy DR (2004) E-cadherin-mediated adhesion inhibits ligand-dependent activation of diverse receptor tyrosine kinases. *Embo J* **23:** 1739-1748

Raghav SK, Waszak SM, Krier I, Gubelmann C, Isakova A, Mikkelsen TS, Deplancke B (2012) Integrative genomics identifies the corepressor SMRT as a gatekeeper of adipogenesis through the transcription factors C/EBPbeta and KAISO. *Molecular cell* **46:** 335-350

Reiss K, Maretzky T, Ludwig A, Tousseyn T, de Strooper B, Hartmann D, Saftig P (2005) ADAM10 cleavage of N-cadherin and regulation of cell-cell adhesion and beta-catenin nuclear signalling. *Embo J* **24:** 742-752

Reya T, Clevers H (2005) Wnt signalling in stem cells and cancer. *Nature* **434:** 843-850

Reynolds AB, Daniel J, McCrea PD, Wheelock MJ, Wu J, Zhang Z (1994) Identification of a new catenin: the tyrosine kinase substrate p120cas associates with E-cadherin complexes. *Mol Cell Biol* **14:** 8333-8342

Reynolds AB, Roczniak-Ferguson A (2004) Emerging roles for p120-catenin in cell adhesion and cancer. *Oncogene* **23:** 7947-7956

Reynolds AB, Roesel DJ, Kanner SB, Parsons JT (1989) Transformation-specific tyrosine phosphorylation of a novel cellular protein in chicken cells expressing oncogenic variants of the avian cellular src gene. *Mol Cell Biol* **9:** 629-638

Rimm DL, Koslov ER, Kebriaei P, Cianci CD, Morrow JS (1995) Alpha 1(E)-catenin is an actin-binding and -bundling protein mediating the attachment of F-actin to the membrane adhesion complex. *Proc Natl Acad Sci U S A* **92:** 8813-8817

Roberts RB, Min L, Washington MK, Olsen SJ, Settle SH, Coffey RJ, Threadgill DW (2002) Importance of epidermal growth factor receptor signaling in establishment of adenomas and maintenance of carcinomas during intestinal tumorigenesis. *Proc Natl Acad Sci U S A* **99:** 1521-1526

Rodova M, Kelly KF, VanSaun M, Daniel JM, Werle MJ (2004) Regulation of the rapsyn promoter by kaiso and delta-catenin. *Mol Cell Biol* **24:** 7188-7196

Roose J, Molenaar M, Peterson J, Hurenkamp J, Brantjes H, Moerer P, van de Wetering M, Destree O, Clevers H (1998) The Xenopus Wnt effector XTcf-3 interacts with Groucho-related transcriptional repressors. *Nature* **395:** 608-612

Rowan AJ, Lamlum H, Ilyas M, Wheeler J, Straub J, Papadopoulou A, Bicknell D, Bodmer WF, Tomlinson IP (2000) APC mutations in sporadic colorectal tumors: A mutational "hotspot" and interdependence of the "two hits". *Proc Natl Acad Sci U S A* **97:** 3352-3357

Ruzov A, Dunican DS, Prokhortchouk A, Pennings S, Stancheva I, Prokhortchouk E, Meehan RR (2004) Kaiso is a genome-wide repressor of transcription that is essential for amphibian development. *Development* **131:** 6185-6194

Ruzov A, Hackett JA, Prokhortchouk A, Reddington JP, Madej MJ, Dunican DS, Prokhortchouk E, Pennings S, Meehan RR (2009) The interaction of xKaiso with xTcf3: a revised model for integration of epigenetic and Wnt signalling pathways. *Development* **136:** 723-727

Sadot E, Simcha I, Shtutman M, Ben-Ze'ev A, Geiger B (1998) Inhibition of beta-catenin-mediated transactivation by cadherin derivatives. *Proc Natl Acad Sci U S A* **95:** 15339-15344

Sangiorgi E, Capecchi MR (2008) Bmi1 is expressed in vivo in intestinal stem cells. *Nature genetics* **40:** 915-920

Sansom OJ, Reed KR, Hayes AJ, Ireland H, Brinkmann H, Newton IP, Batlle E, Simon-Assmann P, Clevers H, Nathke IS, Clarke AR, Winton DJ (2004) Loss of Apc in vivo immediately perturbs Wnt signaling, differentiation, and migration. *Genes Dev* **18:** 1385-1390

Sarrio D, Perez-Mies B, Hardisson D, Moreno-Bueno G, Suarez A, Cano A, Martin-Perez J, Gamallo C, Palacios J (2004) Cytoplasmic localization of p120ctn and E-cadherin loss characterize lobular breast carcinoma from preinvasive to metastatic lesions. *Oncogene* **23:** 3272-3283

Sasai N, Nakao M, Defossez P-A (2010a) Sequence-specific recognition of methylated DNA by human zinc-finger proteins. *Nucleic Acids Res* **38:** 5015-5022

Sasai N, Nakao M, Defossez PA (2010b) Sequence-specific recognition of methylated DNA by human zinc-finger proteins. *Nucleic Acids Res* **38:** 5015-5022

Sato T, Stange DE, Ferrante M, Vries RG, Van Es JH, Van den Brink S, Van Houdt WJ, Pronk A, Van Gorp J, Siersema PD, Clevers H (2011a) Long-term expansion of epithelial organoids from human colon, adenoma, adenocarcinoma, and Barrett's epithelium. *Gastroenterology* **141:** 1762-1772

Sato T, van Es JH, Snippert HJ, Stange DE, Vries RG, van den Born M, Barker N, Shroyer NF, van de Wetering M, Clevers H (2011b) Paneth cells constitute the niche for Lgr5 stem cells in intestinal crypts. *Nature* **469:** 415-418

Sato T, Vries RG, Snippert HJ, van de Wetering M, Barker N, Stange DE, van Es JH, Abo A, Kujala P, Peters PJ, Clevers H (2009) Single Lgr5 stem cells build crypt-villus structures in vitro without a mesenchymal niche. *Nature* **459:** 262-265

Schepers A, Clevers H (2012) Wnt signaling, stem cells, and cancer of the gastrointestinal tract. *Cold Spring Harb Perspect Biol* **4:** a007989

Schlegelmilch K, Mohseni M, Kirak O, Pruszak J, Rodriguez JR, Zhou D, Kreger BT, Vasioukhin V, Avruch J, Brummelkamp TR, Camargo FD (2011) Yap1 acts downstream of alpha-catenin to control epidermal proliferation. *Cell* **144:** 782-795

Schneider MR, Dahlhoff M, Horst D, Hirschi B, Trulzsch K, Muller-Hocker J, Vogelmann R, Allgauer M, Gerhard M, Steininger S, Wolf E, Kolligs FT (2010) A key role for E-cadherin in intestinal homeostasis and Paneth cell maturation. *PloS one* **5:** e14325

Schwitalla S, Fingerle AA, Cammareri P, Nebelsiek T, Goktuna SI, Ziegler PK, Canli O, Heijmans J, Huels DJ, Moreaux G, Rupec RA, Gerhard M, Schmid R, Barker N, Clevers H, Lang R, Neumann J, Kirchner T, Taketo MM, van den Brink GR, Sansom OJ, Arkan MC, Greten FR (2013) Intestinal tumorigenesis initiated by dedifferentiation and acquisition of stem-cell-like properties. *Cell* **152:** 25-38

Seidel B, Braeg S, Adler G, Wedlich D, Menke A (2004) E- and N-cadherin differ with respect to their associated p120ctn isoforms and their ability to suppress invasive growth in pancreatic cancer cells. *Oncogene* **23:** 5532-5542

Shibamoto S, Hayakawa M, Takeuchi K, Hori T, Miyazawa K, Kitamura N, Johnson KR, Wheelock MJ, Matsuyoshi N, Takeichi M, et al. (1995) Association of p120, a tyrosine kinase substrate, with E-cadherin/catenin complexes. *The Journal of cell biology* **128:** 949-957

Shibata H, Takano H, Ito M, Shioya H, Hirota M, Matsumoto H, Kakudo Y, Ishioka C, Akiyama T, Kanegae Y, Saito I, Noda T (2007) Alpha-catenin is essential in intestinal adenoma formation. *Proc Natl Acad Sci U S A* **104:** 18199-18204

Shibata H, Toyama K, Shioya H, Ito M, Hirota M, Hasegawa S, Matsumoto H, Takano H, Akiyama T, Toyoshima K, Kanamaru R, Kanegae Y, Saito I, Nakamura Y, Shiba K, Noda T (1997) Rapid colorectal adenoma formation initiated by conditional targeting of the Apc gene. *Science* **278:** 120-123

Shroyer NF, Helmrath MA, Wang VY, Antalffy B, Henning SJ, Zoghbi HY (2007) Intestine-specific ablation of mouse atonal homolog 1 (Math1) reveals a role in cellular homeostasis. *Gastroenterology* **132:** 2478-2488

Shtutman M, Zhurinsky J, Simcha I, Albanese C, D'Amico M, Pestell R, Ben-Ze'ev A (1999) The cyclin D1 gene is a target of the beta-catenin/LEF-1 pathway. *Proc Natl Acad Sci U S A* **96:** 5522-5527

Siegel R, Desantis C, Jemal A (2014) Colorectal cancer statistics, 2014. *CA Cancer J Clin* **64:** 104-117

Silvis MR, Kreger BT, Lien WH, Klezovitch O, Rudakova GM, Camargo FD, Lantz DM, Seykora JT, Vasioukhin V (2011) alpha-catenin is a tumor suppressor that controls cell accumulation by regulating the localization and activity of the transcriptional coactivator Yap1. *Sci Signal* **4:** ra33

Skoudy A, Gomez S, Fabre M, Garcia de Herreros A (1996) p120-catenin expression in human colorectal cancer. *Int J Cancer* **68:** 14-20

Slorach EM, Chou J, Werb Z (2011) Zeppo1 is a novel metastasis promoter that represses E-cadherin expression and regulates p120-catenin isoform expression and localization. *Genes Dev* **25:** 471-484

Smalley-Freed WG, Efimov A, Burnett PE, Short SP, Davis MA, Gumucio DL, Washington MK, Coffey RJ, Reynolds AB (2010) p120-catenin is essential for maintenance of barrier function and intestinal homeostasis in mice. *J Clin Invest* **120:** 1824-1835

Smalley-Freed WG, Efimov A, Short SP, Jia P, Zhao Z, Washington MK, Robine S, Coffey RJ, Reynolds AB (2011) Adenoma formation following limited ablation of p120-catenin in the mouse intestine. *PLoS ONE* **6:** e19880

Smith AL, Dohn MR, Brown MV, Reynolds AB (2012) Association of Rho-associated protein kinase 1 with E-cadherin complexes is mediated by p120-catenin. *Mol Biol Cell* **23:** 99-110

Smith AL, Friedman DB, Yu H, Carnahan RH, Reynolds AB (2011) ReCLIP (Reversible Cross-Link Immuno-Precipitation): An Efficient Method for Interrogation of Labile Protein Complexes. *PLoS ONE* **6:** e16206

Smits R, Ruiz P, Diaz-Cano S, Luz A, Jagmohan-Changur S, Breukel C, Birchmeier C, Birchmeier W, Fodde R (2000) E-cadherin and adenomatous polyposis coli mutations are synergistic in intestinal tumor initiation in mice. *Gastroenterology* **119:** 1045-1053

Snippert HJ, van der Flier LG, Sato T, van Es JH, van den Born M, Kroon-Veenboer C, Barker N, Klein AM, van Rheenen J, Simons BD, Clevers H (2010) Intestinal crypt homeostasis results from neutral competition between symmetrically dividing Lgr5 stem cells. *Cell* **143:** 134-144

Solimini NL, Luo J, Elledge SJ (2007) Non-oncogene addiction and the stress phenotype of cancer cells. *Cell* **130:** 986-988

Soto E, Yanagisawa M, Marlow LA, Copland JA, Perez EA, Anastasiadis PZ (2008) p120 catenin induces opposing effects on tumor cell growth depending on E-cadherin expression. *The Journal of Cell Biology* **183:** 737-749

Soubry A, van Hengel J, Parthoens E, Colpaert C, Van Marck E, Waltregny D, Reynolds AB, van Roy F (2005) Expression and Nuclear Location of the Transcriptional Repressor Kaiso Is Regulated by the Tumor Microenvironment. *Cancer Res* **65:** 2224-2233

Spring CM, Kelly KF, O'Kelly I, Graham M, Crawford HC, Daniel JM (2005) The catenin p120ctn inhibits Kaiso-mediated transcriptional repression of the beta-catenin/TCF target gene matrilysin. *Experimental Cell Research* **305:** 253-265

Stairs DB, Bayne LJ, Rhoades B, Vega ME, Waldron TJ, Kalabis J, Klein-Szanto A, Lee JS, Katz JP, Diehl JA, Reynolds AB, Vonderheide RH, Rustgi AK (2011) Deletion of p120-catenin results in a tumor microenvironment with inflammation and cancer that establishes it as a tumor suppressor gene. *Cancer Cell* **19:** 470-483

Stanger BZ, Datar R, Murtaugh LC, Melton DA (2005) Direct regulation of intestinal fate by Notch. *Proc Natl Acad Sci U S A* **102:** 12443-12448

Strano S, Munarriz E, Rossi M, Castagnoli L, Shaul Y, Sacchi A, Oren M, Sudol M, Cesareni G, Blandino G (2001) Physical interaction with Yes-associated protein enhances p73 transcriptional activity. *J Biol Chem* **276:** 15164-15173

Su LK, Kinzler KW, Vogelstein B, Preisinger AC, Moser AR, Luongo C, Gould KA, Dove WF (1992) Multiple intestinal neoplasia caused by a mutation in the murine homolog of the APC gene. *Science* **256:** 668-670

Taddei ML, Giannoni E, Fiaschi T, Chiarugi P (2012) Anoikis: an emerging hallmark in health and diseases. *The Journal of pathology* **226:** 380-393

Takahashi K, Suzuki K (1996) Density-dependent inhibition of growth involves prevention of EGF receptor activation by E-cadherin-mediated cell-cell adhesion. *Experimental cell research* **226:** 214-222

Takeda N, Jain R, LeBoeuf MR, Wang Q, Lu MM, Epstein JA (2011) Interconversion between intestinal stem cell populations in distinct niches. *Science* **334:** 1420-1424

Takeichi M (1995) Morphogenetic roles of classic cadherins. *Current opinion in cell biology* **7:** 619-627

Tan CW, Hirokawa Y, Gardiner BS, Smith DW, Burgess AW (2013) Colon cryptogenesis: asymmetric budding. *PloS one* **8:** e78519

Tetsu O, McCormick F (1999) Beta-catenin regulates expression of cyclin D1 in colon carcinoma cells. *Nature* **398:** 422-426

Theveneau E, Mayor R (2012) Cadherins in collective cell migration of mesenchymal cells. *Current opinion in cell biology* **24:** 677-684

Thoreson MA, Anastasiadis PZ, Daniel JM, Ireton RC, Wheelock MJ, Johnson KR, Hummingbird DK, Reynolds AB (2000) Selective uncoupling of p120(ctn) from E-cadherin disrupts strong adhesion. *The Journal of Cell Biology* **148:** 189-202

Torres M, Stoykova A, Huber O, Chowdhury K, Bonaldo P, Mansouri A, Butz S, Kemler R, Gruss P (1997) An alpha-E-catenin gene trap mutation defines its function in preimplantation development. *Proc Natl Acad Sci U S A* **94:** 901-906

Valizadeh A, Karayiannakis AJ, el-Hariry I, Kmiot W, Pignatelli M (1997) Expression of E-cadherin-associated molecules (alpha-, beta-, and gamma-catenins and p120) in colorectal polyps. *Am J Pathol* **150:** 1977-1984

van de Wetering M, Sancho E, Verweij C, de Lau W, Oving I, Hurlstone A, van der Horn K, Batlle E, Coudreuse D, Haramis AP, Tjon-Pon-Fong M, Moerer P, van den Born M, Soete G, Pals S, Eilers M, Medema R, Clevers H (2002) The beta-catenin/TCF-4 complex imposes a crypt progenitor phenotype on colorectal cancer cells. *Cell* **111:** 241-250

van der Flier LG, van Gijn ME, Hatzis P, Kujala P, Haegebarth A, Stange DE, Begthel H, van den Born M, Guryev V, Oving I, van Es JH, Barker N, Peters PJ, van de Wetering M, Clevers H (2009) Transcription factor achaete scute-like 2 controls intestinal stem cell fate. *Cell* **136:** 903-912

van Dop WA, Heijmans J, Buller NV, Snoek SA, Rosekrans SL, Wassenberg EA, van den Bergh Weerman MA, Lanske B, Clarke AR, Winton DJ, Wijgerde M, Offerhaus GJ, Hommes DW, Hardwick JC, de Jonge WJ, Biemond I, van den Brink GR (2010) Loss of Indian Hedgehog activates multiple aspects of a wound healing response in the mouse intestine. *Gastroenterology* **139:** 1665-1676, 1676 e1661-1610

van Es JH, de Geest N, van de Born M, Clevers H, Hassan BA (2010) Intestinal stem cells lacking the Math1 tumour suppressor are refractory to Notch inhibitors. *Nat Commun* **1:** 18

van Es JH, van Gijn ME, Riccio O, van den Born M, Vooijs M, Begthel H, Cozijnsen M, Robine S, Winton DJ, Radtke F, Clevers H (2005) Notch/gamma-secretase inhibition turns proliferative cells in intestinal crypts and adenomas into goblet cells. *Nature* **435:** 959-963

van Roy FM, McCrea PD (2005) A role for Kaiso-p120ctn complexes in cancer? *Nature reviews Cancer* **5:** 956-964

Varelas X, Samavarchi-Tehrani P, Narimatsu M, Weiss A, Cockburn K, Larsen BG, Rossant J, Wrana JL (2010) The Crumbs complex couples cell density sensing to Hippo-dependent control of the TGF-beta-SMAD pathway. *Dev Cell* **19:** 831-844

Vasioukhin V, Bauer C, Degenstein L, Wise B, Fuchs E (2001) Hyperproliferation and defects in epithelial polarity upon conditional ablation of alpha-catenin in skin. *Cell* **104:** 605-617

Vassilev A, Kaneko KJ, Shu H, Zhao Y, DePamphilis ML (2001) TEAD/TEF transcription factors utilize the activation domain of YAP65, a Src/Yes-associated protein localized in the cytoplasm. *Genes Dev* **15:** 1229-1241

Vermeulen JF, van de Ven RA, Ercan C, van der Groep P, van der Wall E, Bult P, Christgen M, Lehmann U, Daniel J, van Diest PJ, Derksen PW (2012) Nuclear Kaiso expression is associated with high grade and triple-negative invasive breast cancer. *PloS one* **7:** e37864

Vleminckx K, Vakaet L, Jr., Mareel M, Fiers W, van Roy F (1991) Genetic manipulation of E-cadherin expression by epithelial tumor cells reveals an invasion suppressor role. *Cell* **66:** 107-119

Vos CB, Cleton-Jansen AM, Berx G, de Leeuw WJ, ter Haar NT, van Roy F, Cornelisse CJ, Peterse JL, van de Vijver MJ (1997) E-cadherin inactivation in lobular carcinoma in situ of the breast: an early event in tumorigenesis. *British journal of cancer* **76:** 1131-1133

Werner S, Beer HD, Mauch C, Luscher B (2001) The Mad1 transcription factor is a novel target of activin and TGF-beta action in keratinocytes: possible role of Mad1 in wound repair and psoriasis. *Oncogene* **20:** 7494-7504

Wildenberg GA, Dohn MR, Carnahan RH, Davis MA, Lobdell NA, Settleman J, Reynolds AB (2006) p120-Catenin and p190RhoGAP Regulate Cell-Cell Adhesion by Coordinating Antagonism between Rac and Rho. *Cell* **127:** 1027-1039

Wong VW, Stange DE, Page ME, Buczacki S, Wabik A, Itami S, van de Wetering M, Poulsom R, Wright NA, Trotter MW, Watt FM, Winton DJ, Clevers H, Jensen KB (2012) Lrig1 controls intestinal stem-cell homeostasis by negative regulation of ErbB signalling. *Nature cell biology* **14:** 401-408

Wyrwicz LS, Gaj P, Hoffmann M, Rychlewski L, Ostrowski J (2007) A common cis-element in promoters of protein synthesis and cell cycle genes. *Acta Biochim Pol* **54:** 89-98

Xiao K, Allison DF, Buckley KM, Kottke MD, Vincent PA, Faundez V, Kowalczyk AP (2003) Cellular levels of p120 catenin function as a set point for cadherin expression levels in microvascular endothelial cells. *The Journal of cell biology* **163:** 535-545

Xiao K, Garner J, Buckley KM, Vincent PA, Chiasson CM, Dejana E, Faundez V, Kowalczyk AP (2005) p120-Catenin regulates clathrin-dependent endocytosis of VE-cadherin. *Mol Biol Cell* **16:** 5141-5151

Yagi R, Chen LF, Shigesada K, Murakami Y, Ito Y (1999) A WW domain-containing yes-associated protein (YAP) is a novel transcriptional co-activator. *Embo J* **18:** 2551-2562

Yamada S, Pokutta S, Drees F, Weis WI, Nelson WJ (2005) Deconstructing the cadherin-catenin-actin complex. *Cell* **123:** 889-901

Yamashita D, Sano Y, Adachi Y, Okamoto Y, Osada H, Takahashi T, Yamaguchi T, Osumi T, Hirose F (2007) hDREF regulates cell proliferation and expression of ribosomal protein genes. *Mol Cell Biol* **27:** 2003-2013

Yan KS, Chia LA, Li X, Ootani A, Su J, Lee JY, Su N, Luo Y, Heilshorn SC, Amieva MR, Sangiorgi E, Capecchi MR, Kuo CJ (2012) The intestinal stem cell markers Bmi1 and Lgr5 identify two functionally distinct populations. *Proc Natl Acad Sci U S A* **109:** 466-471

Yanagisawa M, Anastasiadis PZ (2006) p120 catenin is essential for mesenchymal cadherin-mediated regulation of cell motility and invasiveness. *The Journal of Cell Biology* **174:** 1087-1096

Yanagisawa M, Huveldt D, Kreinest P, Lohse CM, Cheville JC, Parker AS, Copland JA, Anastasiadis PZ (2008) A p120 catenin isoform switch affects Rho activity, induces tumor cell invasion, and predicts metastatic disease. *J Biol Chem* **283:** 18344-18354

Yap AS (1998) The morphogenetic role of cadherin cell adhesion molecules in human cancer: a thematic review. *Cancer Invest* **16:** 252-261

Yoon H-G, Chan DW, Reynolds AB, Qin J, Wong J (2003) N-CoR Mediates DNA Methylation-Dependent Repression through a Methyl CpG Binding Protein Kaiso. *Molecular cell* **12:** 723-734

Zecchini V, Domaschenz R, Winton D, Jones P (2005) Notch signaling regulates the differentiation of post-mitotic intestinal epithelial cells. *Genes Dev* **19:** 1686-1691

Zhang PX, Wang Y, Liu Y, Jiang GY, Li QC, Wang EH (2011) p120-catenin isoform 3 regulates subcellular localization of Kaiso and promotes invasion in lung cancer cells via a phosphorylation-dependent mechanism. *Int J Oncol* **38:** 1625-1635

Zhao B, Wei X, Li W, Udan RS, Yang Q, Kim J, Xie J, Ikenoue T, Yu J, Li L, Zheng P, Ye K, Chinnaiyan A, Halder G, Lai ZC, Guan KL (2007) Inactivation of YAP oncoprotein by the Hippo pathway is involved in cell contact inhibition and tissue growth control. *Genes Dev* **21:** 2747-2761

Zhao B, Ye X, Yu J, Li L, Li W, Li S, Lin JD, Wang CY, Chinnaiyan AM, Lai ZC, Guan KL (2008) TEAD mediates YAP-dependent gene induction and growth control. *Genes Dev* **22:** 1962-1971

Zhou D, Zhang Y, Wu H, Barry E, Yin Y, Lawrence E, Dawson D, Willis JE, Markowitz SD, Camargo FD, Avruch J (2011) Mst1 and Mst2 protein kinases restrain intestinal stem cell proliferation and colonic tumorigenesis by inhibition of Yes-associated protein (Yap) overabundance. *Proc Natl Acad Sci U S A* **108:** E1312-1320

APPENDIX A

CONSEQUENCES OF P120 LOSS IN INTESTINAL ORGANOID CULTURES

Introduction

Recent technological advances have allowed the *ex vivo* culture of primary mouse intestinal tissue (Sato et al, 2009). Originally termed "mini-guts," isolated murine crypts form elaborate structures in 3D Matrigel culture, in which crypt-like domains "bud" from a central lumen. Importantly, all differentiated cell types are seen in these cultures, thus effectively recapitulating many aspects of intestinal biology. The first "organoids" described crypt culture from the small intestine, but the organoid repertoire has been expanded to include: enteroids (small intestine), colonoids (colon), and tumoroids (adenoma), as well as cultures from human cancers and normal tissues (Sato et al, 2011a).

Our previous studies firmly establish p120 as a haploinsufficient tumor suppressor, and increased tumor numbers are seen with monoallelic p120 loss in a variety of mouse tumor models (Chapter 3). However, the phenotype of p120 loss and the exact manner in which it contributes to tumorigenesis has been elusive. These studies are complicated by the fact that many of our *in vivo* observations have been difficult to replicate *in vitro*. Some reasons for this include: 1) CRC cell lines are established from late stage tumors (i.e. adenocarcinomas or metastases) and are not representative of early tumorigenic phenotypes; 2) most CRC cell lines have activating Wnt pathway mutations and/or alterations to the adherens junction; 3) p120 knockdown by siRNA or shRNA reduces p120 expression significantly more than heterozygousity. Therefore, we turned to *ex vivo* enteroid culture as a means to investigate potential mechanisms for cadherin contribution in both early tumorigenesis and crypt maintenance.

Results

The effects of p120 heterozygousity in small intestinal enteroids

Small intestinal enteroid cultures have been established and maintained according to the protocols described in Appendix B, and multiple cultures have been generated from global p120 heterozygous (*p120 +/-*) mice and their WT (*p120 +/+*) littermates. While no overt difference were seen in plating efficiency, these calculations were complicated by the fact that p120 heterozygous tissue had noticeably decreased cell-cell adhesion, making them much more sensitive the manipulations necessary for plating. In fact, to maintain these cultures at similar viability to matched WT lines, differential methodologies were used for passaging to ensure sufficient crypt shearing without excessive dissociation (Appendix B). Otherwise, both culture types readily establish, and reduction of p120 and cadherin complex proteins can be seen by WB and IHC analysis (Figure 23C and Figure 26B).

Although higher tumor counts were consistently seen in p120 heterozygous tumor models, few phenotypic differences are observed in homeostasis in p120 heterozygous mice as compared to WT littermates. Thus, it was quite surprising to see that in 3D culture, *p120+/-* enteroids have a dramatic phenotype and are morphologically distinct from WT controls (Figure 22A). This altered morphology, includes increased budding, increased secondary branching (arrowhead), narrower crypts, and elongated crypt outgrowths. Crypt budding was quantified by sequential counts over the course of 7 days, which reveals a significant budding increase in *p120+/-* cultures (Figure 22B). Interestingly, budding counts remain the same until approximately 4 days post plating, leaving the early budding timeline apparently unchanged. Instead, it appears that the branching phenotype is likely due to development of secondary buds in *p120+/-* enteroids. This phenomenon was rarely seen in the WT cultures, but quite frequent with p120 heterozygousity (Figure 19A, arrowhead). Interestingly, despite the change in crypt buds, no change in proliferation was observed with p120 reduction (Figure 22C) and the same fraction of cycling cells was found in both WT and heterozygous cultures. However, it is possible that the *p120+/-* enteroids still have a higher total number of proliferating cells due to the higher number of crypt units. Higher numbers of crypts and their associated stem cells may increase proliferative, but only in a manner proportional to the other non-proliferative cell types.

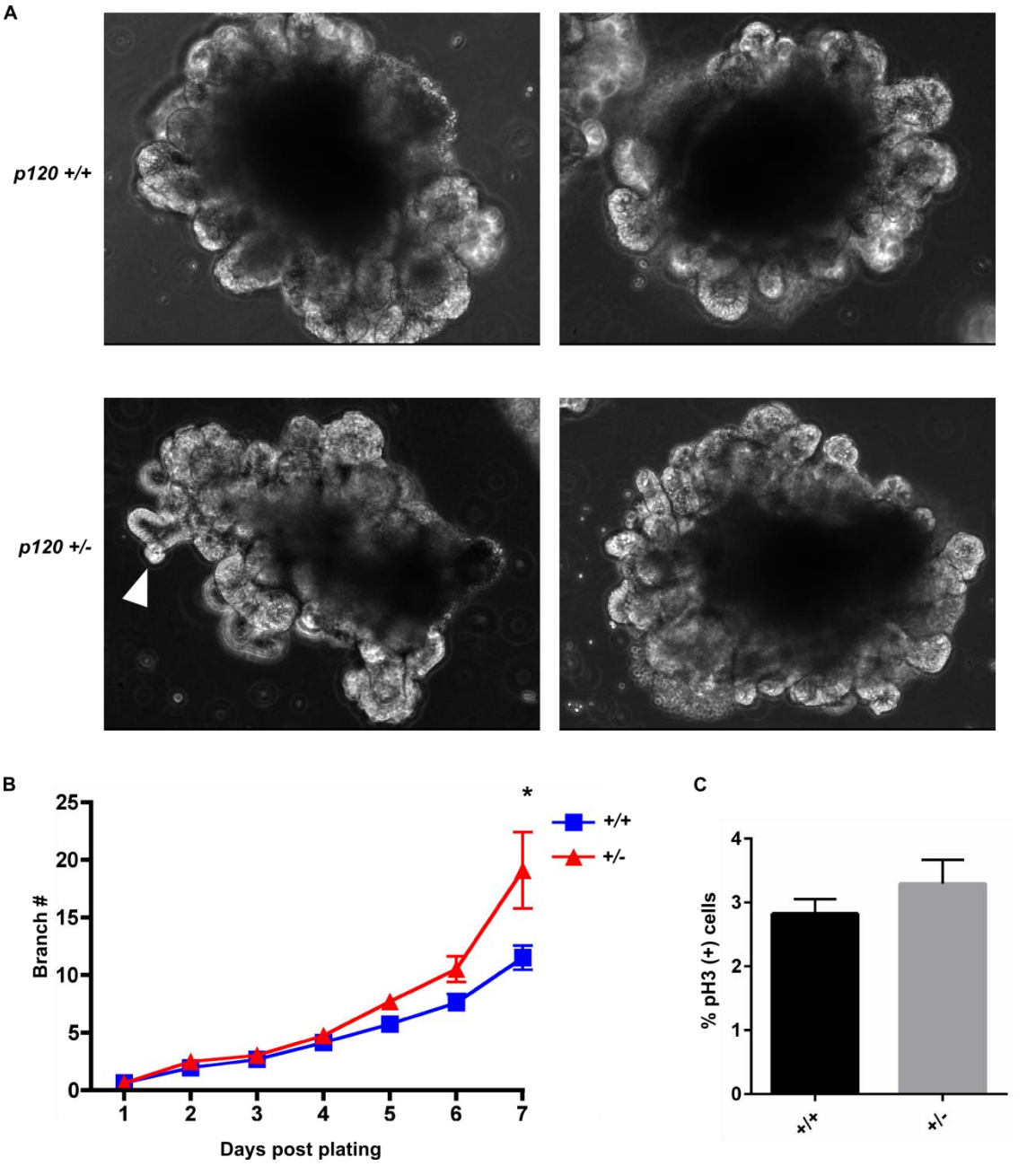

Figure 22. Abnormal morphology and increased branching in p120 heterozygous enteroids. (A) Bright field images from *p120* +/+ (top) and *p120* +/- (bottom) enteroids from cultures 7 days post plating. Heterozygous enteroids show altered morphology, including increased budding, increased secondary branching (arrowhead), narrower crypts, and elongated crypt outgrowths. (B) Enteroid buds were counted daily over 7 days to show a higher number of crypt buds in p120 +/- enteroids. $P < 0.05$. (C) To measure proliferation, enteroids were embedded and stained for phospho-histone H3. Quantification shows similar percentage of pH3 (+) cells. Error bars ± SEM.

To further test whether increased Wnt signaling could drive the enteroid and/or tumor phenotype, mRNA was harvested from *p120+/-* and *p120+/+* enteroids and subjected to qRT-PCR analysis (Figure 23). Interestingly, Wnt targets in the p120 heterozygous enteroids were broadly decreased as compared to their WT controls, as seen for *Axin2*, *c-Myc*, *Tcf7*, and *CyclinD1* (Figure 23A). While markers for most differentiated cell populations reveal little change, it was surprising to see that markers of the ISC, *Lgr5* and *Olfm4*, were decreased by close to 50% in *p120+/-* enteroids despite the presence of more crypt-like structures (i.e. enteroid buds). Thus, although numerous *in vitro* studies have found increased Wnt activation when β-catenin is not sequestered by the cadherin complex, these data suggest that the Wnt pathway is likely not the primary driver of the increased tumorigenesis observed in our mouse models. Furthermore, while western blot analysis revealed the expected decrease in p120, α-catenin, and β-catenin protein, no change in activation of growth signaling pathways was detected (Figure 23C). Thus, the mechanism behind the increased branching in *p120+/-* enteroids, and the driver of increased tumorigenesis *in vivo*, still remains undetermined.

Complete p120 ablation in *ApcMin* tumoroids

While loss of one p120 allele increased tumorigenesis in our *Apc* mouse models, loss of both alleles appears incompatible with tumor cell viability (Chapter 3). However, extensive characterization of p120 null adenoma cells by immunofluorescent staining yielded no mechanistic insight into this requirement (Figure 10). To attempt these studies in a more robust model system, we turned to organoid culture of *ApcMin* tumoroids. Tumors from *ApcMin; Vil-CreER; p120f/f* mice were digested and 3D tumoroid cultures were established according to protocols described in Appendix B. As the liver is required to process TAM in animal models, p120 loss was induced by treatment of 1μM 4-hydroxy-tamoxifen (4-OH TAM), an amount sufficient to induce complete gene KO (Farin et al, 2012). This treatment was continued for 3 days to ensure KO in a manner consistent with our *in vivo* treatment protocol.

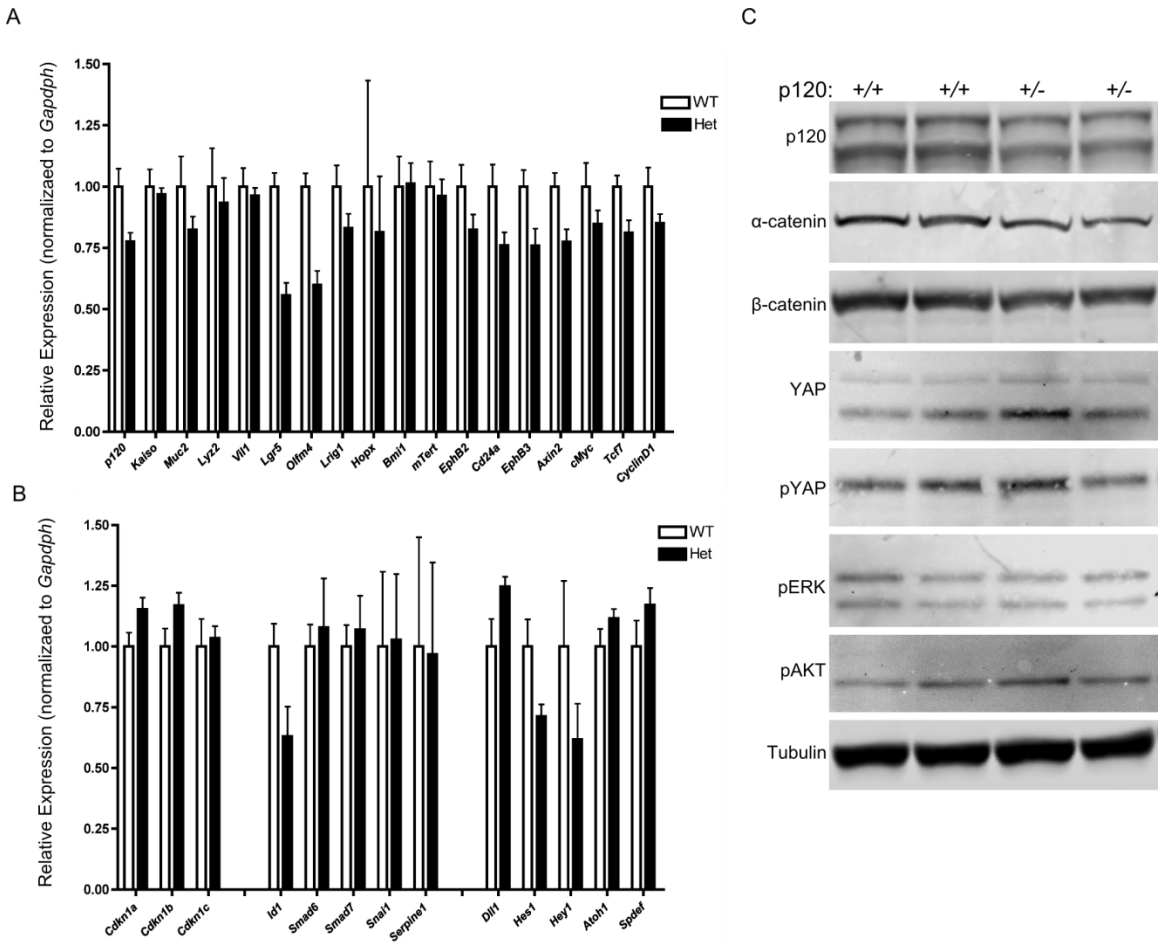

Figure 23. Changes in mRNA and protein expression induced by p120 heterozygousity. *p120 +/+* and *+/-* enteroids were harvested and homogenized in Trizol for mRNA or in RIPA buffer for WB analysis. qPCR analysis of (A) Wnt targets and differentiated cell markers and (B) regulators of proliferation, BMP, and Notch associated genes. (C) Western blot analysis shows expected decrease in p120, α-catenin, and β-catenin with little change in signaling proteins analyzed. Overall, no alterations were identified that are likely to account for the increased budding seen in p120 heterozygous enteroids.

As shown in Figures 24 and 25, induction of p120 KO *ex vivo* yielded striking results. Sequential images of a representative field illustrate loss of the round, spheroid morphology starting at approximated day 3 (last day of TAM treatment) that grew more pronounced over time, as the tumoroids shrink and grew noticeably denser (Figure 24A). While at first thought to be due to a loss of tumoroid viability, immunofluorescent studies confirmed these tumoroids still maintain an epithelial layer, and the change in both size and density is likely due to sloughing of apoptotic cells into the lumen (Figure 25A). In addition to changes in size, KO tumoroids also began to "bud" and develop numerous protrusions that appeared to be outgrowths from the tumoroid body (Figure 24B). Interestingly, the number of outgrowths appeared to proportional to the amount of p120 loss. 4-OH TAM-treated cultures from *ApcMin; Lgr5CreER; p120f/f* mice, which have a much more limited expression of cre recombinase, often showed a similar, but more restricted phenotype as cultures with a *Vil-CreER* driver.

Attempts to induce p120 loss in *ApcMin* tumors *in vivo* yielded very small, clonal patches of null cells that were lost entirely 2-4 weeks post TAM induction. Surprisingly, these cells did not show increased rates of apoptosis and the reason for their loss is still unclear. To determine if p120 null cells were generated by *ex vivo* TAM treatment and whether the phenotype observed by bright field was due to widespread p120 loss, TAM-treated and control tumoroid cultures were paraffin embedded and sectioned for immunofluorescent staining (Figure 25). However, despite continuous 3-day culture with relatively high amounts of 4-OH TAM, tumoroids from all time points were still found to maintain p120 expression. Interestingly, p120 levels appear to be reduced as compared to untreated controls, making it likely that tumoroids display wide-spread loss of one allele, much as we found with tumors from KO mice *in vivo* (Figure 25A). Only small patches of complete p120 KO were found (Figure 25B, arrow), which were generally negative for the apoptosis marker used. Interestingly, numerous apoptotic cells could be found in both TAM and control cultures, and often appeared to be extruded from the epithelial layer (Figure 25B, arrowhead). Thus, it seems likely that p120 null cells could be extruded from the tumoroid monolayer, sloughing into the lumen and contributing to the shrunken, dense cultures observed by bright field.

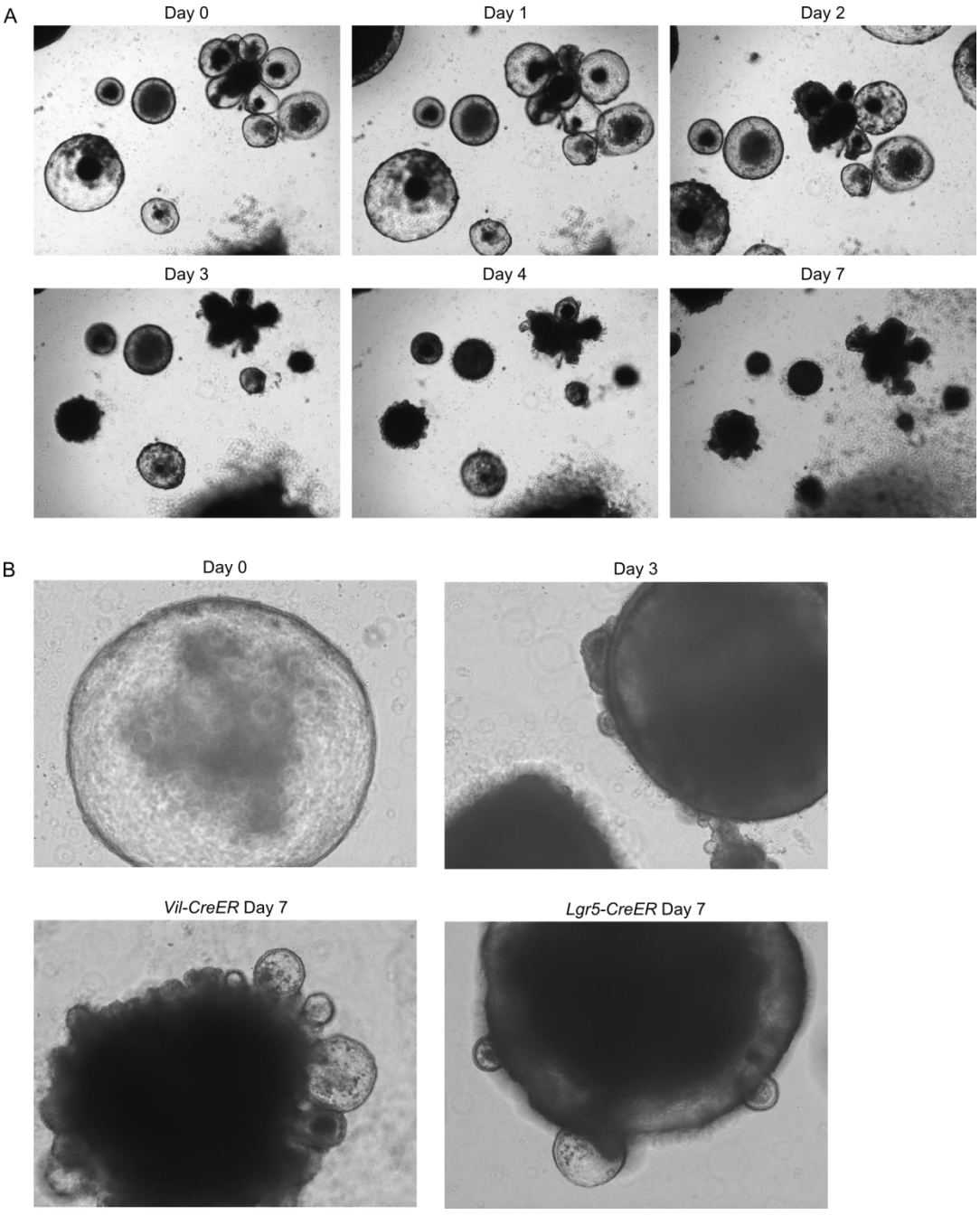

Figure 24. Widespread p120 loss induces cell sloughing and morphological changes *ex vivo*. Tumors from *ApcMin; Vil-CreER; p120f/f* and *ApcMin; Lgr5-CreER: p120f/f* mice were cultured *ex vivo* and p120 KO was induced by 3 day culture with 10μM 4-OH TAM. (A) Time course images show tumoroid "shrinking," likely due to dead cells sloughed into the tumoroid lumen, and altered morphology after TAM treatment. (B) Representative tumoroids show outgrowths of cells induced by p120 KO. Note that *Lgr5-CreER* tumoroids show a more restricted phenotype.

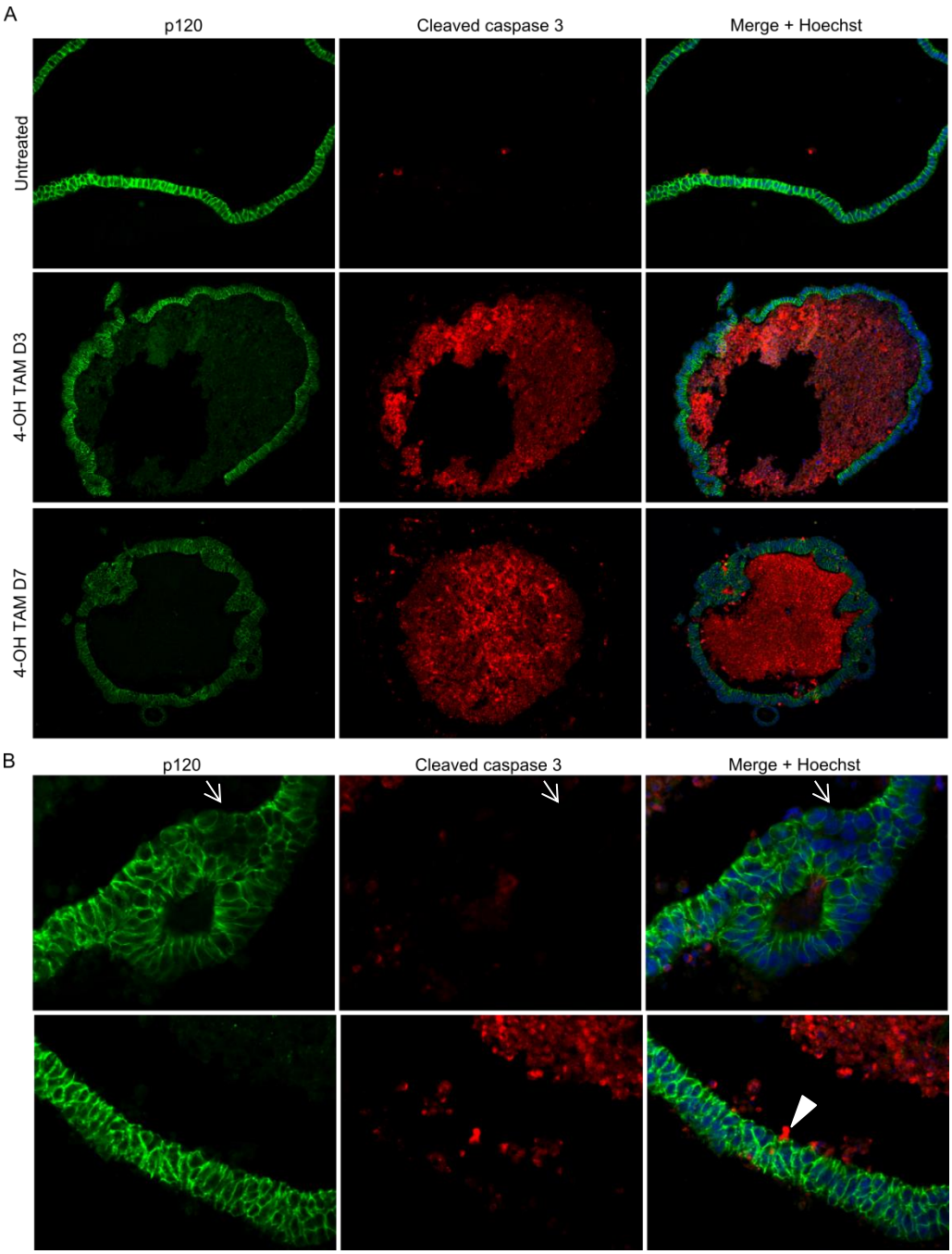

Figure 25. Limited p120 KO observed in *ApcMin* tumoroid cultures. Tumoroid cultures were embedded, sectioned, and stained for p120 (green), cleaved caspase 3 (red), and Hoechst (blue). (A) Representative images from untreated (top), day 3 (middle), and day 5 (bottom). Staining reveals very little p120 KO, although reduced p120 staining suggests widespread loss of one allele. Note morphological changes, as also observed by bright field. (B) As in vivo, very small areas of KO were observed (arrow), yet these areas were usually negative for cleaved caspase 3. Instead, apoptotic cells were most often seen extruding from the monolayer (arrowhead), suggesting cells are sloughed prior to death and not vice versa.

Discussion

Here, we utilized a recently developed *ex vivo* culture system in an attempt to elucidate the function of p120 in intestinal homeostasis and tumorigenesis. Unlike *p120+/-* mice at baseline, we find that enteroid cultures from *p120+/-* mice have a robust branching phenotype, although increased Wnt activation or proliferating cells were not found. Studies with *ApcMin* tumoroid cultures were designed in an effort to induce higher p120 KO that that observed in live mice. Interestingly, tumoroids display the same limited KO pattern seen in the *in vivo* tumor models and p120 KO cells were not more likely to be apoptotic than neighboring tumoroid cells. While this system did not prove to be more robust for elucidating the requirement for p120 in tumorigenesis, the results obtained here, from both enteroid and tumoroid cultures, reveal relevant manifestations of *in vivo* phenotypes which could reflect p120's role in early intestinal tumorigenesis.

Based on the available literature, perhaps the most likely mechanism behind p120's haploinsufficiency *in vivo* is the ability to activate the Wnt pathway by freeing β-catenin from the cadherin complex. However, our results are not consistent with this phenomenon, and instead we find decreased expression of Wnt target genes and stem cell markers in the *p120+/-* enteroids. One complication to this data may be the increased branching and cell numbers in the p120 het enteroids that could theoretically "dilute" the mRNA harvested from a small population such as the ISCs, leading to the decrease seen in Wnt target gene expression. Indeed, the results may be different if samples were instead taken from day 4 enteroids before changes in branching are apparent. However, all other differentiated cell markers, even those that mark the "+4" stem cell, are unchanged.

Interestingly, the branching phenotype observed in *p120+/-* enteroids is further supported by studies in 3D tumoroid cultures. While 4-OH TAM treatment was meant to induce complete p120 loss, reduced fluorescent staining suggests wide-spread loss of one allele, just like that observed in the *p120f/f* tumor models. Therefore, it is likely that the morphological changes induced by TAM treatment are due to loss of one p120 allele, not two. However, the mechanism behind this phenotype, and how it influences tumor formation *in vivo*, is still unknown. The tumoroid outgrowths are reminiscent of crypt "buds" on normal enteroids, thus p120 loss could cause tumoroids dedifferentiation to mediate the budding

phenotype. This has not yet been tested, but based on the qRT-PCR results from normal *p120+/-* enteroids, it is possible that p120 loss reduces overall Wnt-tone in the tumoroids. On the other hand, loss of one p120 allele dramatically increases tumor formation in the *Apc1638* mouse model, where tumor formation is thought to rely on the ability to overcome a minimum threshold of Wnt activation. Thus, while overall these data do not suggest a significant increase in Wnt activation, a substantial decrease in Wnt signaling should cause fewer tumors, instead of the 10-fold increase observed in *Apc1638* mice.

Tumors establish much more readily in p120 heterozygous mice, but are without any other phenotypic difference. Thus whether the branching increase is relevant to tumor formation at all can be debated. However, as phenotypes were consistent in both enteroids and tumoroid cultures, it likely reflects a subtle, but highly functional alteration that may not be apparent until the cells are freed from the confines of the intestinal architecture. Interestingly, while the intestinal crypts appear relatively normal with p120 loss, many organ systems display morphological defects which are most commonly attributed to loss of cell-cell adhesion. Systems such as the mammary and salivary glands display cell sloughing and ductal occlusion, much as seen in the 3D intestinal cultures. Thus, it appears likely that the mechanism behind p120's role in the intestine may still be attributed to altered cell-cell adhesion. Indeed, the only difference noted in the *p120+/-* intestine was a slightly higher rate of cell migration, a common manifestation of altered adhesion. This conclusion would also be consistent with the role observed for E-cadherin and α-catenin in Chapter 3. Together, these data suggest that the intestinal architecture may be unusually efficient at constraining the altered morphology normally induced by p120 loss, thus these dramatic phenotypes only manifest when tissue is cultured *ex vivo*.

Loss of cell-cell adhesion may also be the driving force behind loss of p120 null adenoma cells. Here, we find that treatment with 4-OH TAM leads to rapid cell sloughing, even to the point that tumoroids grow significantly smaller. Much like the results *in vivo*, small pockets of p120 KO cells could be found, but these cells were not generally apoptotic. Cells undergoing apoptosis were readily found, however, and can be seen extruding from the epithelial layer in both untreated and TAM-treated cultures. Interestingly, the intestine is a highly dynamic environment and at the end of their transition up the villus cells are lost by sloughing into the intestinal lumen. This phenomenon can also be observed in *ApcMin* tumors, and cells (both apoptotic and viable) can often be seen in the middle of adenomatous crypts. Thus, this may provide a mechanism for loss of p120 KO cells, which may fall easy prey to extrusion due to lack of adhesion and the ability to participate in collective migration.

While defects in cell-cell adhesion may account for the phenotype observed with p120 heterozygousity and the fate of p120 null cells, this has yet to be conclusively demonstrated. Furthermore, while the *p120+/-* phenotype may be mediated by adhesion defects, how this defect contributes to the increase observed in tumor formation is still unclear. However, here we describe a series of novel, *ex vivo* models which may prove valuable for future studies on both p120 and its binding partner, Kaiso.

APPENDIX B

PROTOCOLS FOR ORGANOID CULTURE AND ANALYSIS

Establishing small intestinal enteroids

Modified from Mahe et. al. (Mahe et al, 2013)

1) Dissect out ~10 cm of small intestine on ice, removing tissue from the stomach to midway down the intestine. Flush with ice cold PBS* until PBS runs clear. Remove the first cm of intestine with the pyloric junction and from there measure 8cm of intestine. Splay open with blunt tip scissors. Wash 2X in cold PBS, 1X in PBS plus 0.01% bleach, and rinse again in PBS. Mince tissue with scissors and transfer into a 15mL conical tube with 5mL cold PBS. Rock at 4^{o} for 15 minutes.

   ** Use purchased 1X PBS, without calcium and magnesium, for washes, incubations, and buffers. This ensures proper pH, and any calcium or magnesium will interfere with chelation*.

   ***To cut down on contamination, use sterile PBS and filter solutions as needed. I do as many steps as possible under the hood.*

2) Remove PBS and vortex on high for 5 seconds. Wash intestinal fragments 2X with 10mL PBS. After final wash, transfer into 5mL fresh chelation buffer (2mM EDTA in PBS*). Rock in cold room for 30 minutes.

   **For 20mL chelation buffer add 0.0117g EDTA*

3) Remove chelation buffer and wash intestinal fragments 2X in cold PBS by gently inverting 4-5 times. Let intestinal fragments settle and remove PBS with a pipet. Add 5mL cold shaking buffer (PBS with 43.3 mM sucrose and 54.9 mM sorbitol*.)

   ** For 500mL, weigh 7.41g sucrose and 5g sorbitol. Add PBS to 500ml. Filter and store at 4^{o}*

4) Shake tubes gently (to the tempo of AC/DC Back in Black) for 2 minutes. After 2 minutes, check for crypts by pipetting 20μL onto glass coverslip (ideally see 5-10 crypts per drop). If crypt yield is lower, filter (step 5), add 5mL more shaking buffer, and shake for 2 more minutes.

5) Filter crypts through 70µm cell strainer into a 50mL conical. Rinse filter with 5mL cold shaking buffer.
6) Count crypts number per 20µL drop and transfer enough volume for 300 crypts per well to a 5mL polystyrene round bottom tube.*

   **If crypts are concentrated enough, you can combine multiple wells per tube and bring pellet up in the appropriate amount of Matrigel*
7) Centrifuge at 150g (~900rpm) for 10 minutes at 4^{o}C. Pour off shaking buffer by quickly dumping into a waste conical. Place tubes upside down on Kim-wipe as you process remaining tubes. After all tubes are processes, aspirate any excess liquid from side of tube. Be sure to remove as much excess water as possible since this will dilute your Matrigel.
8) Resuspend crypts in 50µL Matrigel (BD 356231) per tube*, containing:
   - EGF: 50ng/mL (R&D 2028-EG-200)
     - To aliquot, add 2mL PBS to vial (200ug/vial)
     - Make 9 200uL aliquots + 20 10µL aliquots. Continue to thaw and split 200µL into 10µL aliquots as necessary
   - Noggin: 100ng/mL (1967-NG-025/CF)
     - To aliquot, add 500µL PBS to vial (25ug/vial)
     - 20µl aliquot x 25
   - R-spondin 500ng/mL (VAPRSPON5 from core)
     - Calculated concentration to make 5µg aliquots
     - 500ng will be 1/10th of aliquot volume
   - Wnt3a: 100ng/mL (1324-WNP-010/CF)
     - To aliquot, add 200µL PBS to vial
     - 20µL aliquot x 10

**Store growth factor aliquots at -80^{o}C*

*** When resuspending crypts, be sure to resuspend without adding bubbles and do not pipet up and down excessively, especially for p120+/- cultures*

9) Plate onto 12-well culture plates, forming a mounded dome with Matrigel in the middle of the well.
10) Allow Matrigel to polymerize at 37^{o}C for 30 minutes
11) Overlay Matrigel with 500µL "mini-gut" culture media:
    - Mini-gut culture media
        - Advanced DMEM/F12 (Invitrogen #12634-010)
        - L-Glutamine (Invitrogen #25030)
        - Pen-Strep (Invitrogen #15140-148)
        - Hepes 10µM (Cellgro MT25060CI from core)
        - N2 Supplement 1:100 (Invitrogen #17502-048)
        - B27 Supplement 1:50 (Invitrogen #17504044)

    *** Make 200ml of this media and freeze in 10ml aliquots for plating and splitting. Media will start to lose activity after 4 days at 4^{o}C*

12) Every 4 days, replace media with fresh mini-gut media plus growth factors.
        - 1µL R-Spondin (or 500ng/well)
        - 1µL Noggin
        - 0.25µL EGF
        - 500µL media

Splitting enteroids

1) Aspirate media and wash 1X with cold PBS.
2) Add 1mL cold PBS per well. Coat p1000 pipet tip with 0.1% sterile BSA solution.* Use pipet tip to scrape plug off the bottom and transfer into a 15 mL conical tube on ice.

   **Pipet up and down in BSA to coat tip before pipetting enteroids. This keeps enteroids from sticking inside the pipet tip. Alternative to BSA solution is 0.1% FBS.*
3) Spin down at 200g for 3 minutes at 4^{o} to pellet enteroids
4) Resuspend enteroid pellet in 1mL cold PBS.
5) Shear enteroid buds by pulling into 1mL syringe fitted with a 25G needle. Go up and down 2X for p120+/- and 3-4X for WT (depending on size and quantity of enteroids). Be careful not to over-shear and keep bubbles at a minimum.
6) Spin at 200g for 5 minutes.
7) Gently remove all PBS and the top part of pelleted Matrigel. Sheared crypts should pellet at the very bottom of the Matrigel, most cells scattered throughout are single cells and will not grow.
8) Resuspend in Matrigel as done previously. Refeed as necessary.

Freezing enteroids

1) Harvest enteroid as per "splitting" protocol
2) Spin down 200g for 3 minutes at 4^{o}.
3) Resuspend in organoid freezing media (80% Advanced DMEM F12, 10% heat inactivated FBS, 10% DMSO). I generally freeze 2-3 wells worth of organoids in 1mL.
4) Freeze enteroids at -80^{o}C overnight and transfer to LN storage ASAP.

Establishing ApcMin adenoma organoids

1) Sac 1 4-5 month old *ApcMin* mouse. Harvest whole intestine on ice and flush with cold PBS. Splay intestine open and wash 1Xwith PBS.
2) Spread splayed intestine on bibulous paper. Isolate adenomas with as little normal intestinal epithelium as possible.
3) Add isolated adenomas to 10mL chelation buffer in 15mL conical tube.
    - Chelation buffer (w/2mM EDTA) (Chelation buffer: distilled water with 5.6 mM Na2HPO4, 8.0 mM KH2PO4, 96.2 mM NaCl, 1.6 mM KCl, 43.4 mM sucrose, 54.9 mM D-sorbitol, 0.5 mM DL-dithiothreitol). Make up buffer *without EDTA* and store at 4^{o}C, Add 2mM EDTA directly before tumor isolation.
4) Rock tumor fragments in EDTA chelation buffer at 4^{o} for 1 hour. After 1 hour, shake gently for 2 minutes to completely loosen normal epithelium.
5) Aspirate chelation buffer and wash 1X with PBS. Add 5 mL pre-warmed digestion buffer (37^{o}C)
    - Digestion buffer (10mL)
        - 9.7mL plain DMEM
        - 250µL FBS
        - 100µL Pen-Strep antibiotic
        - 1mg collagenase XI
        - 1.25mg Dispase
6) Rock/shake at 37^{o} for 30 minutes. I generally put tubes on a nutator in a cell culture incubator. Be sure to Parafilm the top of the tube.
7) Shake tubes gently for 2 minutes. Let sit undisturbed for 1 minute for larger particles to settle. Collect supernatant.

8) Spin supernatant down at 200g for 5 minutes. Aspirate digestion buffer and wash pellet 1X with PBS. Spin down at 150g for 3 minutes.

9) Aspirate as much PBS from the pellet as possible and resuspend pellet Matrigel as needed.*

**I generally resuspend in ~1mL Matrigel for 1 aged ApcMin mouse*

*** While not required, I add the standard growth factor compliment (EGF, Noggin, and R-spondin) for the initial plating to help with yield.*

10) Add 50µL cell/Matrigel mix to individual wells on a 12-well plate. Allow Matrigel to polymerize for 30 minutes at 37^{o}C, then overlay with 500µL tumoroid media.

11) Tumoroid media:
    - 196mL Advanced DMEM/F12
    - 4mL Pen-Strep antibiotic

12) Refeed and split as needed. To split cultures, shear 2X with a syringe fitted with 25G needle. Tumoroid cultures are much more sensitive to shearing than standard enteroid cultures.

Paraffin embedding for IHC staining

1) Grow organoids and harvest according to standard splitting protocol. Collect enteroids in a 15 mL conical on ice and spin down at 200g for 3 min at 4°C.
2) Aspirate PBS and as much Matrigel as possible without disturbing pellet. Resuspend in 1mL 10% neutral-buffered formalin. Fix on ice for 20 minutes.
3) As cells are fixing, make up 2% agarose in PBS (10mL PBS + 0.2g agarose).*

   **Dissolve agarose carefully as this is a very small volume. If agarose boils over it will increase the percentage of your gel and decrease staining quality.*
4) Place dissolved agarose in 55°C water bath for at least 10 minutes prior to use.
5) Wash enteroid 3X with ice-cold PBS to remove fixative. Spin down each time at 200g for 3 min at 4°C.
6) On final wash, aspirate as much liquid as possible to prepare for embedding.
7) To prepare for agarose embedding:
   - Lay down a labelled piece of Parafilm to let the agarose plug solidify. Label where each sample plug will go.
   - Use low retention, blunt-tipped pipets (cut tips off normal ones). Using normal pipet tips will cause either enteroid dissociation, premature agarose polymerization, or both.
8) Resuspend enteroids quickly in 90µL agarose. It is a small volume going into a cold tube, so just pipet enough to collect enteroids and pull them up. Spot agarose plug on to labelled Parafilm.

   ** I like to use an excess of agarose, because bubbles in this scenario are a nightmare. But, the smaller your agarose plug the more concentrated your samples will be on the slide. Only spot as much as you need to get the majority of enteroids in the plug*.
9) Let agarose solidify for 10 minutes.
10) Place plug in a labelled biopsy cassette and keep in 70% ethanol at 4° until bringing to the TPSR core.

11) When submitting your samples to the core, be sure to specify “short processing cycle.” Otherwise, they should know what to do. You can see the agarose plug in the paraffin to know when to start cutting.

***Overall, staining seemed most dependent on keeping the samples cold and on ice. Unfortunately, methylene blue stain will not work at colder temperatures, but the agarose is still easy enough to see where to cut in the paraffin block*

Organoid lentiviral infection

Virus production:

1) Infect 2 10cm plates of 293T cells with lentiviral vectors via standard PEI transfection protocol.
    - PEI: Add 2µg vector DNA, 1µg PAX2 packaging plasmid, and 1µg MD2 packaging plasmid to 100µL plain DMEM media. Add 24µL PEI (1mg/mL) and vortex to mix. Let sit at room temp 10-15 minutes. Meanwhile, add 10mL fresh, complete DMEM with heat inactivated FBS. Add PEI mixture drop wise while swirling and incubate overnight.
2) On the following day change media on 293Ts and add 10mL fresh media. Incubate 48 hours.
3) After 48 hours, ensure transfection if possible (GFP/RFP expression, etc.) Collect lentivirus media and filter through a 0.45µm filter. Spin overnight at 8,000g at 4°C.

Enteroid infection (next morning)

4) Harvest enteroids for infection into conical tube on ice using 0.1% BSA coated pipet tips.* Spin down enteroids at 200g for 3 min (4°C) to pellet.

    **I normally do ~2 wells worth per vector, with approximately 50 enteroids per well.*
5) Resuspend in 1mL cold PBS. Dissociate enteroids by passaging through a 25G needle ~8 times.*

    **Shear more or less depending on density and branching in your cultures. The point is to get enteroids to cell clumps without complete dissociation. A good rule-of-thumb is shear 2X what you would to split the cultures.*
6) Spin down dissociated enteroids at 1000g for 5 minutes. Resuspend in 250µL concentrated virus (see step below) and transfer to 5mL polystyrene round bottom tube.
7) To prep virus, after overnight spin pour off media and resuspend each viral pellet in 250µL mini-gut media with:
    - Standard ENR growth factor compliment, 1µg/mL Wnt3a, 8µg/mL polybrene, and 10µM Y27632.

    ** I have never actually seen a virus pellet, but I know that it's there. I test my virus by having a spare plate of 293Ts on hand by adding ~1 drop of the concentrated virus*

mixture. Be sure to add more polybrene for the amount of media used on the cells to keep it at 4-8μg/mL.

8) Spin organoid pellet in concentrated virus at 600g at 32^{o} for 1 hour.
9) Remove tubes from centrifuge and place in rack. Incubate rack at 37^{o} for 6 hours in incubator. Do not disturb the cell/virus pellet.
10) After 6 hours, add 3-4mL PBS to dilute the virus. Spin down at 1000g for 5 minutes at 4^{o}C.
11) Pour off media (similar to enteroid establishment protocol) and aspirate all liquid from the side of the tube.
12) Resuspend organoid pellet in 200mL Matrigel with standard growth factor compliment, 10μM Y27632, and 1μg/mL Wnt3a. Allow to polymerize at 37^{o}C and overlay with plain mini-gut media.
13) Two days post infection, check fluorescence by microscopy. Infected GFP will clearly be in the epithelial cells (and NOT what you can see frequently in the lumen) See Figure 22 for example images.

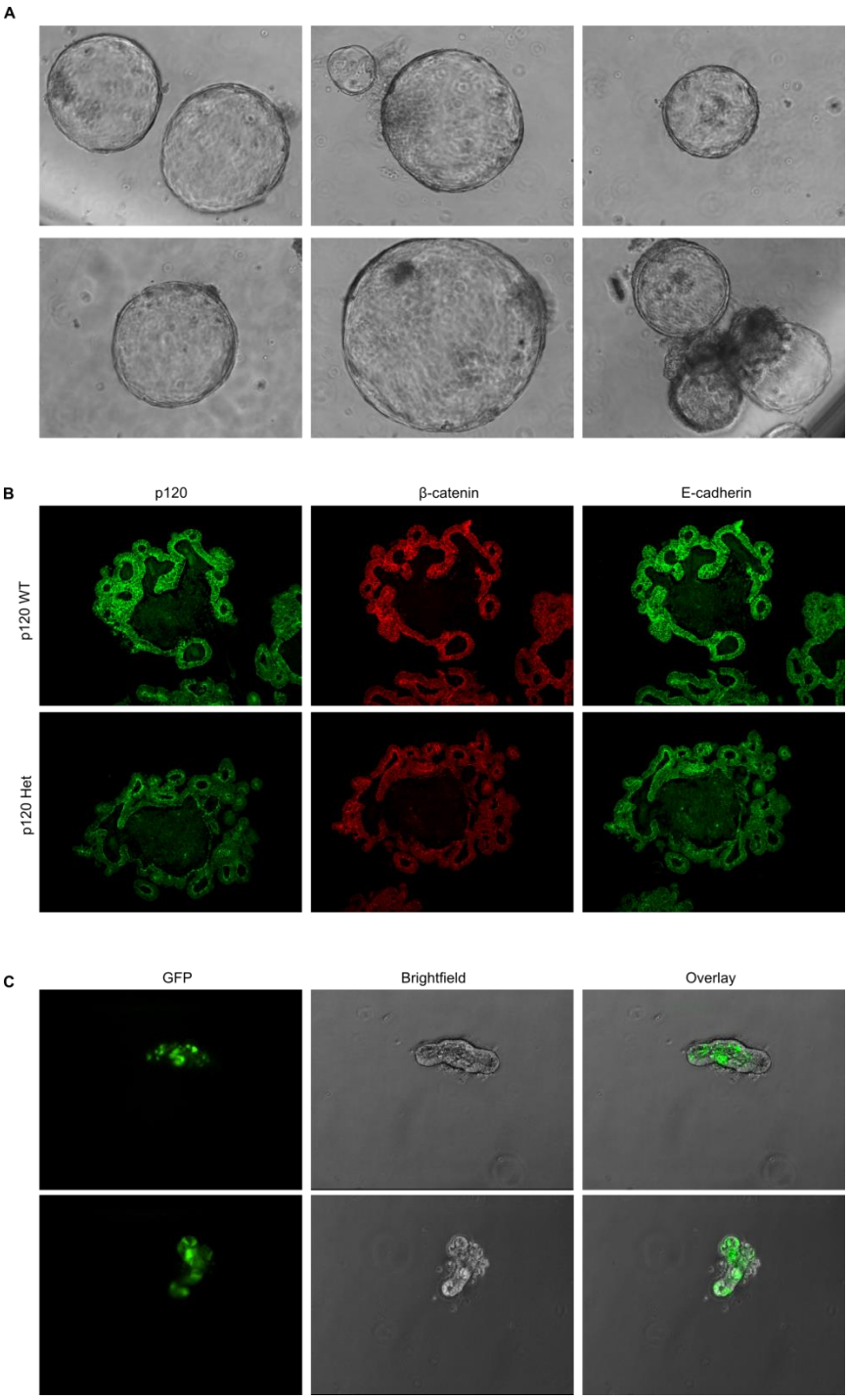

Figure 26. Validation of organoid protocols. (A) *ApcMin* adenoma tumoroids grow as cystic spheroids (B) IHC on FFPE enteroid samples. Note the decrease in staining in the *p120 +/-* enteroids as compared to WT, as expected. (C) Results of GFP infection 2 days post infection. Note epithelial GFP expression. This was maintained over enteroid growth and passaging.